Bioseparations using Surfactant-Aided Size-Exclusion Chromatography

Danielle Horneman

Bioseparations using Surfactant-Aided Size-Exclusion Chromatography

Proefschrift

ter verkrijging van de graad van doctor
aan de Technische Universiteit Delft,
op gezag van de Rector Magnificus prof. dr. ir. J.T. Fokkema,
voorzitter van het College voor Promoties,
in het openbaar te verdedigen op dinsdag 10 oktober 2006 om 12:30 uur

door

Danielle Amanda HORNEMAN

scheikundig ingenieur
geboren te Leiden

Dit proefschrift is goedgekeurd door de promotoren:

Prof. dr. ir. L.A.M. van der Wielen

Prof. dr. ir. J.T.F. Keurentjes

Samenstelling promotiecommissie:

Rector Magnificus	voorzitter
Prof. dr. ir. L.A.M. van der Wielen	Technische Universiteit Delft, promotor
Prof. dr. ir. J.T.F. Keurentjes	Technische Universiteit Eindhoven, promotor
Prof. dr. ir. W. Norde	Wageningen Universiteit
Prof. dr. ir. P.J. Jansens	Technische Universiteit Delft
Prof. dr. ir. G.W.K. van Dedem	Technische Universiteit Delft
Prof. dr. ir. J.H. de Winde	Technische Universiteit Delft
Dr. M.H.M. Eppink	Diosynth/Akzo Pharma

Dr. ir. M. Ottens heeft als begeleider in belangrijke mate aan de totstandkoming van het proefschrift bijgedragen.

Contents

1

Introduction

1.1   Introduction

In most bioprocesses one or more chromatographic steps are used in the purification of the product. Different types of chromatography are possible based on different separation principles. For example affinity chromatography, based on biospecific affinity and ion-exchange chromatography, based on the difference in net charge or distribution of charged groups. In most chromatographic systems, the performance can be optimized in-situ by the proper adjustment of the buffer compositions during adsorption and desorption (Giddings, 1965; Sofer *et al.,* 1997). This is not the case in size-exclusion chromatography. Size-exclusion chromatography (SEC) is based on the difference in size and shape of the components to be separated. It is used for the separation of molecules with a near identical chemical composition such as dimers or oligomers from monomeric products. In SEC, the selectivity is only depending on the volume of the fibers in the gel material and the diameter ratio of the fibers versus the components to be separated (Ogston *et al.*, 1958; Bosma *et al.*, 2000). These parameters cannot be changed in-situ and each specific separation will require a specific gel. Beside this low flexibility, SEC is characterized by a low efficiency due to the limited selectivity of the gel material. High resolution is possible but will result in high eluent and resin consumption, diluted products and long process times, which all will have a negative effect on the costs of the production process (Sofer *et al.*, 1997). There is clearly room for improvements or alternative concepts for this polishing step.

In this thesis an alternative method is proposed which is based on the integration of SEC and a selective mobile phase containing non-ionic micelles. It was demonstrated that the way in which biomolecules and bioparticles partition towards a phase containing non-ionic micelles depends on the same kind of parameters as SEC: the volume of the micelle and the diameter ratio of the micelles and the components to be separated (Liu *et al.,*1994). The main difference with SEC is that the micellar size and shape can be changed in-situ by varying the solution conditions, such as concentration and type of surfactant, temperature and type and concentration of added salts (Evans *et al.,* 1994). In this chapter some background information will be given on SEC in fixed bed as well as in simulated moving bed systems and on the use of non-ionic micelles for the separation of biomolecules and bioparticles. The chapter will conclude with the scope and outline of this thesis

1.2   Size-exclusion chromatography

In size-exclusion chromatography (sometimes also referred to as gel filtration), a column is packed with porous gel particles. These particles consist of fibers and between these fibers pores are formed. Relatively large components do not fit in these pores while

relatively small components can easily enter the pores. When a feed with two different sized components enters the column, both components will travel through the column at different speed (figure 1.1).
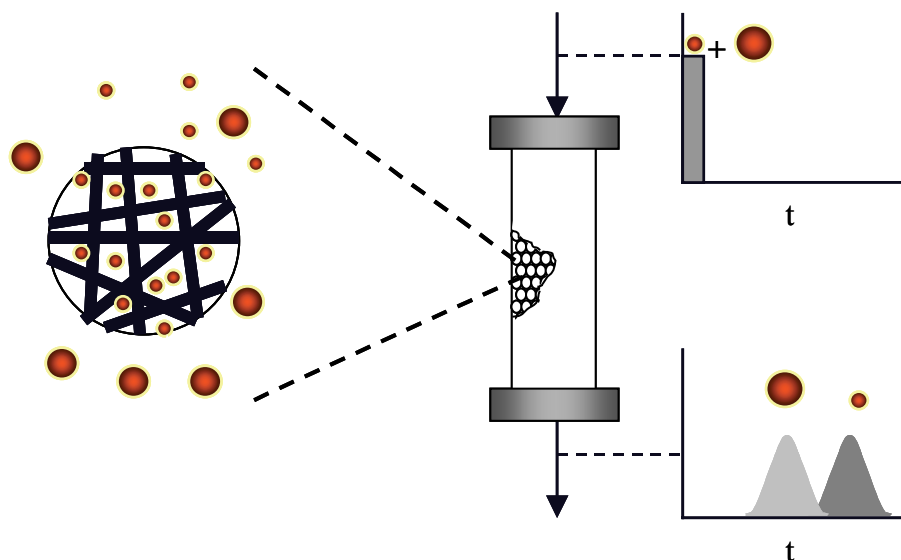

Figure 1.1. *Schematic representation of size-exclusion chromatography*

The distribution and thus the selectivity is depending on the size of the components to be separated, the size of the gel fibers and the volume fraction of the gel-fibres. As too large components are fully excluded and too small components can completely penetrate into the gel particles, SEC has a limited selectivity. As a consequence, only small sample volumes can be handled. This affects the volumetric productivity in a negative manner. For this reason SEC is often used as one of the last purification steps, when the volume that has to be handled has alaready been reduced in the previous steps. Examples of the application of size-exclusion chromatography are the separation of dimers and degradation fragments from monomer recombinant Human Serum Albumin (Berezenco *et al.,* 1996), the application of large scale size-exclusion chromatography in the separation of albumin, IgG and factor IX from plasma (Sofer *et al.,* 1997) and the application of size-exclusion chromatography in the final purification of monoclonal antibodies. A scenario of this last separation is given by Sofer and Hagel (Sofer *et al.,* 1997). This scenario shows that even after the reduction of the starting volume with a factor 16, the size-exclusion chromatography step is still the time limiting step and uses the highest amount of resin volume.

1.2.2   Simulated Moving Bed chromatography

Simulated moving bed chromatography (SMB) is a method that makes more efficient use of the resin by simulating the movement of the resin in the opposite direction of the liquid

flow. In this way continuous separation is possible. The countercurrent operation leads to a very efficient use of the resin material. As a result higher productivity and lower eluent use can be achieved than compared with the conventional fixed bed method. Figure 1.2 gives a simple representation of an SMB and an associated concentration profile. It consists of series of columns in which the liquid and solids move counter currently. The movement of the solids is simulated by moving the columns into the opposite direction of the liquid flow once per switch interval. The solids are always recycled and the liquid can also be recycled depending on the process requirements.
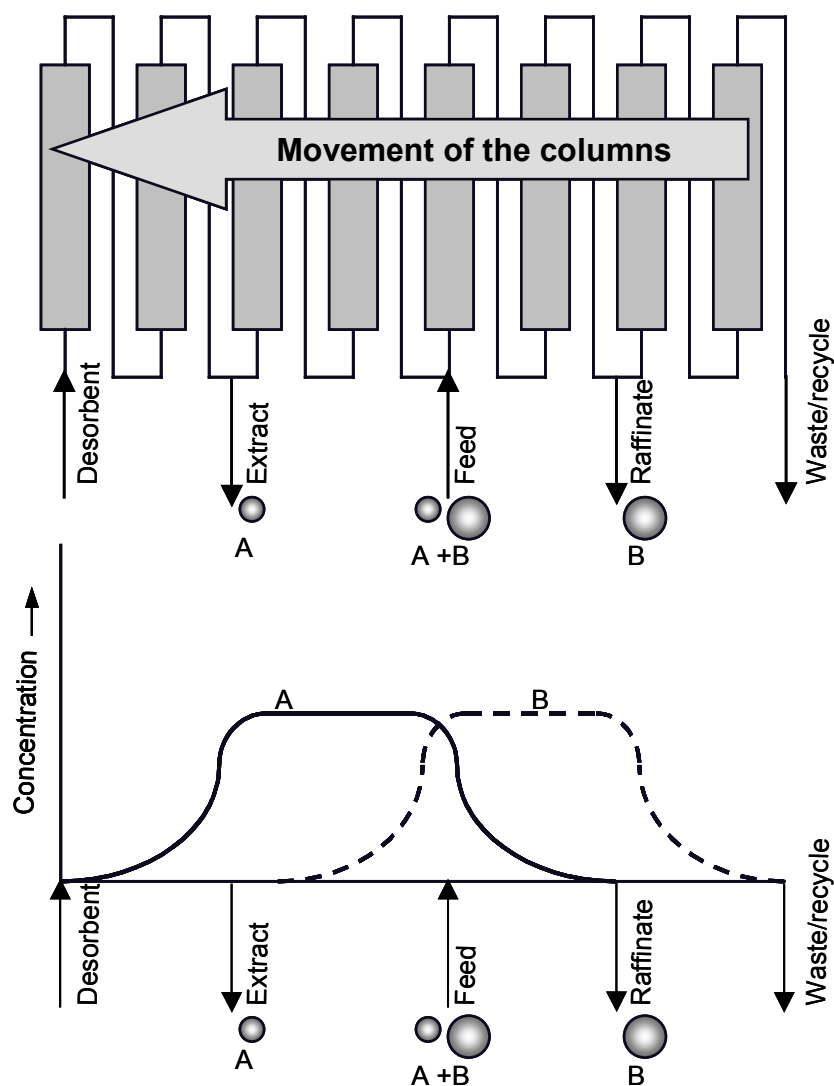
Figure 1.2. *Schematic representation of an SMB. The figure below gives the concentration profiles in the SMB for the separation of two components of different size.*

The feed enters one of the columns in the SMB. In case of size-exclusion chromatography the smaller component will travel slower through the columns than the larger component. By switching the columns before the smaller component reaches the raffinate outlet at the right side of the feeding point this raffinate will only contain the

larger component. The smaller component is moving with the solid phase and is collected at the extract outlet at the left side of the feeding point. Complete separation is possible after proper selection of the liquid flow rates and the simulated solid flow rates.

The first application of SMB described in literature was in the petrochemical industry (Broughton, 1961). Since the last 20 years SMB technology is also more and more used in the fine chemical and pharmaceutical industry. One of the first and also most referred applications is the separation of enantiomers (Pais *et al.,* 1997; Cavoy, *et al.,* 1997; Azevedo *et al.,* 1999). Further, SMB is also used for the separation of amino acids (Walsum *et al.,* 1997), and proteins (Gottschlich *et al.,* 1997; Houwing *et al.,* 2002; Houwing, 2003; Houwing *et al.,* 2003a,). Although SMB technology is applicable for any type of chromatography, only a few studies can be found on SEC in SMB, like the fractionation of dextran polymers (Ruthven *et al.*, 1989) the separation of proteins (Houwing *et al.,* 2003), and multicomponent separations (Mun *et al.,*2003; Ottens *et al.,* 2006). Although SMB can reduce the eluent and resin use in comparison with fixed bed chromatography, SMB does not increase the flexibility or selectivity of SEC.

1.3 Micellar aqueous two phase systems

1.3.1 Micelles

Micelles are self-assembling aggregates composed of surfactant molecules. Surfactants are amphiphilic molecules, which means that they have a hydrophilic part, referred to as the "head" and a hydrophobic part referred to as the "tail". When the surfactant concentration is above the so-called critical micelle concentration (CMC) and above the critical micellar temperature (Krafft temperature) micelles will be formed (Evans *et al.*, 1994). Micelles can be classified by the presence of formally charged groups in its head (Berthod *et al.,* 2000). The head of an ionic surfactant carries a net charge. If the charge is negative, the surfactant is more specifically called anionic; if the charge is positive, it is called cationic. If a surfactant contains a head with two oppositely charged groups, it is termed zwitterionic while non-ionic surfactant has no charge groups in its head.

1.3.2 Aqueous Micellar Two-Phase System (AMTPS)

Upon heating, micellar solutions of most non-ionic surfactants become turbid at a temperature that is known as the cloud point. Above this temperature phase separation takes place. Two phases will be formed; one micellar poor phase and one micellar rich phase. Figure 1.3 shows a typical coexistence curve of a non-ionic surfactant. The region in the curve is the two-phase region. At conditions within this region the micellar solution will separate in a micellar poor and a micellar rich phase. The cloud point is depending on

the molecular structure of the surfactant. For a given non-ionic surfactant the cloud point can be altered by addition of other components like salts or organic compounds (Hinze *et al.*,1993).
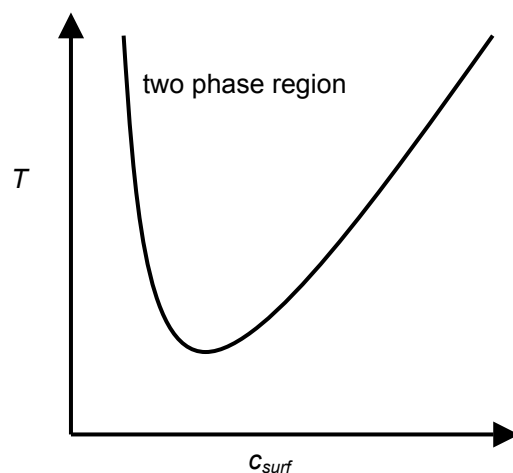

Figure 1.3. *Schematic picture of a coexisting curve of a non-ionic surfactant. At conditions above this curve the micellar solution will separate in two phases.*

1.3.3   Separation using AMTPS

In the first (bio)-application of AMTPS, the separation was not based on the difference in size of the molecules. It was in fact used to separate hydrophobic biomolecules from hydrophilic molecules using the non-ionic surfactant Triton X-114 (Bordier, 1981). The separation is based on the extent of partitioning to the micellar rich phase. This partitioning is dependent on the interaction of the solute of interest and the non-ionic micelle. Hydrophobic proteins will be extracted to the micellar rich phase resulting in high concentration factors for these hydrophobic proteins. This separation method is also called cloud-point extraction. Nowadays cloud-point extraction is still mostly used for the purification of membrane proteins (Hinze *et al.,* 1993; Sanchez-Ferrer, 1994; Saitoh *et al.,* 1995; Tani *et al.,* 1998; Quina *et al.,* 1999,).

This thesis, however deals mainly with the separation of hydrophilic, water-soluble proteins. The first use of AMTPS for this type of separation was described by Blankschtein and coworkers (Nikas *et al*, 1992). There is no attractive interaction between the hydrophilic proteins and the non-ionic surfactant. The distribution of the proteins over the two phases is only depending on the repulsive excluded volume interaction between the micelles and the proteins (Nikas *et. al*., 1992; Liu *et al.,* 1995; Liu *et al.,* 1996). The larger the protein the more it distributes towards the micellar poor

phase as can be seen in figure 1.4. The distribution of the component over the two phases can be influenced by changing the concentration of the micelles or changing the shape or size of the micelles (Liu *et al.*, 1996). The last two characteristics can be changed by altering the type of surfactant, the concentration of salt or the temperature in the system. One of the possible applications is shown by the separation of viruses (bacteriophages) from water-soluble proteins (Liu *et al.,* 1998). At this moment no (industrial) application of AMTPS has been mentioned in literature.
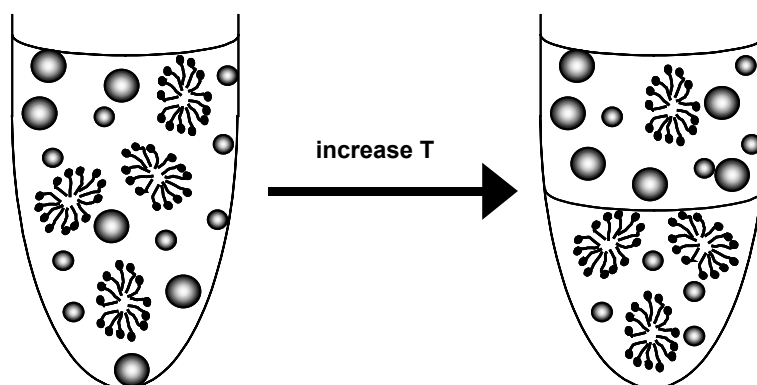

increase T

Figure 1.4. *Schematic representation of the separation of two different sized molecules using an aqueous micellar two-phase system.*

1.4   Scope and outline of this theses

This thesis is part of the STW research project: BIO-separations using Surfactant-Aided gel Filtration Equipment (BIOSAFE, project nr. 790.35.359). The aim of the project was the integration of chromatographic and micellar systems for the purification of relevant biomolecules and biopartcles with increased productivity, selectivity and flexibility. The project was devided in two main research lines:

1. Development and utilization of an integrated gel filtration-micellar system as a chromatographic system for the separation of relevant biomolecules and bioparticles
2. Development of tools for the rational selection of non-ionic surfactants in relation to the components to be separated, solution conditions, control and optimization of the partitioning of biomolecules and bioparticles over gel-micel system

The project was carried out in collaboration with the Eindhoven University of Technology (Ph.D student Dick van Roosmalen, prof. Jos Keurentjes and Dr. Peter van den Broeke). This thesis mainly focuses on the development and utilization of the integrated system

(research line 1) but also some attention is paid to the selection and optimization of such integrated system. In Eindhoven the focus was on the second research line and the results will be presented in the Ph.D. thesis of Dick van Roosmalen.

1.4.1   Outline of the theses

In **chapter 2** the background of surfactant-aided size-exclusion chromatography (SASEC) will be given. Proof of principle will be shown and a model will be presented that predicts the outcome of the experiments performed. In **chapter 3** the design of micellar gradient SMB will be discussed. Using the model presented in chapter 2, the constraints are predicted by this design tool and experimentally verified. **Chapters 4** and **5** will discuss two possible applications of SASEC, viral clearance and the purification of Monoclonal Antibodies. In both examples SASEC is used in fixed bed mode and in SMB mode. **Chapter 6** is the only micellar free chapter of this thesis. It describes the concentration effects of BSA size-exclusion chromatography on the distribution behavior of BSA. The consequences of these concentration effects on fixed bed chromatography and SMB chromatography are discussed. Finally, **chapter 7** provides an outlook on the further application of SASEC and the general requirements of the micelle-gel sytems.

References

Azevedo DCS, Pais, LS, Rodrigues AE. 1999. J. Chromatogr. A. 865: 187-200

Berezenko S, Quirk AV, Wood PC, Woodrow JR, Sleep D, van Urk H, Burton SJ, Stehen J, Goodey AR, Johnson RA. 1996. Patent WO 9637515.

Berthod A, Garcia- Alvarez-Coque, C. 2000. Micellar Liquid Chromatography, Marcel Dekker, New York

Bordier C. 1981. J. Biol. Chem. 256: 1604-1607

Bosma JC, Wesselingh JA. 2000. J. Chromatogr. B 743: 169-180

Broughton DB, Gerhold CG. 1961. US Patent 2985589

Cavoy E, Deltent MF, Lehoucq S, Miggiano D. 1997. J. Chromatogr. 769: 49-57

Das C, Mainwaring R, Langone JJ, 1985. An. Biochem. 45: 27-36

Evans DF, Wennerström H. 1994. The Colloidal Domain, VCH publ., New York.

Felipe X, Law AJR. 1997. J. Dairy research 64: 459-464

Giddings JC. 1965. Dynamics of Chromatography, Marcel Dekker, New York

Gottschlich N, Kasche V. 1997. J. Chromatogr. 765: 201-206

Hinze WL, Pramauro E. 1993 Crit. Rev. Anal. Chem. 24: 133-177

Houwing J, Billiet HAH, van der Wielen LAM. 2003a. AICHE J. 49: 1158-1167

Houwing J, van Hateren SH, Billiet HAH, van der Wielen LAM. 2002. J Chromatogr. A. 952: 85-98

Houwing J. 2003. Separation of proteins by simulated moving bed technology, PhD thesis, Delft University of Technology, Delft

Lazzara MJ, Blankschtein D, Deen WM. 2000 J. Colloid Interface Sc. 226: 112-122

Liu C, Nikas YJ, Blankschtein D. 1995. AIChE J. 41: 991-995

Liu C, Nikas YJ, Blankschtein D. 1996. Biotechnol. Bioeng. 52: 185-192

Liu C, Kamei DT, King JA, Wang DIC, Blankschtein D. 1998. J of Chromatogr, B , 711: 127-138

Liu C, Kamei DT, King JA, Wang DIC, Blankschtein D. 1998. J of Chromatogr, B , 711: 127-138

Mun SY, Xie Y, Kim JH. 2003. Ind. Eng. Chem. Res. 42: 1977-1993

Nikas YJ, Liu C, Srivastava T, Abbot NL, Blankschtein D. 1992. Macromolecules 25: 4797-4806

Ogston G. 1958. Trans Faraday Soc 54:1754-1757

Reuveny S, Lazar A. 1989. Adv. in biotech proc, 11: 45-80.

Ottens M, Houwing J, van Hateren SH, van Balen T, van der Wielen LAM. 2006. Food and Bioproducts processing 84: 59-71

Pais LS, Loureiro JM, Rodrigues AE. 1997. Chem Eng Sci. 52: 245-257

Puvvada, Blankschtein D. 1990. J Chem Phys. 92: 3710-3724

Ruthven DM, Ching CB. 1989. Chem. Eng. Sci. 44: 1011-1038

Saitoh T, Tani H, Kamidate T, Watanabe H. 1995. Trends Anal Chem. 14: 213-217

Sanchez-Ferrer A, Bru R, Garcia-Carmona F. 1994. Crit. Rev. in Biochem. Mol. Biol. 29: 275-313

Sofer G. Hagel L. 1997. Handbook of Process Chromatography, Academic Press.

Tani H, Kamidate T, Watanabe H. 1997. J Chromatogr. 780: 229-241

Tani H, Kamidate T, Watanabe H. 1998. Anal. Sci. 14: 875-888

Van Walsem HJ, Thompson MC. 1997. J. Biotechnol, 59: 127-132

2

Surfactant-Aided Size-Exclusion Chromatography

Abstract

The flexibility and selectivity of size-exclusion chromatography (SEC) for protein purification can be modified by adding non-ionic micelle-forming surfactants to the mobile phase. The micelles exclude proteins from a liquid phase similar to the exclusion effect of the polymer fibers of the size-exclusion resin. This surfactant-aided size-exclusion chromatography technology (SASEC) is demonstrated on the separation of two model proteins; Bovine Serum Albumin (BSA) and myoglobin (Myo). The effect of the added surfactants on the distribution behavior of the proteins is predicted adequately by a size-exclusion model presented in this paper.

Keywords: Micelles, non-ionic surfactants, proteins, size-exclusion chromatography.

2.1 Introduction

Biopharmaceutical products such as biomolecules (hormonal peptides, proteins), and bioparticles (vaccines, viral vectors) have to satisfy extreme purity demands. The purification of molecules with a near-identical chemical composition such as multimers from monomeric products, usually requires costly purification and substantial use of auxiliary materials. In the case of multimer-monomer separation, size-exclusion column chromatography (SEC) is the method commonly used. The selectivity depends on the extent of exclusion of a certain species from uncharged gel particles. Therefore, the key parameters are the porosity of the gel, the degree of cross-linking and the ratio of the diameters of the species to be separated and the diameter of the pores or fibers in the gel.

Because too large species are fully excluded and too small species can completely penetrate the gel particles, this chromatographic column technique has a limited selectivity and a restricted flexibility, as each specific separation requires a specific gel. This is unfortunate, given the relatively high prices of these gel materials. Another limitation is that once a certain gel material is selected, the efficiency of separation can only be improved by reducing the amount to be purified, decreasing the flow or increasing the column length. This affects the volumetric productivity or the product concentration in a negative manner.

Here, we propose an alternative method based on the integration of *non-selective* size-exclusion chromatography and a *selective* mobile phase containing micelles of a specific size. The way in which biomolecules and bioparticles partition towards a phase containing "inert" micelles of nonionic surfactants, depends on the same parameters as in gel filtration chromatography: the volume fraction of micelles and the diameter ratio of solute and micelles (Liu *et al.,* 1998). The larger component will be excluded to a higher extent from the micellar mobile phase than the smaller component, which will elute first. In theory, the gel matrix should act as a practically non-selective "storage" phase for proteins but selectively exclude micelles. Small species elute first, thereby reversing the "normal" chromatographic behavior (figure 2.1).

The average micellar shape and size, and thus the selectivity of the protein separation, can be tuned in-situ by varying the solution conditions, such as concentration and type of surfactants, temperature as well as type and concentration of added salts (Evans *et al.,* 1994). The possibility to vary the solution conditions in-situ adds another degree of freedom to normal SEC. This flexible selectivity makes this method further more suitable for gradient Simulated Moving Bed (SMB) chromatography, which uses the gradient in selectivity to improve the performance of the separation method. It has been shown that

gradient SMB can result in lower solvent consumption and less dilution of the product (Jensen *et al.,* 2000). The analysis of SASEC in SMB technology is not included in this paper.
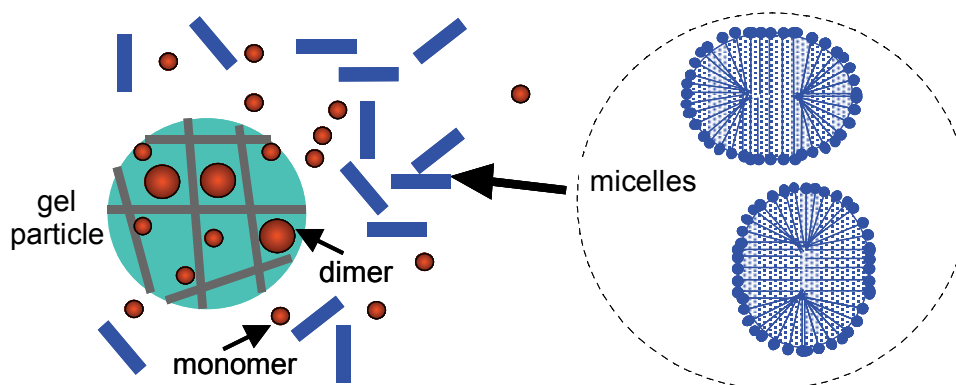

Figure 2.1. *Schematic representation of selective exclusion of large (in this case multimeric) species from the micellar liquid phase in surfactant-aided size-exclusion chromatography.*

The separation described here, is based on the excluded volume interactions between the micelles and the proteins and should not be confused with micellar SEC where attractive interactions between the micelles and proteins are used to increase the selectivity (Herries *et al.,* 1964; Berthod *et al.,* 2000).

The **aim** of this study is to proof the principle of the method described above, and show that micelles can indeed influence the selectivity of size-exclusion chromatography. In this paper we will focus on the influence of the concentration of non-ionic surfactants on the distribution coefficient of proteins. Therefore, pulse experiments on fixed bed gel-filtration are performed with the proteins Bovine Serum Albumin (BSA) and myoglobin (Myo) to determine the distribution coefficients of both proteins as a function of surfactant concentration. The surfactants used in this work are non-ionic alkylpolyoxyethylene glycol ethers. These non-ionic surfactants are used to minimize interactions other than size-exclusion interactions (Nikas *et al.,* 1992).

Furthermore, a model based on excluded volume interactions is presented to predict the influence of micelles on the distribution behavior of proteins.

2.2 Theory

2.2.1 Distribution coefficients in size-exclusion chromatography

The elution of a solute *i* is characterized by its distribution coefficient, K_i, which is defined as the ratio of the solute concentration in the solid phase, $c_{i,s}$, over the solute concentration in the mobile phase, $c_{i,L}$ at equilibrium. Throughout this paper, the solid phase is defined as the total gel volume, including the fibers and the pores of the gel particles.

$$K_i = \frac{c_{i,s}}{c_{i,L}}$$

(2.1)

Relatively large solutes cannot diffuse into the pores and have a *K*-value close to 0, whereas relatively small solutes can diffuse into the pores relatively easily and have higher *K*-values. K_i can be experimentally evaluated by the determination of the experimental elution volume, V_e of a given solute by means of pulse experiments. The elution volume is then normalized to a column-independent distribution coefficient by (Fisher, 1980):

$$K = \frac{V_e - V_0}{V_t - V_0}$$

(2.2)

where V_0 is the volume of the mobile phase in the column and V_t is the total volume of the column.

The distribution coefficient is an important parameter in size-exclusion chromatography. Therefore, many efforts have been undertaken to predict this distribution coefficient from the size and shape of the solute(s) and the size, shape and concentration of the fibers or obstacles (Ogston, 1958; Jansons *et al.,* 1990; Fanti *et al.,* 1990; Wills *et al.,* 1995; Johnson *et al.*, 1996; Lazzara *et al.,* 2000; Bosma *et al.,* 2000). One of the first efforts has been undertaken by Ogston (Ogston, 1958), who has derived a model for the distribution coefficient that is based on the available space fraction for a rigid spherical solute in a random distribution of long fibers. This model is only valid for low solute concentrations and can be written as:

$$K_i = \exp\left(-\phi_f\left(1+\frac{r_i}{r_f}\right)^2\right)$$

(2.3)

where ϕ_f is the volume fraction of fibers in the gel particles and r_i and r_f are the radius of the solute i and the gel fiber, respectively. In this model, the overlap of fibers is neglected. Bosma and Wesselingh (Bosma *et al.,* 2000) extended this model by including the overlap of the fibers:

$$K_i = \exp\left(-\ln\left(\frac{1}{1-\phi_f}\right)\left(1+\frac{r_i}{r_f}\right)^2\right)$$

(2.4)

In many separation processes, more than one single solute and more than one single type of fiber can be present in the system. To describe the steric interactions among these different solutes and fibers, Blankschtein and coworkers (Lazzara *et al.,* 2000) developed a generalized excluded volume model. In this model, all volumes excluded to a solute due to the presence of all types of fibers and solutes, including the solute itself, are calculated in each phase. They derived the following general equation:

$$K_i = \exp\left(-\sum_j \chi_{ij,s} + \sum_j \chi_{ij,L}\right)$$

(2.5)

where the dimensionless number $\chi_{ij,k}$ is the total excluded volume of solute i and a set of objects j per volume of phase k and is defined as:

$$\chi_{ij,k} = x_{j,k} U_{ij,k}$$

(2.6)

Where $x_{j,k}$ is the number concentration of component j in phase k (#/m^3) and $U_{ij,k}$ is the excluded volumes between i and j in phase k. The excluded volume of two convex particles can be calculated by the following general expression (Jansons *et al.,* 1990; Fanti *et al.,* 1990; Wills *et al.,* 1995; Johnson *et al.*, 1996; Lazzara *et al.,* 2000):

$$U_{ij} = V_i + \frac{S_i H_j + S_j H_i}{4\pi} + V_j$$

(2.7)

where V_i, S_i and H_i are the volume, the surface area and the integral of the mean curvature of component i, respectively. With this expression, it is possible to calculate the excluded volume between two convex objects of any shape or size.

The distribution coefficient of a spherical solute in SEC with only one type of fiber can now be calculated using equations 2.5 to 2.7. Assuming that the length of the fibers is substantially larger than the fiber radius, i.e. $l_f >> r_f$, the distribution coefficients becomes:

$$K_i = \exp\left(-\phi_f\left(1+\frac{r_i}{r_f}\right)^2 - \left(\phi_{i,s}-\phi_{i,L}\right)\left(1+\frac{r_i}{r_i}\right)^3\right)$$

(2.8)

where ϕ_i is the volume fraction of the solute i. The first term in the exponent on the right hand side of equation 2.8 describes the steric interactions between the fiber and the protein in the solid phase. The second term describes the steric self-interaction among the protein molecules themselves in the solid and liquid phase. For dilute protein solutions, the second term can be neglected and equation 2.8 equals the well-known Ogston relation (eq. 2.3).

2.2.2   Surfactant-aided size-exclusion chromatography

To describe the retention behavior of a single protein in surfactant-aided SEC (SASEC), 3 components are present: the protein (1), the fiber (2) and the micelle (3). Only the micelles and the protein can be present in both phases (solid phase and liquid phase). Using equation 2.5, the distribution coefficient of the protein now becomes:

$$K_1 = \exp\left(-\chi_{11,s} - \chi_{12,s} - \chi_{13,s} + \chi_{11,L} + \chi_{13,L}\right)$$

(2.9)

For dilute protein solutions, the parameters $\chi_{11,s}$ and $\chi_{11,L}$ can be neglected because the excluded volume due to the presence of protein molecules is relatively small compared to the total accessible volume. To calculate the excluded volume for proteins due to the presence of micelles, the size and shape of the micelles has to be known. This can be predicted by using a molecular-thermodynamic model of micellization (Puvvada *et al.,* 1990; Nagarajan *et al.,* 1991). Puvvada and Blankschtein only studied alkylpolyoxyethylene glycol ethers with a relatively short polyoxyethylene chain as the hydrophilic head group and regarded this as a compact head group. This approach does not give satisfactory results with respect to the size prediction when the polyoxy-ethylene chain consists of more than 8 oxy-ethylene units. For these large polyoxyethylene chain lengths, the head group is regarded as a polymeric chain (Nagarajan *et al.,* 1991). The micelle is then modeled as a hydrophobic core surrounded by a coronal a polymer solution consisting of polyoxyethylene chains (figure 2.2). Both models predict micelles formed by the surfactants used in this study ($C_{12}E_{23}$ and $C_{16}E_{20}$) to be globular and not cylindrical. For spherical micelles, the radius of the micelles is taken as the sum of the radius of the hydrophobic core and the thickness of the hydrophilic corona. The radius of

the hydrophobic core can be estimated from the hydrocarbon chain length of the surfactant. The extended hydrocarbon tail length is the maximum possible length of the chain and can be calculated by (Tanford, 1980):

$$l_{max} = 1.5 + 1.265(n_c - 1) \qquad (2.10)$$

where n_c is the number of carbon atoms in the hydrocarbon chain. Hydrocarbon chains in the liquid state are not fully extended and thus the hydrocarbon tail length is always smaller than the extended tail length. For $C_{12}E_{23}$ the hydrocarbon tail length is estimated to be about 75 % of the extended hydrocarbon tail length (Tanford *et al.,* 1977, Tanford, 1980) and for $C_{16}E_{20}$ the length is estimated to be about 62% of the extended hydrocarbon tail length (Tanford *et al.,* 1977).
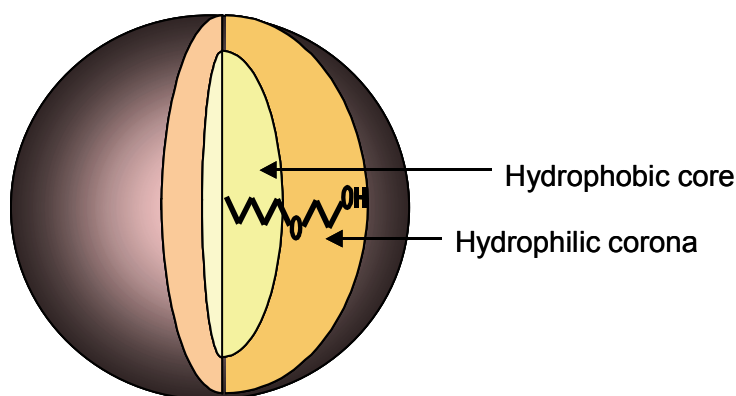

Figure 2.2. *Schematic representation of a spherical micelle with a hydrophobic core and a hydrophilic corona.*

In this study, the thickness of the hydrophilic corona is taken from the simulation results of Nagarajan (Nagarajan *et al.,* 1991), which corresponds with experimental work of Tanford (Tanford *et al.,* 1977). From the study of Tanford can be deduced that the hydrophobic core cannot be a perfect sphere when the micelles are formed by one of the two surfactants used in this study, as there is simply not enough space in the spherical core to contain all the hydrophobic tails (Tanford *et al.,* 1977). Therefore, the hydrophobic core must have an oblate shape. An oblate micelle is defined by three semi-axes r_m, r_m and $\eta_m r_m$ where $\eta_m < 1$. The semi-axes r_m and $\eta_m r_m$ are assumed to be 4.13 nm and 3.66 nm for $C_{12}E_{23}$ and 4.69 nm and 3.77 nm for $C_{16}E_{20}$ (Tanford, 1980). The distribution

coefficient of a spherical solute (dilute solution) now becomes (Jansons *et al.,* 1990; Lazzara *et al.,* 2000):

$$K_i = \exp\left(\frac{-\ln\left(\frac{1}{1-\phi_f}\right)\left(1+\frac{r_i}{r_f}\right)^2 - (\phi_{m,s} - \phi_{m,L}) \cdot}{\left(1+\frac{1}{\eta_m}\left(\frac{r_i}{r_m}\right)^3 + \frac{3}{2}\left(\frac{r_i}{r_m}\right)^2 \frac{g(\eta_m)}{\eta_m} + \frac{3}{2}\left(\frac{r_i}{r_m}\right)\frac{f(\eta_m)}{\eta_m}\right)}\right)$$

$$f(\eta_m) = 1 + \eta_m^2 \left(1 - \eta_m^2\right)^{-1/2} \cosh^{-1}\left(\eta_m^{-1}\right) \tag{2.11}$$

$$g(\eta_m) = \eta_m + \left(1 - \eta_m^2\right)^{-1/2} \cos^{-1}\left(\eta_m\right)$$

2.3   Materials and Method

2.3.1   Equipment

The pulse experiments were performed on an FPLC system, controlled by Unicorn version 2.01 (Amersham Pharmacia Biotech Benelux). The concentration of the proteins in the outlet of the column was determined on-line by a spectrophotometer at two different wavelengths (280 nm and 405 nm). During the break-through experiments, the concentration of the surfactants was measured on-line at 206 nm. The density of the eluent was also determined in all experiments.

2.3.2   Column

An XK16 column from Pharmacia Biotech was used in the system. The column was packed with Sephacryl^{TM} S300 HR (Amersham Biosciences BV, cat no. 17-0599-01) up to a height of 7 cm. The volume fraction of the gel fibers, ϕ_f, has been determined with salt pulses. Small salt molecules (NaCl) can diffuse into all the pores of the gel. The difference between the elution volume of NaCl and the geometrical volume of the column gives the volume of the gel fibers. A value of 0.08 was found for this gel, the radius of the gel fiber, r_f was assumed to be 1.5 nm. This assumption has been made by fitting known distribution coefficients of calibration proteins (data provided by Amersham Pharmacia Biotech) to the Ogston equation (equation 2.4). The dead volume of the system (total volume between injection point and spectrophotometer minus the column volume itself) is determined by pulses of dextran blue and BSA. The void volume of the packed column is determined by dextran blue pulses.

2.3.3   Experiments

Pulses of 0.5 ml containing 10 g/l BSA (Sigma, cat no A 7906) or 1.5 g/l Myo from horse heart (Sigma cat no. M18882, > 90% pure) in a surfactant-buffer solution were injected. In all experiments, a 10 mM phosphate buffer, pH 6.8 containing 0.1 M NaCl and a known concentration of surfactant was used as eluent. The surfactants used in these experiments were the non-ionic surfactants $C_{12}E_{23}$ (Acros organics, cat no 228345000) and $C_{16}E_{20}$ (Acros organics, cat no 344295000). Various surfactant concentrations between 0 and 20% (w/w) were used in the eluent. In order to determine the distribution coefficient of the surfactants, break-through curves of the surfactants were measured at the different surfactant concentrations.

2.4   Results and discussion

2.4.1   Distribution coefficients of BSA and Myo as function of surfactant concentration; experimental results

The pulse response curves already show the effect of the presence of micelles on the elution behavior of the proteins. Figure 2.3 shows some examples of the pulse response curves measured in the BSA-$C_{12}E_{23}$ systems. As expected, it shows an increase in elution volume of BSA with increasing surfactant concentration. From these measured pulse response curves the distribution coefficients of the protein have been determined, using equation 2.2, where the elution volume is the volume corresponding to the peak of the pulse response curve. The elution volume and the void volume are both corrected for the dead volume of the system. The results of these calculations can be seen in figure 2.4, which shows the distribution coefficient as function of the surfactant concentration. The protein distribution coefficient increases with increasing surfactant concentration, which indicates that the proteins are indeed excluded to a higher extent from the mobile phase into the gel phase at higher surfactant concentration. The micelles formed by the two different surfactants, $C_{12}E_{23}$ and $C_{16}E_{20,}$ have about the same size and shape but differ in hydrophobicity. Figure 2.4 shows that there is no significant difference in distribution coefficients of the proteins between the two different micelle-gel systems. This indicates that the effect on the distribution coefficient is indeed mainly determined by the size and shape of the micelle.
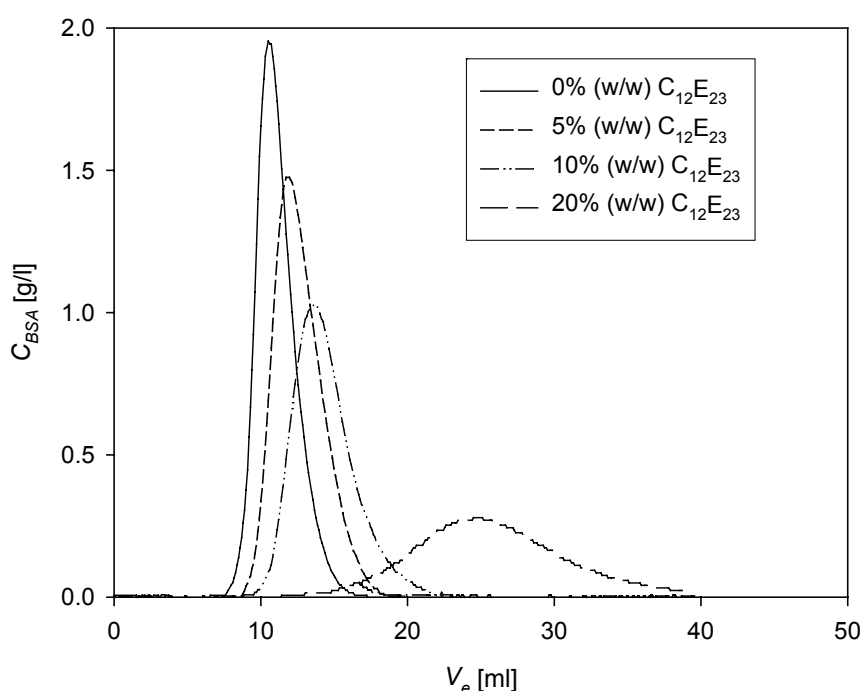
Figure 2.3. *Pulse response curves of BSA at different concentrations of $C_{12}E_{23}$. $C_{BSA,F}$ = 10 g/l, pulse volume = 0.5 ml.*

Figure 2.4 also shows that in this case a selective gel has been used. The distribution coefficients of BSA and MYO at 0% (w/w) of surfactant are less than unity and BSA has a smaller distribution coefficient than Myo. Increasing the surfactant concentration has, however, a larger influence on the distribution coefficient of BSA than of Myo. The distribution coefficient of BSA changes from 0.39 at 0% (w/w) up to 2 at a concentration of 20% (w/w) of $C_{12}E_{23}$, while the distribution coefficient of Myo only changes from 0.6 up to 1.5 in the same concentration range. This difference of influence on two different sized proteins proves that changing the surfactant concentration in the mobile phase can change the selectivity of SEC. The ability to change the selectivity in-situ, improves the flexibility of this separation method.

The data further show that introducing micelles in the mobile phase increases the distribution coefficients of the proteins beyond the normal range found in SEC, i.e. between 0 and 1. Values of K_{BSA} up to 2 can be achieved at a concentration of 20% (w/w) of $C_{12}E_{23}$.
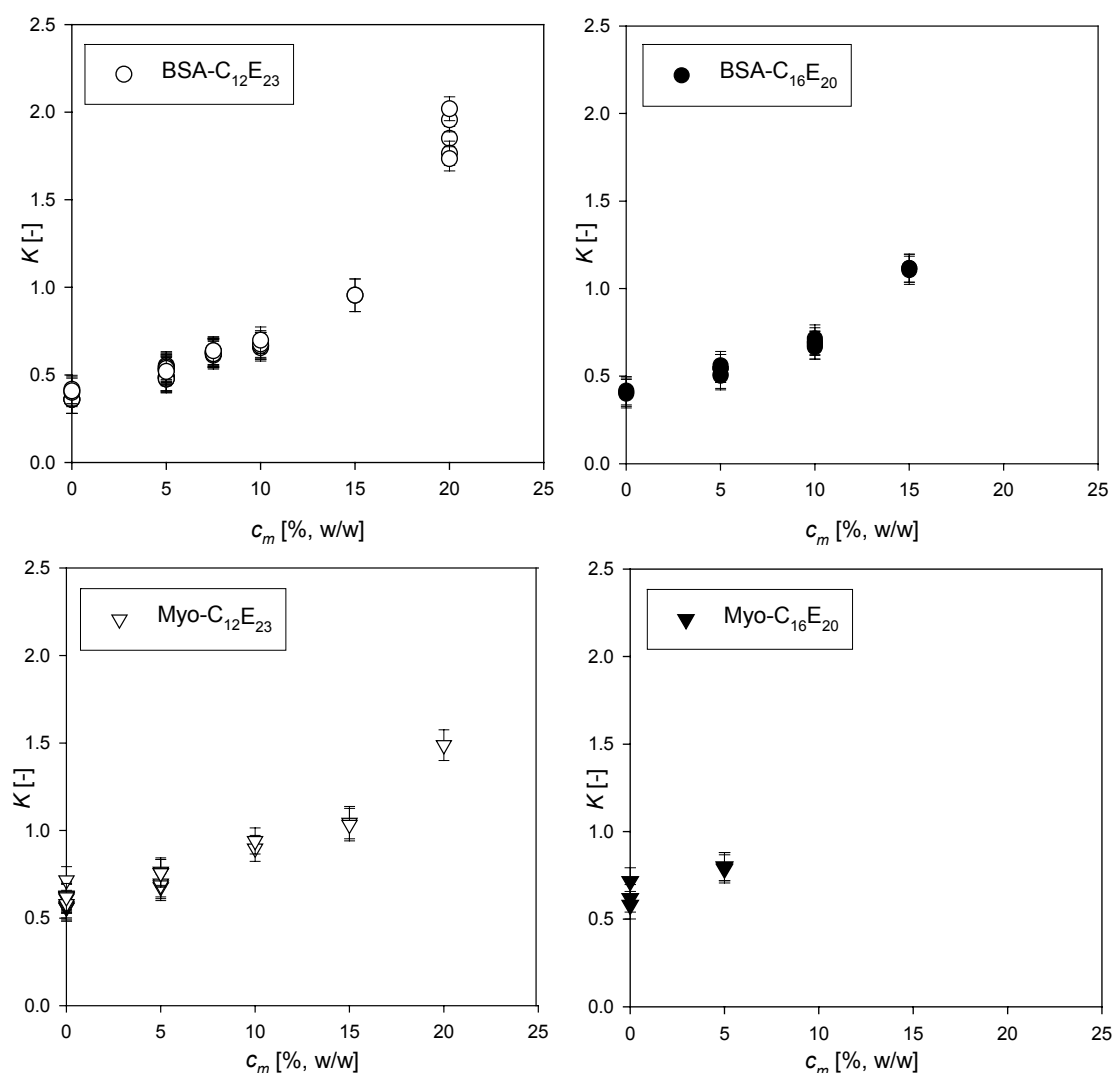
Figure 2.4. *Distribution coefficients of BSA (circles) and myoglobin (triangles) as function of surfactant concentration, for the two tested surfactants $C_{12}E_{23}$ and $C_{16}E_{20}$.*

2.4.2 Distribution coefficients of the micelles, experimental and model results.

The distribution of the micelles into the solid phase has to be known before any prediction can be made of the distribution coefficient of the proteins. Figure 2.5 shows the experimentally determined distribution coefficients of the surfactants. It shows an increase in K-values at increasing surfactant concentration. Thus also the micelles themselves are more excluded from the mobile phase into the solid phase at higher surfactant concentrations. Using equations 2.5 to 2.7, the distribution coefficients of the micelles can be predicted. To do so, all experimentally determined weight fractions were recalculated to volume fractions by:

$$\phi_{in} = \frac{w_{in}\,\rho\,N_{av}}{M_w N} V_m \qquad\qquad (2.12)$$

where w_{in} is the mass fraction of the micelles in the eluent, ρ is the density of eluent, M_w is the molar mass of one surfactant molecules, N is the aggregation number of the micelle (the number of surfactant molecules per micelle) and V_m is the volume of a micelle. The aggregation number of $C_{12}E_{23}$ and $C_{16}E_{20}$ are 50 and 70 respectively (Nagarajan *et al.,* 1991).

The model prediction (equations 2.5-2.7) of the distribution coefficients is represented as a line in figure 2.5. The model prediction is in good agreement with the experimentally determined distribution coefficients of the surfactants and is therefore used in the further calculations.
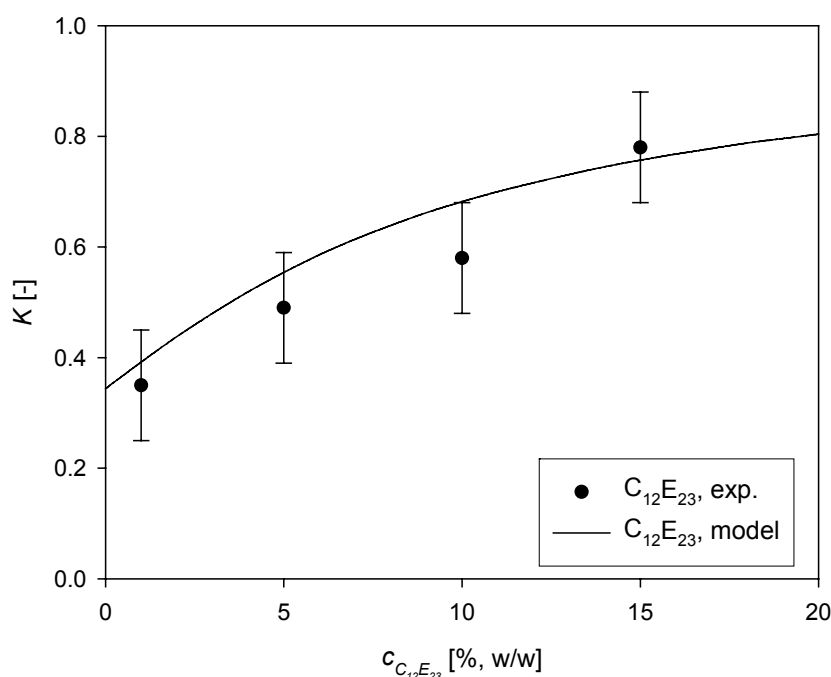
Figure 2.5.   *Comparison between the model predictions of the distribution coefficient of $C_{12}E_{23}$ and the experimentally found values as function of the concentration of $C_{12}E_{23}$.*

2.4.3   Distribution coefficients of the proteins as function of surfactant concentration; modeling results.

Equation 2.11 is now used to predict the distribution coefficient of BSA and Myo as function of the concentration of surfactant in the mobile phase. Figures 2.6 and 2.7 compare the predicted *K*-values with the average of the experimentally found K-values

using $C_{16}E_{20}$ and $C_{12}E_{23}$ as surfactant.

Figure 2.6. *Comparison between the model predictions of the distribution coefficients of BSA and Myo using equation 2.11 and the average of the experimentally found K-values for BSA and Myo as function of the concentration of $C_{12}E_{23}$.*
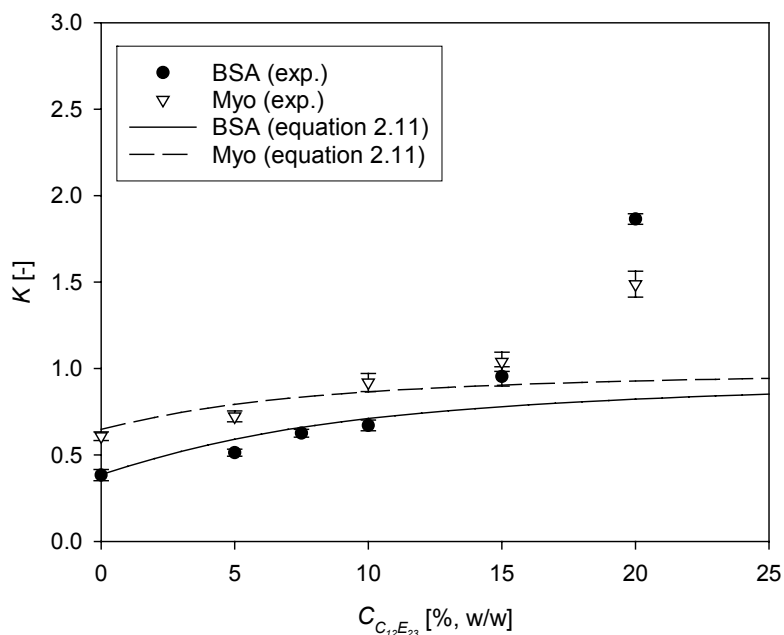

Figure 2.7. *Comparison between the model predictions of the distribution coefficients of BSA and Myo using equation 2.11 and the average of the experimentally found K-values for BSA and Myo as function of the concentration of $C_{16}E_{20}$.*
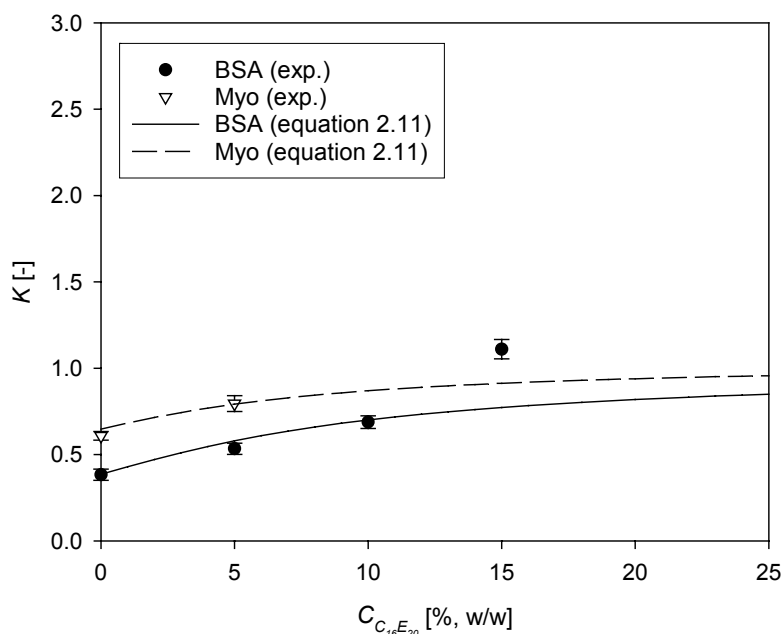
Up to a concentration of 10% (w/w) of surfactant in the mobile phase, the model predictions are in good agreement with the experimental results. At higher concentrations, the model predicts that the distribution coefficient of the proteins is becoming almost constant, while the experimental data show a further increase of the distribution coefficients at higher concentrations of surfactant.

The model described by equation 2.11 does not take into account the possible overlap of the micelles at high concentrations. The excluded volume for the proteins, due to the presence of the micelles, will be underestimated by this model. The distribution coefficient of micelles levels off (figure 2.5), which means that the concentration ratio of the micelles in the mobile and the solid phase becomes constant. The concentration difference between the two phases thus increases with increasing surfactant concentration. This will cause a higher driving force and the protein will distribute more into the solid phase, than predicted without fiber overlap.

At low surfactant concentrations this overlap can be neglected but at higher concentrations the overlap will influence the distribution behavior of the other solutes (Lazarra, Blankschtein and Deen, 2000). In the same way as the original Ogston relation was extended for fiber overlap, the model described here can be extended for the overlap of the micelles (Bosma and Wesselingh, 2000; Lazarra, Blankschtein and Deen, 2000). Equation 2.11 than becomes:

$$
K_i = \exp\left(
\begin{array}{l}
-\ln\left(\dfrac{1}{1-\phi_f}\right)\left(1+\dfrac{r_i}{r_f}\right)^2 - \\[2ex]
\left(\ln\left(\dfrac{1}{1-\phi_{m,s}}\right) - \ln\left(\dfrac{1}{1-\phi_{m,L}}\right)\right)\cdot \\[2ex]
\left(1+\dfrac{1}{\eta_m}\left(\dfrac{r_i}{r_m}\right)^3 + \dfrac{3}{2}\left(\dfrac{r_i}{r_m}\right)^2\dfrac{g(\eta_m)}{\eta_m} + \dfrac{3}{2}\left(\dfrac{r_i}{r_m}\right)\dfrac{f(\eta_m)}{\eta_m}\right)
\end{array}
\right)
\tag{2.13}
$$

Figures 2.8 and 2.9 compare the results of equation 2.13 with the experimental data. The prediction of the distribution coefficient of BSA and Myo is now in good agreement with the experimental results. Even better results may be achieved when other interactions between the micelles and proteins are incorporated in the model besides the steric interactions. The associated increase in model complexity should be balanced against the increase in model accuracy.
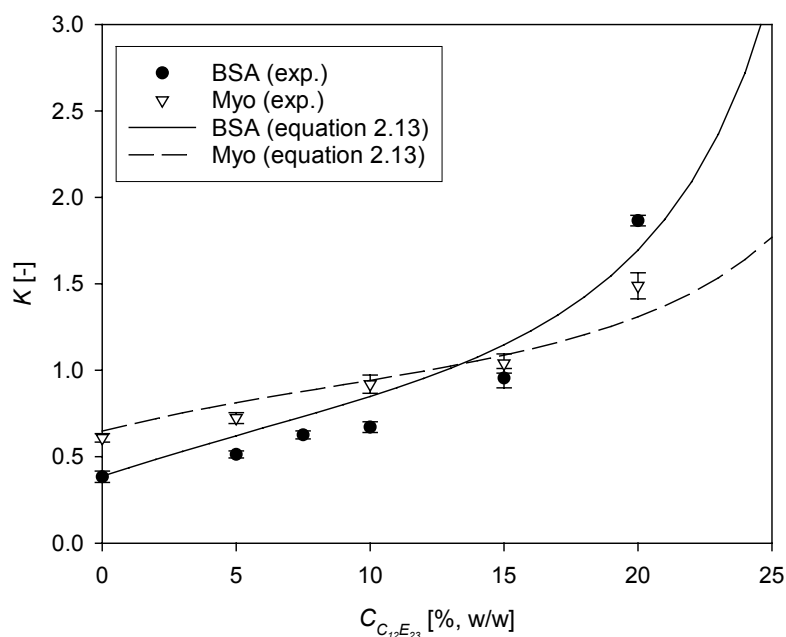
Figure 2.8. Comparison between the model predictions of the distribution coefficients of BSA and Myo using equation 2.13 and the average experimentally found K-values for BSA and Myo as function of the concentration of $C_{12}E_{23}$.
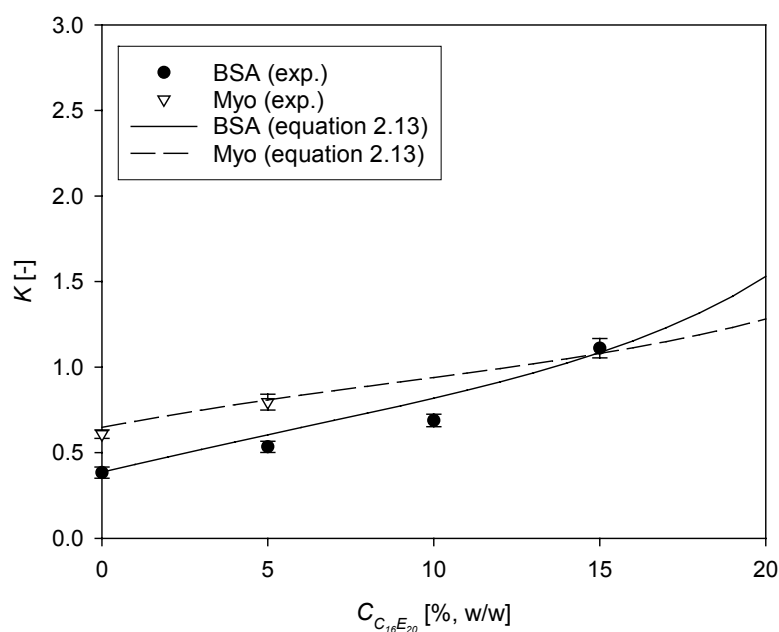
Figure 2.9. Comparison between the model predictions of the distribution coefficients of BSA and Myo using equation 2.13 and the average experimentally found K-values for BSA and Myo as function of the concentration of $C_{16}E_{20}$.

2.4.4 Future Outlook

The case described in this paper shows the ability to change the selectivity in-situ by using SASEC. Using the chosen combination of gel and surfactant for the separation of BSA and Myo is probably not the best choice for applying this SASEC method in fixed bed chromatography. The gel is still selective, which means that first a certain threshold concentration of surfactant should be reached before improvement of the selectivity will occur. Figure 2.4 shows that at about 15% (w/w) the elution behavior of normal SEC is reversed. At higher surfactant concentrations the selectivity will improve. To improve the selectivity at lower surfactant concentrations ($\phi_{m,s}$ - $\phi_{m,L}$) should be increased and/or r_m should be decreased (see eq. 2.13). This is possible by using for example long cylindrical micelles with a small diameter. Long cylindrical micelles will have a lower distribution towards the solid phase compared to spherical micelles. This will results in a higher values for ($\phi_{m,s}$ - $\phi_{m,L}$).

An improvement of selectivity is not even necessary when gradient simulated moving bed chromatography (gradient-SMB) is used (Jensen *et al.,* 2000, Houwing *et al.,* 2002). Normal SMB can already reduce resin and eluent consumption and maintain a high product concentration at the same time. With gradient-SMB the resin and eluent consumption can be further reduced and even more concentrated products can be reached. Another advantage of using SMB-chromatography is that the surfactants can be separated from the product in the same unit operation, if necessary (this doesn't have to be necessary as some surfactants are being used in industrial practice to formulate the end product).

2.5 Conclusions

The elution time, and thus the distribution coefficient of a protein, during size-exclusion chromatography is increased by using nonionic surfactants above their CMC in the mobile phase. This increase is different for proteins of different sizes, what implies that changing the surfactant concentration in the mobile phase changes the selectivity of the separation in-situ. The ability of changing the selectivity makes SASEC more flexible than the conventional SEC for protein purification and will probably decrease the size of SEC equipment and reduce the eluent consumption.

The model presented in this paper is based solely on the excluded volume interactions between the proteins, micelles and the fibers. It does describe qualitatively the influence of non-ionic micelle-forming surfactant on the distribution of proteins. An even more accurate description of the behavior may be achieved when other interactions between

the micelles and proteins are incorporated in the model besides the steric interactions. The associated increase in model complexity should be balanced against the increase in model accuracy.

Nomenclature

$c_{i,k}$	concentration of solute i in phase k
K_i	distribution coefficient of component i
l_{max}	extended hydrophobic tail length
H_i	integral of mean curvature of component
N_{av}	Avogadro number
M_w	molecular weight
N	aggregation number
n_c	number carbon atoms in hydrocarbon tail
r_i	radius of component i
S	selectivity
S_i	surface area of component i
U_{ij}	excluded volume between components i and j
V_e	elution volume
V_i	volume of component i
V_0	void volume
V_t	total volume of column
x_i	number concentration of component i
$\eta_m r_m$	semi-axis of globular micelle
ρ	density
ϕ_i	volume fraction of component i
χ_{ij}	steric interaction parameter between components i and j

Sub and superscripts

f	gel fiber
s	solid phase
m	micelle
L	liquid phase

References

Berthod A, Garcia-Alvarez_Coque C. 2000. Micellar liquid chromatography, Chromatographic Science Series 83, Marcel Dekker, New York

Bosma JC, Wesselingh JA. 2000. J. Chromatogr. B 743: 169-180

Evans DF, Wennerström H. 1994. The Colloidal Domain, VCH publ., New York

Fanti LA, Glandt ED. 1990. J. Colloid Interface Sc. 135: 385-395

Fisher L. 1980. Gel filtration Chromatography, Elsevier/North-Holland, Amsterdam

Herries DG, Richards FM, Bishop W. 1964. J. Phys. Chem. 68: 1842-1853

Houwing J, van Hateren SH, Billiet HAH, van der Wielen LAM. 2002. J Chromatogr. A. 952: 85-98

Jansons KM, Phillips CG. 1990. J Colloid Interface Sc. 137: 75-91

Jensen TB, Reijns TGP, Billiet HAH, van der Wielen LAM. 2000. J. Chromatogr. A 873: 149-162

Johnson EM, Deen WM. 1996. J Colloid Interface Sc. 178: 749-756

Lazzara MJ, Blankschtein D, Deen WM. 2000. J. Colloid Interface Sc. 226: 112-122

Liu C, Kamei DT, King JA, Wang DIC, Blankschtein D. 1998. J. Chromatogr. B, 711: 127-138

Nagarajan R, Ruckenstein E. 1991. Langmuir 7: 2934-2969

Nikas YJ, Liu C, Srivastava T, Abbot NL, Blankschtein D. 1992. Macromolecules 25: 4797-4806

Ogston G. 1958. Trans Faraday Soc 54:1754-1757.

Puvvada S, Blankschtein D. 1990. J Chem Phys 92: 37103724

Tanford C, Nozaki Y, Rhode MF. 1977. J Phys Chem 81: 1555-1560

Tanford C. 1980. The Hydrophobic Effect Formation of Micelles and Biological Membranes, Wiley, New York

Wills PR, Georgalis Y, Dijk J, Winzor DJ. 1995. Biophysical Chem 57: 37-46

3

Micellar gradients in size-exclusion simulated moving bed chromatography

Abstract

The selectivity of size-exclusion chromatography (SEC) can be modified by adding non-ionic micelles to the mobile phase. Surfactant-aided size-exclusion chromatography (SASEC) can therefore very well be performed in a gradient mode on a simulated moving bed (SMB), as is reported in this paper. A method has been developed for correctly positioning a micellar gradient over an SMB. The method is applied for size-exclusion chromatography with the non-ionic surfactant $C_{12}E_{23}$ as gradient forming solute, and demonstrated by applying it to a relevant chromatographic protein separation problem.

Keywords: Bioseparation, protein purification, simulated moving bed, size-exclusion chromatography, surfactants, gradient elution, chromatography

3.1   Introduction

Size-exclusion chromatography (SEC) is a method commonly used for the purification of near identical biopharmaceutical products such as biomolecules (hormonal peptides, proteins), and bioparticles (vaccines, viral vectors). The selectivity depends on the difference of exclusion of various species in a mixture from uncharged gel particles. Therefore, the key parameters are the porosity of the gel, the degree of cross-linking and the characteristic dimensions of the species to be separated and the pores or fibers in the gel. Each gel has a specific selectivity for each specific separation. This selectivity cannot be changed once the gel material has been chosen, making SEC a technique with a limited flexibility.

As surfactants are often part of the last stage in the protein purification step (formulation), they constitute an ideal candidate as modifier for selectivity during SEC. In surfactant-aided size-exclusion chromatography (SASEC), adding non-ionic surfactants to the mobile phase results in increasing distribution coefficients of the solutes to be separated (Horneman *et al.,* 2004; Roosmalen *et al.,* 2004; Horneman *et al.,* 2004a). The way in which biomolecules and bioparticles partition towards the mobile phase containing "inert" micelles of nonionic surfactants, depends on additional parameters when compared to 'normal' size-exclusion chromatography: the volume fraction of micelles, the specific dimensions of the micelles (the modifying solutes) and the specific dimensions of the solutes to be separated (the target solutes) (Liu *et al.,* 1998; Horneman *et al.,* 2004; Roosmalen *et al.,* 2004; Horneman *et al.,* 2004a). The average micellar shape and size, and thus the distribution coefficients of the target solutes can be tuned in-situ by varying the solution conditions, such as concentration and type of surfactants, temperature as well as type and concentration of added salts (Evans *et al.,* 1994). The selectivity can now be changed in-situ by changing the solution conditions. This makes SASEC more flexible than normal SEC. It makes SASEC also interesting for gradient simulated moving bed (SMB) technology (Jensen *et al.,* 2000 and 2000a; Houwing *et al.,* 2002, 2002a and 2003; Abel *et al.,* 2002 and 2004).

SMB chromatography is a counter-current continuous separation technology. A continuous feed is fractionated in two or more product streams as can be seen in 0. The more retained product will move with the solid flow towards the extract outlet, whereas the less retained product will move with the liquid flow towards the raffinate outlet. The main advantages of SMB are the reduced solvent and solid consumption compared to the discontinuous fixed bed technology. The solvent consumption can be further reduced in a closed loop SMB. In that case the outcoming liquid of section IV is (partly) recycled to the desorbent (dotted line in 0). In pharmaceutical production, however, a closed loop is not always an option due to the risk of back contamination.

Gradient SMB can further improve the performance of the separation (Jensen *et al., 2000* and 2000a). Gradient SMB uses a variation in the distribution coefficients of the target solutes. A relatively low distribution coefficient in sections I and II facilitates the elution of the target solute whereas a relatively high distribution coefficient in sections III and IV increases the loading capacity of the solids. As a result, less solvent is needed and the throughput can be increased. Another result is that higher product concentrations can be achieved in gradient SMB (Jensen *et al., 2000*).

The variation of distribution coefficients over SMB systems can be established by different types of gradients; temperature gradients (Migliorini *et al.,* 2001), pressure gradients (Denet *et al.,* 2001; Di Giovanni *et al.,* 2001), solvent gradients (Jensen *et al.,* 2000 and 2000a; Antos *et al.,* 2001 and 2002; Abel *et al.,* 2002 and 2004) where the solvent is *not adsorbable* to the solid phase and solute gradients where the modifying solute is *adsorbable* to the solid phase (Houwing *et al.,* 2002, 2002a and 2003). The last type of gradient requires a more complicated flow selection procedure in order to direct the solute gradient in the correct position (Houwing *et al.,* 2002 and 2003).

Size-exclusion chromatography in SMB has gained an increased interest in the purification of biotechnology products but so far, it is only used in an isocratic mode (Houwing *et al.,* 2003a; Mun *et al.,* 2003; Geisser *et al.,* 2005). With SASEC, a micellar gradient can be used in the SMB. The principle of SASEC has been described and experimentally proven in a previous paper using fixed bed chromatography (Horneman *et al.,* 2004). It was found that the distribution coefficient of the tested proteins was increased with increasing micelle concentration. Also the distribution coefficient of the micelles was influenced by the micelle concentration. In order to use SASEC in gradient SMB, a flow selection procedure to position the micellar gradient in the SMB is needed. This kind of flow selection procedure has been described for salt gradients in ion exchange chromatography (Houwing *et al.,* 2002 and 2003). This paper will further extend this procedure for positioning a micellar gradient in an open loop SEC-SMB. The procedure is verified with several gradient-positioning experiments. The effects of micellar gradients on the area of separation are discussed. Finally, the potential of the separation technique is demonstrated for a relevant pharmaceutical separation, which is the separation of the monoclonal IgG from its dimer.

3.2 Theory

3.2.1 Isotherm of the micelles

Non-ionic micelles show a partitioning behavior towards the solid gel phase. To correctly position the gradient, this partition behavior has to be known. The distribution coefficient of the non-ionic micelles was determined as function of the micelle concentration (Horneman *et al.,* 2004). It was found that the distribution coefficient of an arbitrarily shaped solute *i* can be described by the excluded volume theory (Lazzara *et al.,* 2000; Horneman *et al.,* 2004):

$$K_i = \exp\left(-\sum_j \chi_{ij,s} + \sum_j \chi_{ij,L}\right) \tag{3.1}$$

where the dimensionless number $\chi_{ij,k}$ is the total excluded volume of solute *i* and a set of objects *j* per volume of phase *k* and is defined as:

$$\chi_{ij,k} = x_{j,k} U_{ij,k} \tag{3.2}$$

where $x_{j,k}$ is the number concentration of component *j* in phase *k* (#/m^3) and $U_{ij,k}$ is the excluded volumes between *i* and *j* in phase *k*. The excluded volume of two convex particles can be calculated by the following general expression (Jansons *et al.,* 1990; Lazzara *et al.,* 2000):

$$U_{ij} = V_i + \frac{S_i H_j + S_j H_i}{4\pi} + V_j \tag{3.3}$$

where V_i, S_i and H_i are the volume, the surface area and the integral of the mean curvature of component *i,* respectively. With this expression, it is possible to calculate the excluded volume of two convex objects of arbitrary shape or size. Thus in case of non-ionic micelles in SEC, the distribution coefficient of these micelles can be calculated by:

$$K_m = \exp\left(-\chi_{mf,s} - \chi_{mm,s} + \chi_{mm,L}\right) \tag{3.4}$$

where the subscript *m* stands for the micelles and *f* for the fibers in the gel particles of the solid phase.

3.2.2 Gradient shape

Two main different gradients can be defined, a top and a bottom gradient. A top gradient is the gradient that results in high distribution coefficients of the target solutes above the feed point and a bottom gradient is a gradient that results in high distribution coefficients below the feed point (0). Only a top-gradient can improve loading capacity and or reduction of solvent usage (Houwing *et al.,* 2003). There are two different types of modifying solutes to form a gradient. The first type is a modifying solute that increases the *K*-values of the target solutes, for example micelles in SASEC. The second type is a modifying solute that decreases the *K*-values of the target solutes, for example salt in ion-exchange chromatography. When the *K*-value is increased, high concentration of the modifying solute is needed above the feed to have a top-gradient. When the *K*-value is decreased high concentration is needed below the feed.
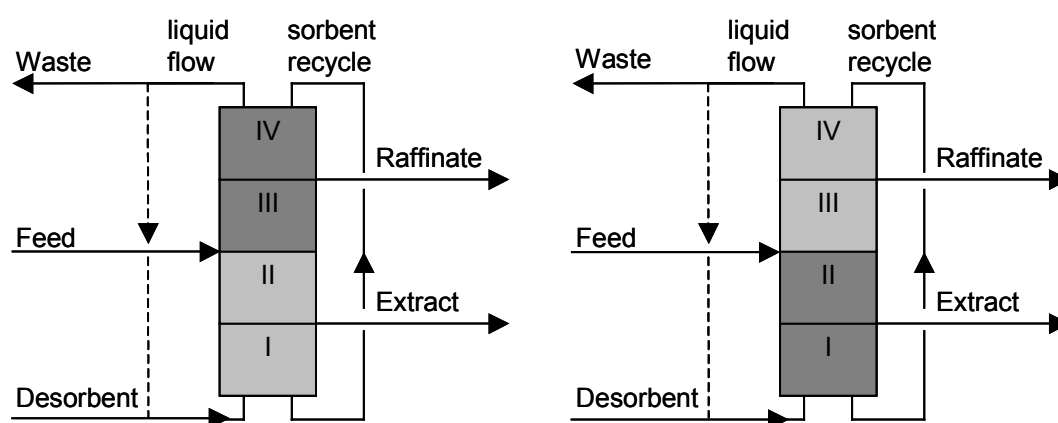
Figure 3.1. *Schematic representation of an SMB with a top-gradient (left) and an SMB with a bottom-gradient (right). A dark color represents a high affinity for the solid phase*

3.2.3 Wave velocity

For a top gradient of a modifying solute, this solute can be introduced with the desorbent or the feed. Depending on the selection of the flows in the SMB the modifying solute can either move upwards or downwards in the SMB. The movement of the modifying solute in the SMB is depending on the velocity of the front of the concentration waves. A wave can be a diffuse or a shock wave. A wave is diffuse when higher concentrations displace lower concentrations relative to the direction of the liquid flow. A wave is a shock wave when a lower concentration displaces a higher concentration. For both waves, it is possible to define the front velocity (Rhee *et al.,* 1971):

Diffuse wave
$$w = \frac{\beta v_s \left(m - \dfrac{\partial q}{\partial c} \right)}{\left(1 + \beta \dfrac{\partial q}{\partial c} \right)}$$

(3.5)

Shock wave
$$w = \frac{\beta v_s \left(m - \dfrac{\Delta q}{\Delta c} \right)}{\left(1 + \beta \dfrac{\Delta q}{\Delta c} \right)}$$

Where: β is the column phase ratio defined by *(1-ε)/ε*, where ε is the column porosity, v_s is the interstitial solids velocity, $\partial q/\partial c$ is the slope of the isotherm at a specific concentration and $\Delta q/\Delta c$ is the slope of the chord of the isotherm, *m* is the flow rate ratio of liquid to the solid phase which can be calculated in a SMB by correcting the actual liquid flow for the simulated flow of bed porosity and dead volume (Migliorini *et al.,* 1999)*:*

$$m = \frac{\Phi_L \tau - V_c \varepsilon - V_d}{V_c (1 - \varepsilon)}$$

(3.6)

where, Φ_L is the volumetric flow rate, τ is the switch time, V_c is the column volume, V_d is the dead volume and ε is the column porosity. A positive wave indicates that the modifying solute will move upwards with the liquid phase. This is the case when *m* > $\partial q/\partial c$ or *m* > $\Delta q/\Delta c$ for a diffuse or shock wave, respectively.

3.2.4   Upward and downward gradient

There are two possibilities to create a top-gradient. The first is an upward gradient of the modifying solute. Therefore the modifying solute is added at the desorbent when it decreases the distribution coefficients of the target solutes or at the feed when it increases the distribution coefficients. The modifying solute will be transported predominantly by the liquid phase. The lower 2 sections will be saturated with the desorbent (c_I = c_{II} = c_D). At the feed inlet, the feed and the flow from section II are mixed resulting in an increased or decreased concentration in section III and IV compared to the concentration in sections I and II. Examples of an upward gradient profile are given in figures 3.2a and 3.2b for the two different types of modifying solutes.

The second possibility is a downward gradient of the modifying solute. Therefore the modifying solute is added to the feed when it decreases the distribution coefficients or to the desorbent when it increases the distribution coefficients. Consequently, the modifying

solute will predominantly be transported by the solid phase. The sections above the feed inlet will be saturated with the desorbent ($c_{III} = c_{IV} = c_D$). The feed will have a different concentration, which will cause a different concentration in the sections below the feed compared to the concentration above the feed inlet. Figures 3.2c and figure 3.2d show the examples of a downward gradient for the two types of modifying solute.
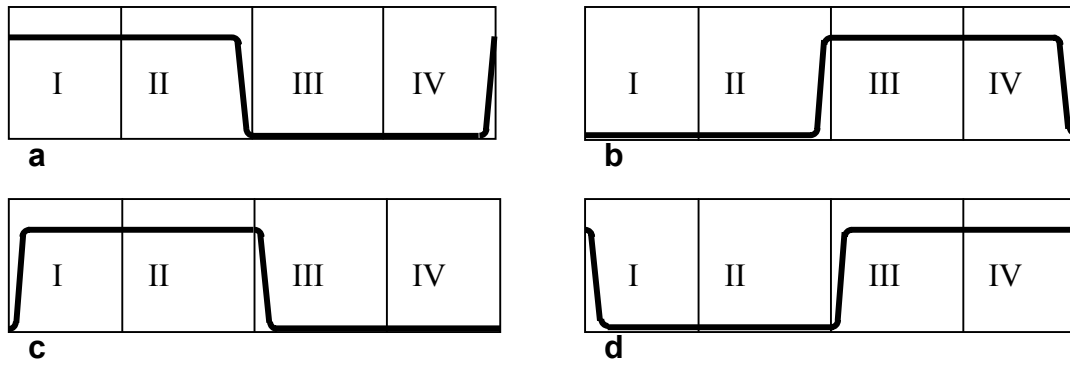
Figure 3.2. Concentration profile of the modifying solute in an SMB, a: upward gradient with an affinity decreasing solute, b: upward gradient with an affinity increasing solute, c: downward gradient with an affinity decreasing solute, d: downward gradient with an affinity increasing solute

3.2.5 Concentration of the modifying solute

In an upward gradient, c_{III} is the unknown concentration whereas c_{II} is the unknown concentration in a downward gradient. The unknown concentration can be calculated with the mass balance over the feed point:
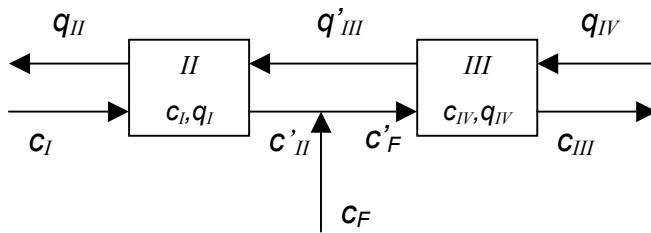
$$m_{II} c_I + (m_{III} - m_{II}) c_F - m_{III} c_{III} + q_{IV} - q_{II} = 0 \tag{3.7}$$

It is assumed that there are no fronts in between sections I and II and between sections III and IV. The concentration in section I will thus be equal to that in section II and the concentration in section III will thus be equal to that in section IV.

3.2.6 Flow selection

Depending on the front shapes of the concentration waves, the constraints of the flow ratios can be defined; these are given in table 3.1.

Table 3.1. Constraints of the flow ratios for positioning a gradient

Gradient	Front	Front shape	*m*
Upward	1	Diffuse	$m_I, m_{II} > \left(\dfrac{\partial q}{\partial c}\right)_{c_D}$
		Shock	$m_I, m_{II} > \left(\dfrac{\Delta q}{\Delta c}\right)_{c_{III} - c_D}$
	2	Shock	$m_{III}, m_{IV} > \left(\dfrac{\Delta q}{\Delta c}\right)_{c_D - c_{III}}$
		Diffuse	$m_{III}, m_{IV} > \left(\dfrac{\partial q}{\partial c}\right)_{c_{III}}$
Downward	1	Shock	$m_I, m_{II} < \left(\dfrac{\Delta q}{\Delta c}\right)_{c_{II} - c_D}$
		Diffuse	$m_I, m_{II} < \left(\dfrac{\partial q}{\partial c}\right)_{c_{II}}$
	2	Diffuse	$m_{III}, m_{IV} < \left(\dfrac{\partial q}{\partial c}\right)_{c_D}$
		Shock	$m_{III}, m_{IV} < \left(\dfrac{\Delta q}{\Delta c}\right)_{c_{II} - c_D}$

A slightly different solution was given by Houwing (Houwing *et al.,* 2002 and 2003) for the constraints of a downward gradient. The main difference is the assumption of the concentration in the section III and IV. Houwing considers this as an unknown concentration. In order to calculate this concentration it was assumed that no front exists between section IV and the waste outlet. This assumption makes it possible to calculate the concentration in section IV by a mass balance over the desorbent point. This assumption seems to be valid in the experiments described in these papers (Houwing *et al.,* 2002 and 2003). This is probably due to the relatively small difference in salt concentration in the feed and desorbent. In general, however, this assumption cannot automatically be made. In many gradients, there will exist a front at the end of section IV that will cause a concentration difference between the raffinate and the waste. In this paper it is stated that the concentration in sections III and IV is equal to the concentration

in the desorbent. The concentration of the modifying solute in the desorbent is introduced to column 1. This column will become the last column of section IV after one switching time. The m-value in section IV is chosen such that this desorbent concentration is not completely replaced by another concentration before the next switch time. After several switches the concentration in sections III and IV will thus be equal to the desorbent concentration. The same results will be obtained for the cases described in Houwing (Houwing *et al.,* 2003) with the procedure described in this paper. The constraints given in table 3.1 are not defined for one specific modifying solute but can be used for each modifying solute as long as the distribution behavior of this modifying solute is only depending on its own concentration. If the distribution coefficient is also influenced by the concentration of the target solutes, a more complicated flow selection procedure is needed.

3.3 Material and Methods

3.3.1   Equipment

An 8-column carousel SMB was used for the SMB experiments. In total 4 Shimadzu LC-8A pumps were used for the desorbent, feed, extract and raffinate flow respectively. The actual flow rates were determined by monitoring the change in weight during the experiment using Mettler Toledo balances (PG-S). The concentration of surfactant in the raffinate and waste outlet was monitored by an Shimadzu UV-Vis detector (SPD-10AV) at 204 and 220 nm and the concentration in the extract flow was monitored by a Shimadzu UV/VIS photodiode array detector (SPD-M10Avp) at all the wavelengths between 200 and 300 nm.

3.3.2   Columns

Sephacryl^{TM} S300 (GE Healthcare, catalogue No. 17-0599-01) was packed in in-house made stainless steel columns with a diameter of 2 cm and a length of 10 cm. The columns were packed at 3 ml/min for 1 hour followed by a flow rate of 8 ml/min for 3 hours. The reproducibility of the packing procedure was checked by pulse experiments with dextran blue. The void volume was determined from the same pulse experiments. An average void fraction of 0.40 ± 0.02 was found for each column.

3.3.3   Experiments

The gradient experiments were performed using an open loop SMB. Before each experiment, the columns were regenerated with a 10 mM phosphate buffer, pH 6.8, containing 0.15 M NaCl. For the upward gradient experiments a feed concentration of 4%

(w/w) of $C_{12}E_{23}$ (Acros organics, catalogue No. 228345000) in buffer was used. The desorbent was a surfactant free phosphate buffer. For the downward gradient experiments, the desorbent had a surfactant concentration of 4% (w/w) while the feed was a surfactant free phosphate buffer.

To measure the concentration profile in the SMB system, samples were taken at the inlet of one of the columns exactly halfway each switch-interval of the columns. To take the samples, an injection valve with a sample loop was placed before this column. At the time of sampling the sample loop was disconnected from the main flow path. The sample loop, filled with the sample, was emptied by injecting air in the sample loop. The sample loop was then loaded again with buffer and reconnected within the main flow path. The volume of the sample loop was only 0.3 ml and taking samples had no effect on the experimental results.

The samples were analyzed on an UV-Vis spectrophotometer (GE Healthcare, Ultrospec 2000) at 204, 220, 260 and 280 nm.

3.3.4   Simulation tool

The surfactant concentration profile in the SMB was simulated using a dynamic model programmed in Matlab. The concentration profiles in the liquid and solid phase of each column were calculated by:

$$\frac{\partial c_L}{\partial t} = -v \frac{\partial c_L}{\partial x} - \beta \cdot k_o a \left(c_s^{eq} - c_s \right)$$

(3.8)

$$\frac{\delta c_s}{\delta t} = \beta \cdot k_o a \left(c_s^{eq} - c_s \right)$$

(3.9)

The axial dispersion is omitted from these equations but implemented in the overall mass transfer coefficient, $k_o a$ (Ruthven *et al.,* 1984; Guiochon *et al.,* 1994):

$$\frac{1}{k_o a} = \frac{2 d_p K \beta}{v} + \frac{d_p}{6} \left(\frac{K}{k_L} + \frac{1}{k_s} \right)$$

(3.10)

The first term describes the dispersion, the second term the mass transfer resistance at the liquid side and the third term describes the mass transfer resistance at the solid side. The mass transfer coefficients at the liquid side, k_L and at the solid side, k_s are calculated by:

$$k_L = Sh_L \frac{D_L}{d_p} \tag{3.11}$$

$$k_S = Sh_S \frac{D_S}{d_S} \tag{3.12}$$

The Sherwood number on the liquid side is calculated by (Guiochon *et al.,* 1994):

$$Sh_L = \frac{1.09}{\varepsilon} \mathrm{Re}^{0.33} Sc^{0.33} \tag{3.13}$$

For the Sherwood number on the solid side a value of 10 is used (Bosma *et al.,* 2000). The diffusion coefficient of $C_{12}E_{23}$ in liquid is assumed to be $5 \cdot 10^{-11}$ m^2/s. The solid diffusion coefficient is calculated using the liquid diffusion coefficient (D_L), the radius of the micelle and the fiber fraction in the gel, ϕ_f, and the radius of the gel fiber (Vonk, 1994).

$$D_S = D_L \exp\left(-\phi_f^{0.5} \frac{r_m}{r_f}\right) \tag{3.14}$$

3.4   Results and Discussion

3.4.1   Downward gradient: area of operation

The surfactants used, form oblate shaped micelles which are defined by three semi-axes r_m, r_m and $\eta_m r_m$ where $\eta_m<1$. The semi-axes r_m and $\eta_m r_m$ are assumed to be 4.13 nm and 3.66 nm for $C_{12}E_{23}$ (Tanford, 1980; Horneman *et al.,* 2004).

The area of operation has been determined for a downward gradient using table 3.1 and the isotherm determined from equations 3.2 to 3.4 for $C_{12}E_{23}$ (Horneman *et al.,* 2004).

This area is shown in figure 3.3 for $c_{C12E23,D}$ = 4% (w/w). The boundaries of the area are given by 4 lines, related to the following constraints:

- $m_{III}=m_{II}$: Above this line, feed can be added.
- $m_{III}^{max} (0)$: This line gives the maximum m_{III} value when c_{II} equals 0. Only m_{III} values smaller than the $m_{III}^{max}(0)$ value will result in a downward movement of the micelles.
- $m_{III}^{max}(c_{surf})$: This line gives the maximum m_{III}-value, which is equal to the $\Delta q/\Delta c$ of the micelle at the concentration c_{II}. This concentration is calculated from the feed

mass balance. Only m_{III}-values smaller than the m_{III}^{max} (c_{surf}) value corresponding to the same c_{II} will result in a downward movement of the micelles. Note that this is the area **above** this line.

- m_{II}^{max} (c_{surf}): This line gives the maximum m_{II}-value, the $\partial q/\partial c$ of the micelles at the concentration c_{II}. Only m_{II} values smaller than the $m_{II}^{max}(c_{surf})$ value corresponding to the same c_{II} will result in a downward movement of the micelles in section II.

The shaded area in figure 3.3 thus gives the area in which a downward gradient of the micelles is possible.
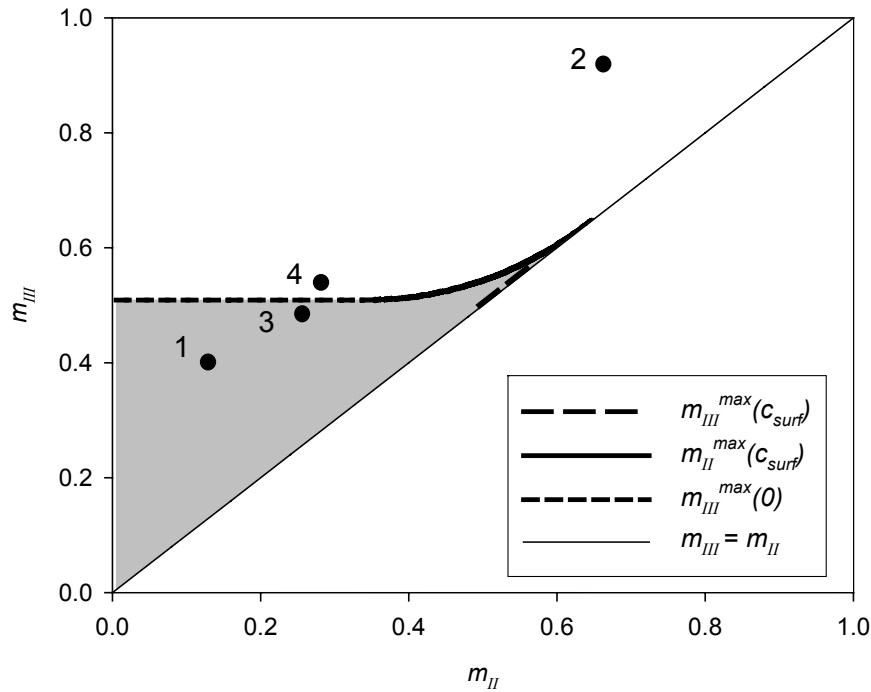
Figure 3.3. *Area of operation for a downward-top gradient of $C_{12}E_{23}$ with $c_D = 4\%$ (w/w).*

3.4.2 Downward gradient: results of gradient experiments

Experiments have been performed at the m_{III}-m_{II} values given in figure 3.3. The values of all m-values, the actual flows and switching times are given in table 3.2. The results of these experiments are shown in figure 3.4.

The m-values of experiment 1 have been chosen within the area of operation. Based on the constraints given in table 3.1 it can be predicted that micelles will move downwards in each section. This prediction agrees very well with the experimental results as can be seen in figure 3.4a. This figure shows a clear gradient profile in the SMB. The concentration in sections III and IV equals the desorbent concentration (4%, w/w) while

the concentration in sections I and II is lower. The line in figure 3.4a gives the concentration profile halfway the switch time predicted by the dynamic SMB model. This model predicts the concentration profile reasonably well. Only the concentration in section II is predicted to be higher than found during the experiments.

Table 3.2. Parameters in the downward gradient experiments

Parameter	exp. 1	exp.2	exp. 3	exp. 4
m_I [-]	0.33	0.87	0.43	0.47
m_{II} [-]	0.14	0.67	0.24	0.27
m_{III} [-]	0.40	0.93	0.49	0.53
m_{IV} [-]	0.13	0.67	0.24	0.27
τ [s]	251	251	240	251
F [ml/min]	1.20	1.21	1.20	1.20
D [ml/min]	4.74	7.18	5.42	5.37
R [ml/min]	1.21	1.19	1.20	1.20
E [ml/min]	0.90	0.91	0.91	0.91
c_D [%, w/w]	4.4	4.4	3.4	3.7
c_{II} [%, w/w][1]	2.02	[2]	0.32	[2]

    1)   Concentration calculated with feed balance (equation 3.7)

    2)   Cannot be calculated because the operation point is outside the area of operation

The *m*-values of experiment 2 are far out of the area of operation. Figure 3.4b shows that there is a gradient formed in the SMB but not the desired downward-top gradient. The micelles added with the desorbent are transported with the liquid flow through section I and II instead of being moved with the solids to section IV. The gradient that is formed is an upward-bottom gradient. Figure 3.5 gives the area of operation to position an upward gradient when the micelles are added to the desorbent. The dot in this figure gives the operation point of this experiment. This point has been chosen on the boundary of this area, which explains the formation of this gradient. Note that this is a **bottom** gradient using this micelle as modifying solute. In a bottom gradient the loading capacity is decreased in section III and IV while the elution is made more difficult in section I and II. No improvement of a separation can be achieved when this type of gradient is used
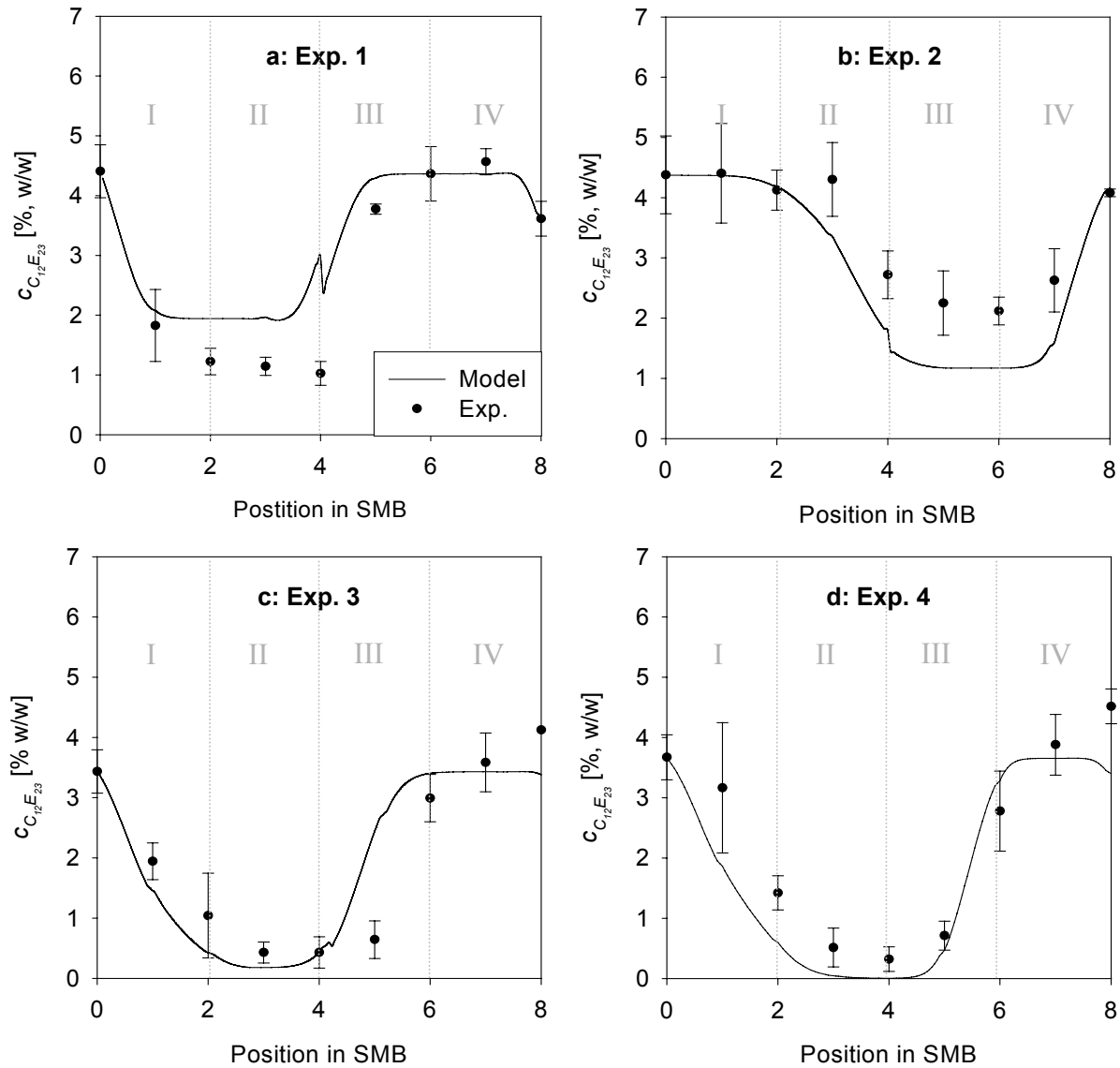
Figure 3.4. *Experimental and simulated concentration profiles at steady state for the downward gradient experiments*

Experiments 3 and 4 have *m*-values close to the boundary of the area of operation. Both experiments show a gradually decrease in concentration in sections I and II. At correct chosen *m*-values there should be no front in between section I and II. In experiment 3 the maximum allowed value of m_I is 0.38. The experimental value of m_I is above this maximum value (see table 3.2). The micelles are thus transported with the liquid flow in section I instead of with the solid phase. In section II the micelles are again transported predominantly with the solid phase preventing a higher concentration in this section. A front between the two sections is formed. This is also predicted by the dynamic model as

can be seen in figure 3.4c. The same is the case in experiment 4. In this experiment, however, also m_{III} is above the maximum allowed value. Therefore the constraint of m_I cannot be calculated from equation 3.7 and table 3.1 but the dynamic model shows again that the micelles are transported with the liquid flow in section I instead of with the solid phase (see figure 3.4d). Due to the high value of m_I, the concentration of micelles will be higher in section I. This will influence the distribution behavior of the components that have to be retained in this section during a separation. Whether or not this is a problem, depends on the isotherms of the components to be separated.

In experiment 4, the front between section II and III is more shifted towards the raffinate outlet. This is because the m_{III} has been chosen just above the maximum value. This is also very well predicted by the dynamic model. In experiment 3 the m_{III} value has been chosen correctly but almost the same results have been found as in experiment 4. The dynamic model, however predicts a front closer to the feed point. It is possible that the error margin in the experimentally determined isotherm of the micelles is somewhat too large to choose a point this close to the boundary of m_{III}. The chosen value of m_{III} can therefore be outside the actual area of operation. Another possibility is that the correlations used to describe the mass transfer coefficient are not accurate enough. If the mass transfer resistance is larger than predicted, the front between the loaded and unloaded parts of the columns will be broader than predicted (Houwing *et al.*, 2003a).
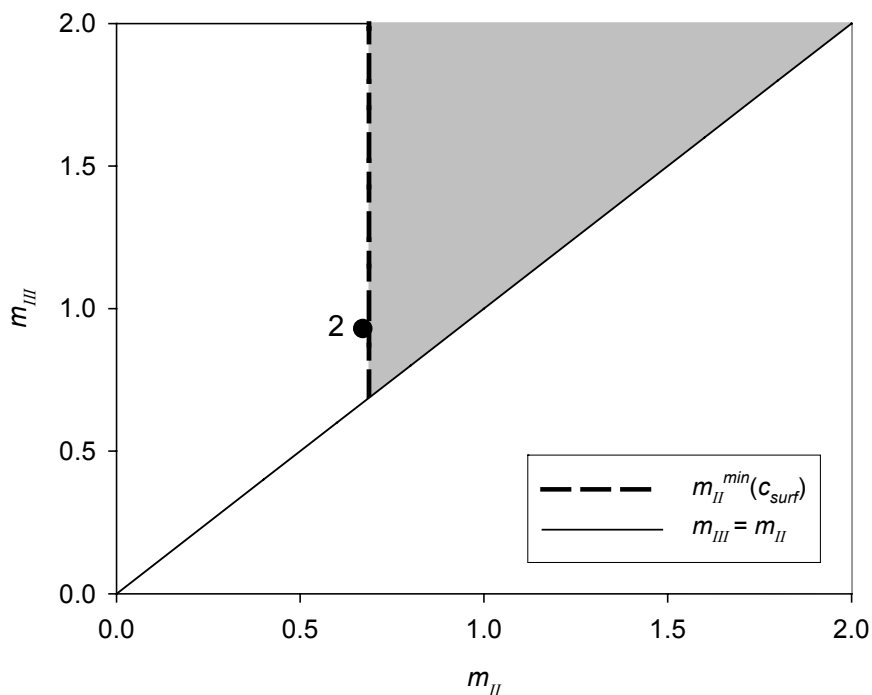

Figure 3.5. *Area of operation for an upward-bottom gradient of $C_{12}E_{23}$ with c_D = 4.4% (w/w).*

3.4.3   Upward gradient: area of operation

Using the isotherm determined in previous work (Horneman *et al.*, 2004), an area of operation has been constructed in the case of an upward top-gradient using c_F = 4% (w/w). This area is shown in figure 3.6.
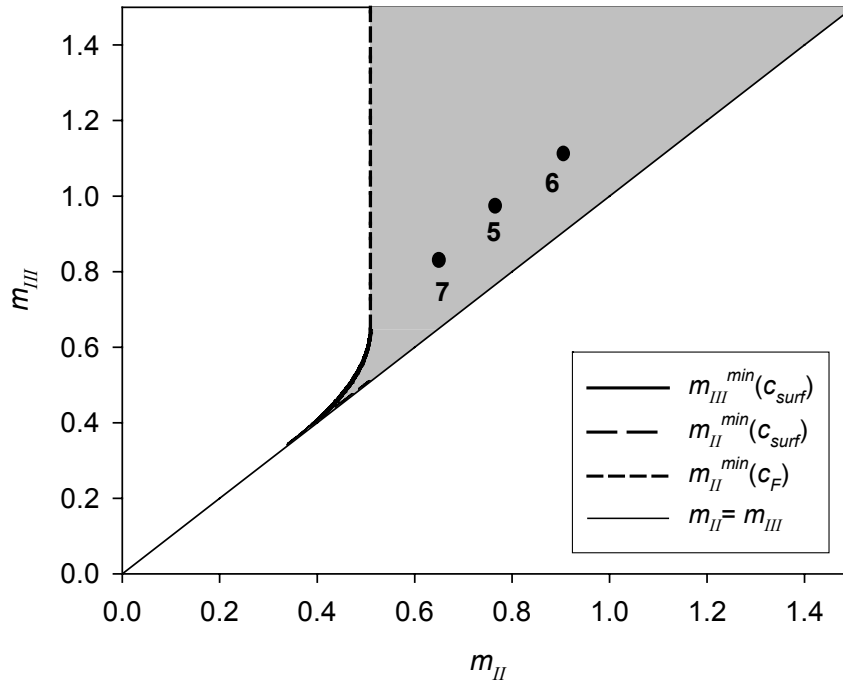
Figure 3.6. *Area in which an upward gradient is possible, c_F = 4% (w/w).*

The boundaries of the area are given by 4 lines:
- m_{III}=m_{II}: Above this line, feed can be added.
- $m_{II}^{min}(c_F)$: This line gives the minimum m_{II} value when c_{III} equals the feed concentration. The concentration cannot be larger than this concentration. All values above this point will result in an upward movement of the micelle.
- $m_{III}^{min}(c_{surf})$: This line gives the minimum m_{III} value, which is equal to the $\partial q/\partial c$ of the micelle at the concentration c_{III}. This concentration is calculated from the feed mass balance. Only m_{III} values higher than the $m_{III}^{min}(c_{surf})$ value corresponding to the same c_{III} will result in an upward movement of the micelle. Note that this is the area **below/to the right** of this line.
- $m_{II}^{min}(c_{surf})$: This line gives the minimum m_{II} value, which is equal to the $\Delta q/\Delta c$ of the micelle at the concentration c_{III}. This concentration is calculated from the feed mass balance. Only m_{II} values higher than the $m_{II}^{min}(c_{surf})$ value corresponding to

the same c_{III} will result in an upward movement of the micelle.
The shaded area in figure 3.6 thus gives the area in which an upward gradient of the micelle is possible.

3.4.4 Upward gradient: experimental results

Three experiments have been performed at the m_{III}, m_{II} values given in figure 3.6. The actual flows, *m*-values and switching times are given in table 3.3. All the upward experiments had *m*-values within the area of operation. In all cases an upward gradient was indeed formed as can be seen in figure 3.7.

Table 3.3.   Experimental parameters

Parameter	exp. 5	exp. 6	exp. 7
m_I [-]	0.98	1.15	0.81
m_{II} [-]	0.75	0.92	0.57
m_{III} [-]	0.98	1.15	0.80
m_{IV} [-]	0.75	0.91	0.81
τ [s]	301	301	301
F [ml/min]	0.91	0.90	0.90
D [ml/min]	6.44	7.11	5.76
R [ml/min]	0.90	0.91	0.89
E [ml/min]	0.89	0.91	0.90
c_F [%, w/w]	3.7	3.7	3.7
c_{III} [%, w/w][1)]	1.5	1.1	2.5

1)   Concentration calculated with feed balance (equation 3.7)

During experiment 5, surfactant was still found in section I and II, which was not expected. The concentration is expected to be equal to the desorbent concentration, which was zero in these experiments. The other 2 experiments show a concentration closer to zero than the first experiment. The last two experiments clearly show the effect of chosen *m*-values on the concentration of surfactant in section III and IV. Experiment 7 was performed at a point close to the boundary of the area. The concentration of surfactant in section III is higher than found in experiment 6 that was performed at a point further away from this boundary. The same was seen in the downward experiments; the closer the m-values were to the boundaries the larger the difference in concentration of surfactant in section II and III. Larger concentration difference means also larger difference in distribution coefficients and thus larger effects on the separation performance. However, close to the boundaries the effects of possible mass transfer

limitations are relatively large (Houwing *et al.,* 2003a) and should be accounted for in designing the separation process.

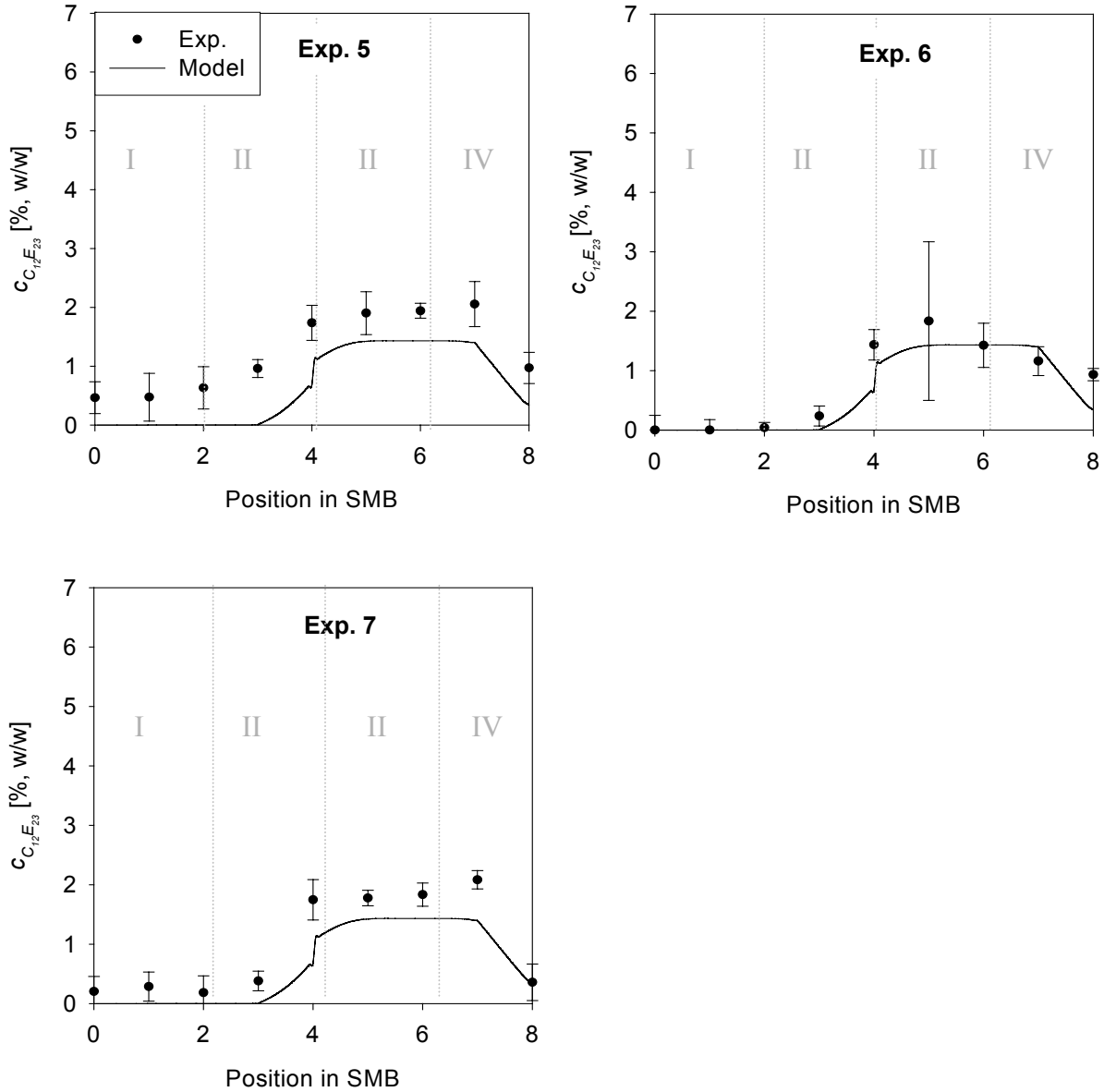***Figure 3.7.*** *Experimental and simulated concentration profiles at steady state for the upward gradient experiments.*

3.4.5 Selecting gradient mode for the separation of IgG monomers and dimers

The results presented in this paper show that it is possible to create a micellar gradient in size-exclusion SMB. It also shows that a positioning procedure is necessary to place the

gradient in the correct position. A top-gradient can be formed by two different gradients: an upward or a downward gradient. The choice between the two gradients is depending on the distribution coefficients of the target solutes compared to the distribution behavior of the modifying solute. The operation point should fulfill both the constraints for positioning the gradient and those of complete separation. The constraints of complete separation are:

$$K_2(c_{II}) \quad < \quad m_I \tag{3.15a}$$

$$K_1(c_{II}) \quad < \quad m_{II} \quad < \quad K_2(c_{II}) \tag{3.15b}$$

$$K_1(c_{III}) \quad < \quad m_{III} \quad < \quad K_2(c_{III}) \tag{3.15c}$$

$$m_{IV} \quad < \quad K_2(c_{III}) \tag{3.15d}$$

where K_i is the distribution coefficient of target solute i and the size of solute 1 is larger than that of solute 2. The constraints of positioning the gradient are given in table 3.1. Target solutes with a relative high distribution coefficient compared to the wave velocity of the micelles will need a downward gradient whereas target solutes with a relative low distribution coefficient compared to the wave velocity of the micelles need an upward gradient. An example will be given of both gradients and of the effects of these gradients on the area of separation.
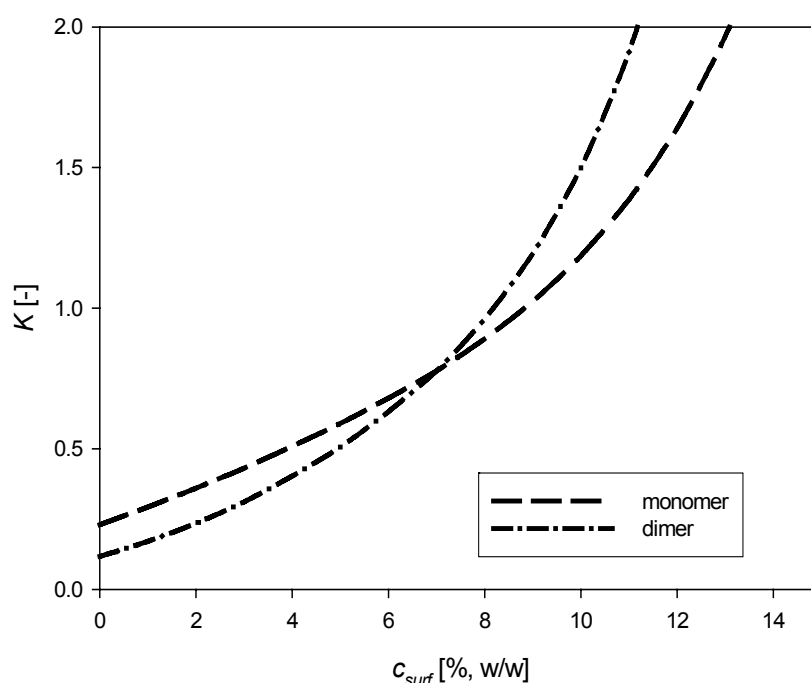

Figure 3.8. *Distribution coefficient of IgG monomer and dimer as function of concentration of $C_{12}E_{23}$ in the mobile phase*

An example of the application of a downward gradient is the separation of IgG monomers and IgG dimers using $C_{12}E_{23}$ as non-ionic surfactant and Sephacryl^{TM} S300 as solid stationary phase. The distribution coefficient of IgG can be calculated using equation 3.1. It is assumed that both monomer and dimer are spherical with $r_{monomer}$ = 5.5 nm and r_{dimer} = 7.0 nm. The calculated distribution coefficients are shown in figure 3.8 as function of the surfactant concentration.

At low surfactant concentration, the distribution coefficients of both monomer and dimer are relatively low, and therefore a downward gradient is needed. Figure 3.9 shows the area of separation with a desorbent surfactant concentration of c_D = 4% (w/w). Figure 3.9 also shows the area of complete separation in case of normal SEC. It is obvious upon inspecting figure 3.9 that significantly higher throughputs can be achieved when using the novel SASEC technology instead of conventional SEC.
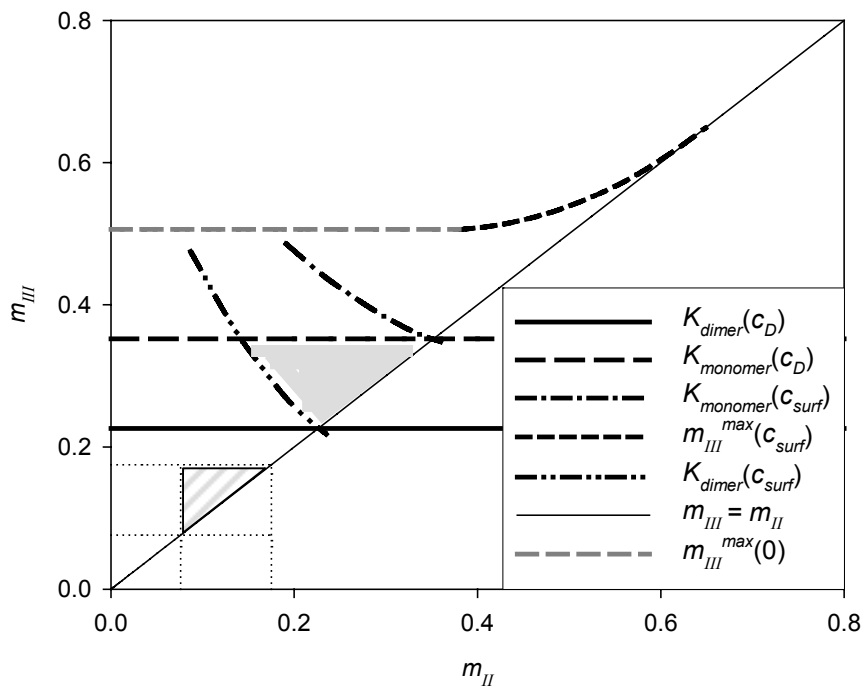
Figure 3.9. *Separation area of monomer IgG and dimer IgG in case of SEC-SMB (striped area) and in case of SASEC-SMB (solid area) using a downward gradient at c_D = 3% (w/w) with $C_{12}E_{23}$ as non-ionic surfactant*

At higher concentrations of $C_{12}E_{23}$, the distribution coefficients of IgG monomer and dimer will increase to values that are relative high compared the wave velocity of the micelles. In that case an upward gradient is needed for the separation. Figure 3.10 shows the area of separation in case of an upward gradient with c_D = 9.9% (w/w) and c_F = 12% (w/w). The area of separation has increased considerably. Substantially higher throughputs can

be achieved under these conditions ((m_{III}-m_{II})|$_{opt}$: SEC: 0.1, SASEC downward gradient: 0.2, SASEC upward gradient: 0.85!).

In both examples not only substantially higher throughputs can be reached but also *concentration* of the product is now possible. Until now, it was never possible to concentrate the desired product during SEC. To achieve product concentration of the extract product, the m_I-value should be chosen below the m_{III}-value. To achieve product concentration of the raffinate product, the m_{IV}-value should be chosen above the m_{II}-value. None of these two constraints is possible in normal SEC, where the K-values are constant in the whole SMB. In the newly presented method SASEC-SMB, both constraints can be fulfilled when the micelle gradient is correctly positioned.
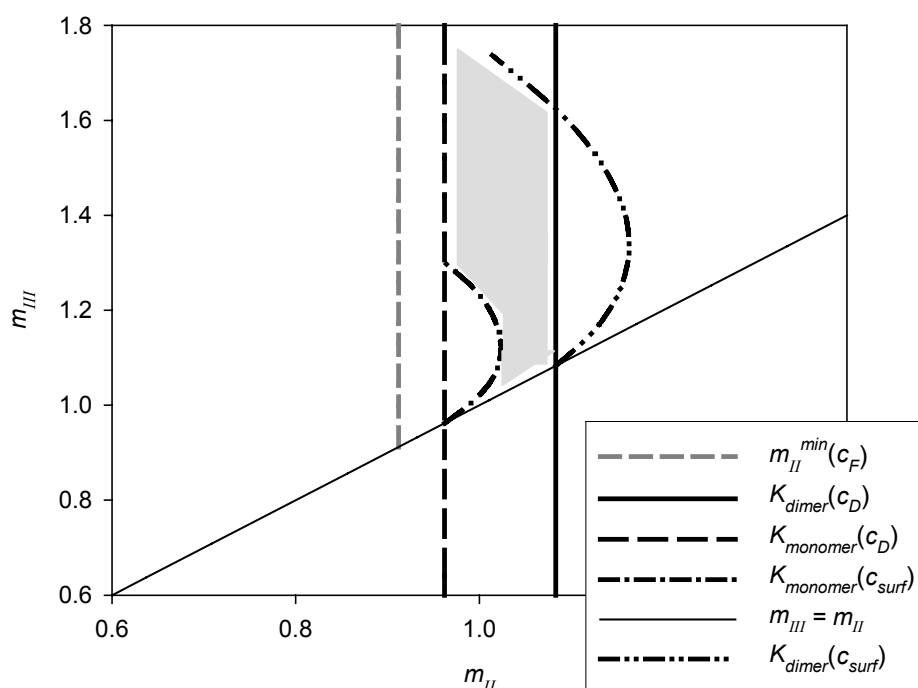
Figure 3.10. *Separation area of monomer IgG and dimer IgG in case of SASEC-SMB (solid area) using an upward gradient at c_D = 9.9% (w/w) and c_F = 12% (w/w) with $C_{12}E_{23}$ as non-ionic surfactant*

The two examples presented here do not necessarily give the most optimized separation conditions. It might very well be that better results can be obtained using another non-ionic surfactant. Other sizes or dimensions of the micelles have a large effect on the distribution behavior of the target solutes as well as on the distribution behavior of the micelles. This makes SASEC-SMB a very flexible separation method. By changing the solution conditions other separations can be performed on the same gel material. In this way not only protein-protein separations are possible but the technique is also

conveniently suited for the separation or removal of much larger molecules as for example during viral clearance. The application of SASEC-SMB chromatographic purification is further experimentally investigated in our lab and will be reported in the next two chapters.

3.5   Conclusion

This paper demonstrates the possibility to position a micellar gradient in SEC-SMB, both theoretically and experimentally. The micelles, formed by non-ionic surfactants exhibit a distribution behavior that is dependent on the concentration of these surfactants. A flow selection procedure is thus needed to place this gradient in the correct position and this selection method is developed and reported in this paper. This general method has been applied in this paper to surfactant-aided size-exclusion SMB chromatography. For both upward and downward gradients, an area was calculated in which the m_{II} and m_{III} values should be chosen to get the correct gradient. Experiments confirmed the correct formation of the gradient as long as all the *m*-values were chosen within this area.

The distribution coefficient of the target solutes will increase at higher surfactant concentration. The choice between an upward or downward gradient is depending on the target solutes that have to be separated and the modifying solute used for this separation. Using the correct gradient will result in significantly higher throughputs and concentration of the product, which is not possible in conventional SEC-SMB. It further results in lower solvent use compared to normal SEC-SMB.

Acknowledgements

Nomenclature

$c_{i,k}$	concentration of component *i* in phase *k*
q	concentration in solid phase at equilibrium with mobile phase
d_p	particle diameter
D	diffusion coefficient
H_i	integral of the mean curvature of component *i*
K_i	distribution coefficient of component *i*

k	mass transfer coefficient
$k_o a$	overall mass transfer coefficient
m	flow rate ratio
r_i	radius of component i
Re	Reynolds number
S_i	surface area of component i
Sc	Schmidt number
Sh	Sherwood number
U_{ij}	excluded volume between components i and j
V_i	volume of component i
V_c	volume of the column
V_d	dead volume
v_s	interstitial solid velocity
w	front velocity
x_i	number concentration of component i

ρ	density
ϕ_i	volume fraction of component i
χ_{ij}	steric interaction parameter between components i and j
Φ_L	volumetric flow rate
β	column phase ratio
ε	column porosity
τ	switch time

Sub and superscripts

eq	equilibrium
f	gel fiber
s	solid phase
surf	surfactant
m	micelle
L	liquid phase
F	feed
R	raffinate
E	extract
D	desorbent

References

Abel S, Mazotti M, Morbidelli M. 2002. J. Chromatogr. A 944: 23-39

Abel S, Mazotti M, Morbidelli M. 2004. J. Chromatogr. A 1026: 47-55

Antos D, Seidel-Morgenstern A. 2001. Chem. Eng. Sc. 56: 6667-6682

Antos D, Seidel-Morgenstern A. 2002. J. Chromatogr. A 944: 77-91

Bosma JC, Wesselingh JA. 2000. J. Chromatogr. B 743: 169-180

Denet F, Hauck W, Nicoud RM, Di Giovanni O, Mazzotti M, Jaubert JN, Morbidelli M. 2001. Ind. Eng. Chem. Res. 40: 4603-4609

Di Giovanni O, Mazzotti M, Morbidelli M, Denet F, Hauck W, Nicoud RM. 2001. J. Chromaotgr. A 919: 1-12

Evans DF, Wennerström H. 1994. The Colloidal Domain, VCH publ., New York

Geisser A, Hendrich T, Boehm G, Stahl B. 2005. J. Chromatogr. A 1092: 17-23
Guiochon GS, Golshan-Shirazi S, Katti AM. 1994. Fundamentals of Preparative and Nonlinear Chromatography, Academic Press, Boston

Horneman DA, Wolbers M, Zomerdijk M, Ottens M, Keurentjes JTF, van der Wielen LAM. 2004. J. Chromatogr. B 807: 39-45

Horneman DA, Ottens M, van den Broeke LJP, van Roosmalen D, Keurentjes JTF, van der Wielen LAM. 2004a. Patent EP1491246

Houwing J, van Hateren SH, Billiet HAH, van der Wielen LAM. 2002. J Chromatogr. A. 952: 85-98

Houwing J, Billiet HAH, van der Wielen LAM. 2002a. J. Chromatogr. A 994: 189-201

Houwing J, Jensen TB, van Hateren SH, Billiet HAH, van der Wielen LAM. 2003, AIChE J. 49: 665-674

Houwing J, Billiet HAH, van der Wielen LAM. 2003a. AICHE J. 49: 1158-1167

Jansons KM, Phillips CG. 1990. J Colloid Interface Sc. 137: 75-91

Jensen TB, Reijns TGP, Billiet HAH, van der Wielen LAM. 2000. J. Chromatogr. A 873: 149-162

Jensen TB, Billiet HAH, van der Wielen LAM. 2000a. WO patent 00/33934

Lazzara MJ, Blankschtein D, Deen WM. 2000. J. Colloid Interface Sc. 226: 112-122

Liu C, Kamei DT, King JA, Wang DIC, Blankschtein D. 1998. J. Chromatogr. B, 711: 127-138

Migliorini C, Mazzotti M, Morbidelli M. 1999. AIChE J 45: 1411-1421

Migliorini C, Wendlinger M, Mazzotti M. 2001. Ind. Eng. Chem. Res. 40: 2606-2617

Mun SY, Xie Y, Kim JH, Wang NHL. 2003. Ind. Eng. Chem. Res. 42: 1977-1993

Rhee HK, Aris R, Amundson NR. 1971. Phil. Trans. Roy. Soc. Lond. A 269: 187-197

Ruthven DM. 1984. Adsorption and adsorption processes, Wiley, New York

Tanford C. 1980. The Hydrophobic Effect Formation of Micelles and Biological Membranes, Wiley, New York

van Roosmalen D, Lazzara MJ, van den Broeke LJP, Keurentjes JTF, Blankschtein D. 2004. Biotechnol. Bioeng. 87: 695-703

Vonk P. 1994. Ph.D. Thesis, University of Groningen, Groningen

4

Viral clearance using surfactant-aided size-exclusion chromatography in fixed bed and simulated moving bed systems

Abstract

Surfactant-aided size-exclusion chromatography (SASEC) is applied to the viral clearance of blood proteins, taking BSA as an example. Fixed bed systems as well as simulated moving bed (SMB) systems are examined. SASEC shows a better performance of this separation in terms of log reduction value (*LRV)*, productivity of BSA, yield on BSA and solvent consumption compared to normal size-exclusion chromatography (SEC) in fixed bed as well as in SMB systems.

Keywords: viral clearance, surfactants, size-exclusion chromatography, simulated moving bed, protein purification.

4.1 Introduction

Biopharmaceutical products have to be free of possible viral contaminations. Virus contamination can arise from the source cell line or other biological starting material or by viruses introduced accidentally during the production process. One of the steps to assure the safety of the product is a sufficient ability of viral clearance during the purification process. Viral clearance can be achieved by either virus inactivation or by virus removal. Examples of virus inactivation treatments are: heat treatment, irradiation, ethanol treatment, pH treatment or solvent/detergent treatment (Kalyanpur, 2002; Burnouf *et al.,* 2004). Most of these treatments are very effective for enveloped viruses. Non-enveloped viruses, however, often show a higher physicochemical resistance (FDA, 1998). When it is possible to break this resistance, the treatment will also often result in the denaturation of the target product. Not all viruses can thus be inactivated with these methods. Therefore, each purification process must at least have one step that is effective in virus removal. Examples of purification steps that are also effective in virus removal are chromatographic techniques and filtration (Levy *et al.,* 1998; Burnouf *et al.,* 2003). Of all chromatographic techniques, gel filtration or size-exclusion chromatography is not commonly known as a very good performing method for viral clearance. The main disadvantage of SEC is the limited selectivity and resolution, which can only be increased by increasing the column length or decreasing the sample load. Recently it has been shown that the selectivity and thus the resolution of size-exclusion chromatography can be changed in-situ, by using non-ionic surfactants in the mobile phase (Horneman *et al.,* 2004 and 2004a, van Roosmalen *et al.,* 2004). These non-ionic surfactants form micelles at very low concentration. The way in which biomolecules and bioparticles partition towards a phase containing "inert" micelles, depends on the same parameters as in gel filtration chromatography: the volume fraction of micelles and the diameter ratio of solute and micelles. These parameters and thus the selectivity can be changed in-situ by varying the solution conditions, such as concentration and type of surfactants, temperature, and the addition of salts (Evans *et al.,* 1994; Horneman *et al.,* 2004; van Roosmalen *et al.,* 2004).

This paper will demonstrate the application of surfactant-aided size-exclusion chromatography (SASEC) in viral clearance. As an example the separation of BSA and bacteriophage ϕ29 is examined. BSA is used as a model for the human blood protein HSA. As a blood product, HSA can be contaminated by several viruses like HIV, hepatititus A virus (HAV), hepatitis B virus (HBV) and hepatitis C virus (HCV) (Adcock *et al.,* 1998). These viruses have different sizes ranging from 20 to 150 nm. Bacteriophage ϕ29 has a size of about 42 nm (Anderson *et al.,* 1966; Meijer *et al.,* 2001) and represents a medium sized virus. The potential of viral clearance using SASEC is shown in both fixed bed and simulated moving bed chromatography.

4.2   Theory

4.2.1   Size-exclusion chromatography

The distribution coefficient in size-exclusion chromatography is defined as the ratio of the solute concentration in the solid phase, $c_{i,s}$ over the solute concentration in the mobile phase, $c_{i,L}$ at equilibrium. Throughout this paper, the solid phase is defined as the total gel volume, including the fibers and the pores of the gel particles.

$$K_i = \frac{c_{i,s}}{c_{i,L}}$$ (4.1)

In size-exclusion chromatography this distribution coefficient can be described by an excluded volume model that describes the steric interactions among the solutes and the fibers (Ogston, 1958; Bosma *et al.,* 2000; Horneman *et al.,* 2004). In this model, all volumes excluding a solute due to the presence of all types of fibers and solutes, including the solute itself, are calculated in each phase. The general equation (Lazzara *et al.,* 2000) is given by:

$$K_i = \exp\left(-\sum_j \chi_{ij,s} + \sum_j \chi_{ij,L}\right)$$ (4.2)

where the dimensionless number $\chi_{ij,k}$ is the total excluded volume of solute *i* and a set of objects *j* per volume of phase *k* and is defined as:

$$\chi_{ij,k} = x_{j,k} U_{ij,k}$$ (4.3)

Where $x_{j,k}$ is the number concentration of component *j* in phase *k (#/m³)* and $U_{ij,k}$ is the excluded volumes between *i* and *j* in phase *k*. The excluded volume of two convex particles can be calculated by the following general expression:(Jansons *et al.,* 1990; Lazzara *et al.,* 2000)

$$U_{ij} = V_i + \frac{S_i H_j + S_j H_i}{4\pi} + V_j$$ (4.4)

where V_i, S_i and H_i are the volume, the surface area and the integral of the mean curvature of component *i,* respectively. With this expression, it is possible to calculate the excluded volume between two convex objects of any shape or size.

4.2.2   Surfactant-aided size-exclusion chromatography

In surfactant-aided size-exclusion chromatography a non-ionic surfactant is added to the mobile phase at a concentration exceeding the critical micelle concentration. Now extra volume is excluded from a solute due to the presence of micelles. The distribution coefficient can again be predicted with equations 4.2 to 4.4. There is only one component extra in both phases: the micelle formed by the non-ionic surfactants. For example when the micelle has an oblate shape, the distribution coefficient of a spherical solute *i* becomes:

$$K_i = \exp\left(\begin{array}{l} \left[-\ln\left(\dfrac{1}{1-\phi_f}\right)\left(1+\dfrac{r_i}{r_f}\right)^2 -\left(\ln\left(\dfrac{1}{1-\phi_{m,s}}\right)-\ln\left(\dfrac{1}{1-\phi_{m,L}}\right)\right)\right]\cdot \\[4mm] \left(1+\dfrac{1}{\eta_m}\left(\dfrac{r_i}{r_m}\right)^3 +\dfrac{3}{2}\left(\dfrac{r_i}{r_m}\right)^2\dfrac{g(\eta_m)}{\eta_m}+\dfrac{3}{2}\left(\dfrac{r_i}{r_m}\right)\dfrac{f(\eta_m)}{\eta_m}\right)- \\[4mm] \left(\phi_{i,s}-\phi_{i,L}\right)\cdot\left(1+\dfrac{r_i}{r_i}\right)^3 \end{array} \right) \qquad (4.5)$$

with:

$$f(\eta_m) = 1 + \eta_m^2\left(1-\eta_m^2\right)^{-1/2}\cosh^{-1}\left(\eta_m^{-1}\right)$$

$$g(\eta_m) = \eta_m + \left(1-\eta_m^2\right)^{-1/2}\cos^{-1}\left(\eta_m\right)$$

Where *r* is the radius, ϕ is the volume fraction. The subscripts *f* and *m* indicate the gel fiber and the micelle. An oblate micelle is defined by three semi-axes r_m, r_m and $\eta_m r_m$ where $\eta_m < 1$. The concentration of micelles in the gel phase can be calculated using the distribution coefficient of the micelle itself. This distribution coefficient can again be calculated using equations 4.2 to 4.4 (Horneman *et al.,* 2004). The last term describes the steric self-interaction among the protein molecules themselves in the solid and liquid phase. For dilute solute solutions this term can be neglected.

4.2.3   Model description of concentration profiles in chromatography

Concentration profiles were simulated by numerical integration of the mass balance equations on the liquid and solid phase:

$$\frac{\partial c_{i,L}}{\partial t} = -v\frac{\partial c_{i,L}}{\partial z} + D_{ax}\frac{\partial^2 c_{i,L}}{\partial z^2} - \frac{1-\varepsilon}{\varepsilon}\frac{\partial c_{i,s}}{\partial t} \qquad (4.6a)$$

$$\frac{\partial c_{i,s}}{\partial t} = k_0 a\left(c_{i,s}^{eq} - c_{i,s}\right) \qquad (4.6b)$$

where v is the interstitial velocity, ε is the void fraction in the column, $k_o a$ is the overall mass transfer coefficient, calculated by:

$$\frac{1}{k_o a} = \frac{d_p}{6}\left(\frac{K}{k_L} + \frac{1}{k_s}\right) \tag{4.7}$$

where k_L and k_s are the mass transfer at the liquid side and solid side respectively. These can be calculated from the Sherwood number. For the Sherwood number on the solid side a value of 10 is used (Bosma *et al.*, 2000). K is the distribution coefficient, which depends on all actual volume fractions as is shown in equation 4.5. The liquid diffusion coefficient of BSA is $D_{BSA} = 6 \cdot 10^{-11}$ m^2/s (Sober, 1970). The diffusion coefficient of bacteriophage is calculated from the Stokes-Einstein relation which gives $D_{\phi 29} = 5 \cdot 10^{-12}$ m^2/s. The intraparticle diffusion coefficient, D_s was calculated from these liquid diffusion coefficients (Vonk, 1994):

$$D_s = D_i \exp\left(-\phi_f^{0.5} \frac{r_i}{r_f}\right) \tag{4.8}$$

For spatial discretization of the convection term a second order backward discretization scheme was used. The axial dispersion was approximated by numerical dispersion (Guiochon *et al.,* 1994). The resulting system of ODE's is solved in time by a fourth order Runga-Kutta method.

4.2.4 Separation performance

The performance of the separation is described in terms of virus log reduction (*LRV*), Yield of product (*Y*), Productivity (*PR*), product concentration (c_{BSA}) and solvent consumption (*CS*). In the fixed bed experiments, these terms are defined as:

$$LRV = \frac{c_{\phi 29\_in} V_{inj}}{c_{\phi 29\_out} V_{out}} \tag{4.9}$$

$$PR = \frac{c_{BSA\_in} V_{inj} Y}{\Delta t_{cycle} V_s} \tag{4.10}$$

$$CS = \frac{\Delta t_{cycle} \Phi}{c_{BSA\_in} V_{inj} Y} \tag{4.11}$$

where V_{inj} is the volume of the sample injected to the column, V_{out} is the volume collected as product, Δt_{cycle} is the cycle time, which is the time between two sample injections and Φ is the flow rate.

In the SMB experiments these terms are defined as:

$$LRV = \frac{c_{\phi 29,F} \Phi_F}{c_{\phi 29,E} \Phi_E}$$ (4.12)

$$PR = \frac{c_{BSA,F} \Phi_F Y}{V_s}$$ (4.13)

$$CS = \frac{\Phi_D}{c_{BSA,F} \Phi_F Y}$$ (4.14)

Where the subscripts *D*, *F* and *E* stand for desorbent, feed and extract.

4.3 Materials and method

4.3.1 Fixed bed experiments

Column

An Omnifit column from BioRad was used in a FPLC Äkta Explorer (GE Healthcare). The column was packed with Sephacryl^{TM} S300 HR (Amersham Biosciences BV, cat no. 17-0599-01) up to a height of 6.7 cm. The volume fraction of the gel fibers, ϕ_f, has been determined from the responses to salt pulses. Small salt molecules (NaCl) can diffuse into all the pores of the gel. The difference between the elution volume of NaCl and the geometrical volume of the column gives the volume of the gel fibers. A value of 0.08 was found for this gel, the radius of the gel fiber, r_f was assumed to be 1.5 nm (Horneman *et al.,* 2004). The dead volume of the system (total volume between injection point and spectrophotometer minus the column volume itself) is determined by pulses of dextran blue and BSA. The void volume of the packed column is determined by dextran blue pulses.

Experiments

Pulses of 0.5 ml containing 2.5 g/l BSA (Sigma, cat no A 7906) and about $1.5*10^9$ phages/ml (DSMZ, DSM 5546) in a surfactant-buffer solution were injected. In all experiments, a 10 mM phosphate buffer, pH 6.8 containing 0.1 M NaCl and a known concentration of surfactant was used as eluent. The flow was kept constant at 1 ml/min. The surfactant used in these experiments was the non-ionic surfactant $C_{12}E_{23}$ (Acros organics, cat no 228345000). Various surfactant concentrations between 0 and 20% (w/w) were used in the eluent.
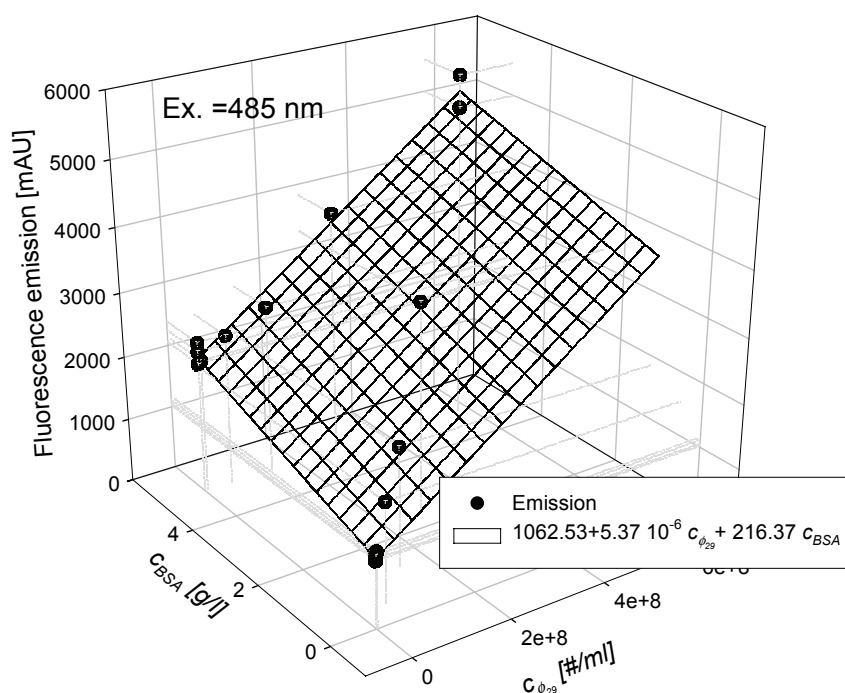
Figure 4.1. *Fluorescence calibration curve for $\phi29$ as function of the concentration of BSA*

Analyses

The samples were collected using a fraction collector (Frac-920, GE Healthcare). The protein concentration was determined off-line by a spectrophotometer (Ultrospec 2000, GE Healthcare) at 280 nm. The concentration of phages was determined using a PicoGreen® dsDNA quantification reagent (Molecular Probes, p11496). This is a fluorescent nucleic acid stain for quantification of double stranded DNA in solution. The samples were excited at 485 nm and the fluorescence emission intensity was measured at 520 nm using a fluorescence microplate reader (Tecan). A calibration curve was made, which also included the effect of the concentration of BSA on the analysis (Figure 4.1).

4.3.2   SMB experiments

Equipment

An 8-column carousel SMB was used for the SMB experiments. The SMB consisted of 3 sections with respectively 3, 3 and 2 columns (see figure 4.2). In total 3 Shimadzu LC-8A pumps were used for the desorbent, feed, and extract flow. The actual flow rates were determined by monitoring the change in weight during the experiment using Mettler Toledo balances (PG-S). The concentration of surfactant in the extract waste outlet was monitored by a Shimadzu UV-VIS detector (SPD-10AV) at 280 nm.
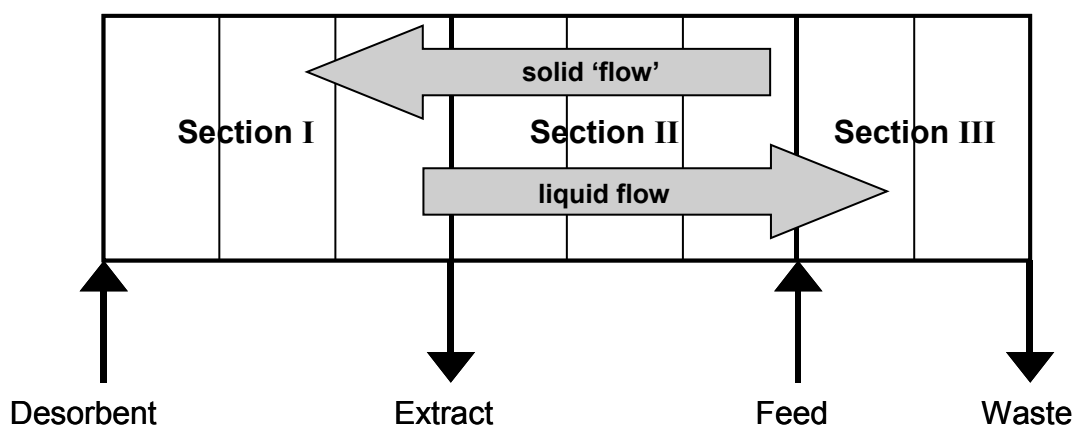
Figure 4.2. *SMB set-up used in the experiments*

Columns

The in-house made stainless steel columns had a diameter of 2 cm and a length of 10 cm. The columns were packed with Sephacryl^{TM} S300 HR (GE Healthcare, cat no. 17-0599-01) at 3 ml/min for 1 hour followed by a flow rate of 12 ml/min for 3 hours. The reproducibility of the packing procedure was checked by pulse experiments with dextran blue. The void volume was determined from the same pulse experiments. An average void fraction of 0.4 ± 0.02 was found for each column.

Experiments

Before each experiment the columns were 'regenerated' with a 10 mM phosphate buffer, pH 6.8, containing 0.15 M NaCl. After this step the feed inlet was changed to a 5 g/l BSA solution without ϕ29. When the BSA concentration was constant in the SMB, the feed was changed again to a 5g/l BSA solution containing the bacteriophage ϕ29. In the experiments with a surfactant gradient, the gradient was first positioned before the feed was changed to a BSA solution.

To measure the concentration profile in the SMB system, samples were taken at the inlet of one of the columns exactly halfway each switch-interval of the columns. To take the samples, an injection valve with a sample loop was placed before this column. At the time of sampling the sample loop was disconnected from the main flow path. The sample loop, filled with the sample, was emptied by injecting air in the sample loop. The sample loop was then loaded again with buffer and reconnected within the main flow path. The volume of the sample loop was only 0.3 ml and taking samples had no effect on the experimental profiles.

4.4   Results and discussion

4.4.1   Fixed bed experiments

The influence of $C_{12}E_{23}$ on the distribution behavior of BSA has been described previously (Horneman *et al.,* 2004). The influence of the same surfactant on the bacteriophage ϕ29 has been determined by pulse experiments using different surfactant concentrations in the mobile phase. Table 4.1 shows that although the micelle concentration influences the distribution behavior of BSA it does not influence the behavior of ϕ29. The diameter of ϕ29 is in the range of 42-60 nm (van Regenmortel *et al.,* 2000), which is larger than the pore size of S300, which is 13 nm (Hagel *et al.,* 1996). Diffusion of ϕ29 into the pores is thus not possible.

Table 4.1.   K-values of phi29 and BSA at different surfactant concentrations

c_{C12E23} [%, w/w]	$K_{\phi29}$ [-]	K_{BSA}[1] [-]
0	0	0.39
2.5	0	N.A.
5	0	0.51
7.5	0	0.63
10	0	0.67

1)   Data taken from Horneman *et al.*, 2004

Resolution

With a K-value of 0 for ϕ29, the selectivity is excellent. The resolution, however determines how good the separation really is. This resolution is depending on the difference in retention volumes and on the width of both response curves.

$$R = \frac{V_{e2} - V_{e1}}{\frac{1}{2} \cdot (W_1 + W_2)}$$

(4.15)

where V_e is the elution volume and W_i is the width of pulse *i*. These response curves are influenced by the *K*-value but also by the length of the column, flow rate, sample size and mass transfer characteristics (Giddings, 1965). In conventional SEC, a high resolution can only be obtained by increasing column length or decreasing the flow rate or the sample load. All these changes will also result in a reduced performance in terms of yield, productivity, solvent consumption and/or product concentration. SASEC is a tool to influence the resolution by changing the *K*-values, by changing only the solvent

conditions. This is demonstrated by the separation of BSA and ϕ29. Figures 4.3 and 4.4 show the pulse response curves in case of surfactant concentrations of 0 and 10% (w/w) in the mobile phase, respectively.
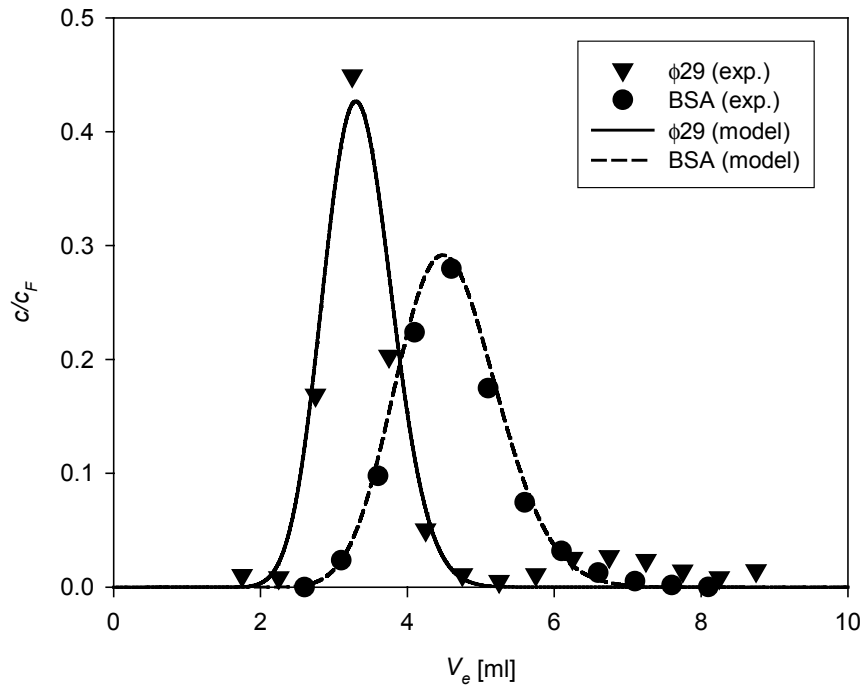

Figure 4.3. *Elution profiles of ϕ29 and BSA at 0% (w/w) of $C_{12}E_{23}$*
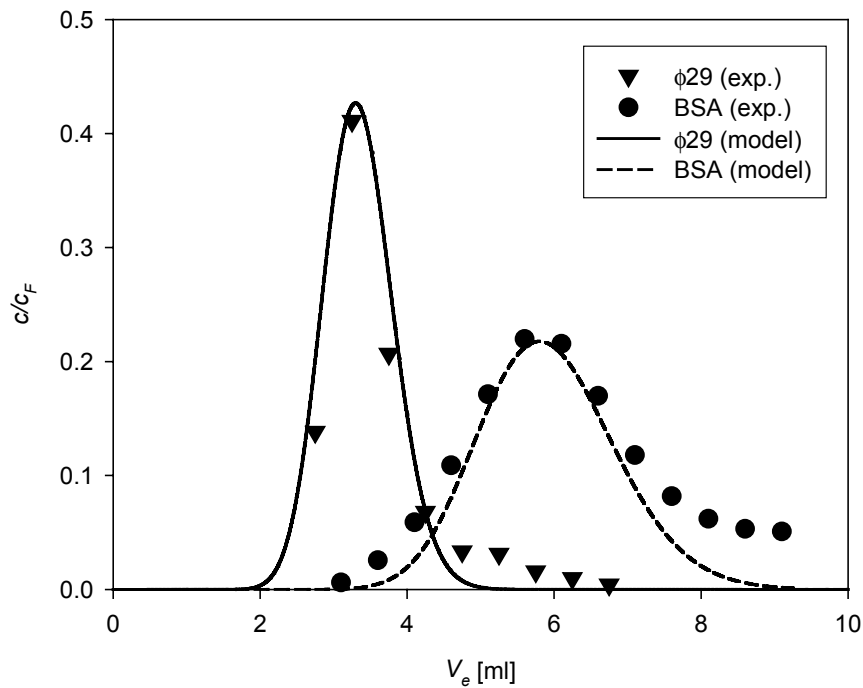

Figure 4.4. *Elution profiles of ϕ29 and BSA at 10% (w/w) of $C_{12}E_{23}$*

At 0% (w/w) the resolution is equal to 0.5. Adding 10% (w/w) of surfactant to the mobile phase increased the resolution to a value of 1. This higher resolution means that a higher *LRV* can be achieved with the same yield on BSA. Table 4.2 shows the differences in performance of the experiments. In the first two columns a comparison is made at a yield of 85 %. At this yield a substantially higher LRV is reached with SASEC. The LRV with SEC is even below 1, which cannot be considered as virus removal. Only, the productivity is less and the solvent consumption is higher with SASEC than with SEC. This is only due to the increase in cycle time in SASEC.

The last two columns of table 4.2 show the differences in performance at a LRV of 3.21. To reach this LRV-value in SEC, only a small fraction of BSA can be collected. As a result the productivity and yield decrease and the solvent consumption increases substantially.

Table 4.2. Comparison of yield (Y), productivity (PR) and solvent consumption (CS), log reduction value (LRV) using SEC (first and third column) and SASEC (second and last column)

	Comparison at Y = 0.85		Comparison at LRV=3.21	
	SEC	**SASEC**	**SEC**	**SASEC**
$c_{C_{12}E_{23}}$ [%, w/w]	0	10	0	10
Y	**0.85**	**0.85**	0.26	0.85
PR [g BSA/10^{-3} m^3 /d]	25.1	20.1	7.5	20.1
CS [l/g BSA]	10.7	13.4	35.8	13.4
LRV	0.87	3.21	**3.21**	**3.21**
c_{BSA} [g/l]	0.2	0.16	0.09	0.16

Concentration of BSA

Adding surfactant to the mobile phase does not significantly effect the product concentration of BSA. It remains diluted in both cases. In order to also solve this problem SASEC-SMB should be used.

4.4.2   SMB experiments

Area of separation

The SMB used in this paper contains only 3 sections (figure 4.2). In section II and III separation takes place, while in section I BSA is eluted. Normally a fourth section is used

to retain the other component at the other side of the SMB. In this paper this other component is $\phi 29$ cannot be retained because it is too large to enter the pores of the gel particles. Therefore section IV is omitted in this SMB.

The optimal way to use the SASEC concept in an SMB is by using a surfactant gradient. This gradient should have a low surfactant concentration in the first two sections and a high concentration in section III. In this the loading capacity of BSA will be increased in section III while a low surfactant concentration in section I and II facilitates the elution of BSA in these sections. Two types of gradients can be formed: an upward gradient, in which the surfactants are predominantly transported with the liquid flow, or a downward gradient in which the surfactant is predominantly transported with the solid phase (Houwing *et al.*, 2004) The constraints for separation in both cases are given in table 4.3. The derivation of these constraints is given elsewhere (Horneman *et al.*, 2006). In this paper the surfactant used is $C_{12}E_{23}$. This surfactant forms oblate shaped micelles that can be described by two radii of 4.13 nm and 3.66 nm, respectively (Horneman *et al.*, 2004). The formed micelles have a concave curved isotherm. This type of isotherm results in a shock front during loading of the column with a solution with increased surfactant concentration and a diffuse front during elution with a solution with a decreased surfactant concentration.

Table 4.3. Constraints for the flow ratios for positioning a gradient of $C_{12}E_{23}$ and the separation of BSA and phi29

Gradient	Front	Front shape	m
Upward	1	Shock	$\left(\dfrac{\Delta q}{\Delta c}\right)_{c_{III}-c_{D}}, \; K_{BSA} < m_{I}$ $\left(\dfrac{\Delta q}{\Delta c}\right)_{c_{III}-c_{D}}, \; K_{\phi 29} < m_{II} < K_{BSA}$
	2	Diffuse	$\left(\dfrac{\partial q}{\partial c}\right)_{c_{III}}, \; K_{\phi 29} < m_{III} < K_{BSA}$
Downward	1	Diffuse	$K_{BSA} < m_{I} < \left(\dfrac{\partial q}{\partial c}\right)_{c_{II}}$ $K_{\phi 29} < m_{II} < \left(\dfrac{\partial q}{\partial c}\right)_{c_{II}}, \; K_{BSA}$
	2	Shock	$K_{\phi 29} < m_{III} < \left(\dfrac{\Delta q}{\Delta c}\right)_{c_{II}-c_{D}}, \; K_{BSA}$

Figure 4.5 shows the distribution behavior of this surfactant compared to that behavior of BSA and ϕ29. In combination with the constraints in table 4.3 it can be seen that below 11% (w/w) of surfactant a downward gradient should be chosen. Above this concentration an upward gradient should be chosen. To prevent high viscosities in the SMB, a downward gradient is chosen. For all experiments the surfactant concentration in the desorbent was set to 9.5% (w/w).
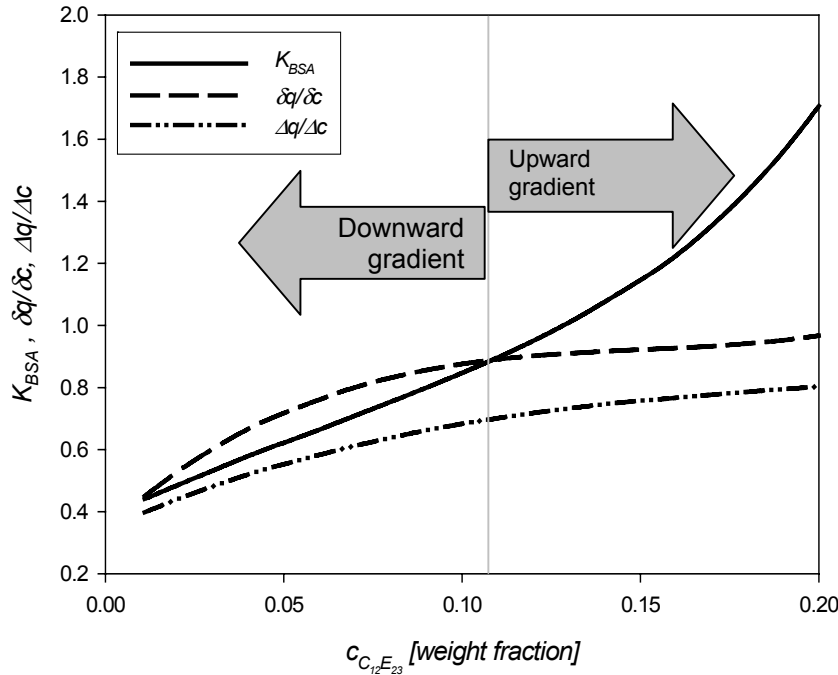
Figure 4.5. *Distribution behavior of ϕ29, BSA and $C_{12}E_{23}$ as function of the concentration of $C_{12}E_{23}$.*

With the constraints given in table 4.3, the area of separation is constructed at this desorbent concentration. This area of separation is given in Figure 4.6. The line m_I^{max} gives the m_{III} and m_{II} values at which the concentration of surfactant in section II becomes such that $K_{BSA} = \delta q/\delta c$. Above this line the constraint for m_I cannot be fulfilled. The boundary of m_{III} is further only depending on the constraints of $C_{12}E_{23}$, because K_{BSA}

$> \left(\dfrac{\Delta q}{\Delta c}\right)_{c_{II}-c_D}$ as can be seen in figure 4.5. In the same way it can be seen that m_{II} is only

depending on the constraint of BSA because $K_{BSA} < \left(\dfrac{\partial q}{\partial c}\right)_{c_{II}}$. The dark gray area in

Figure 4.6 represents the area of separation for the case that no surfactants are used.

From comparison of these two areas it can already be seen that a higher productivity is possible in SASEC-SMB compared to SEC-SMB
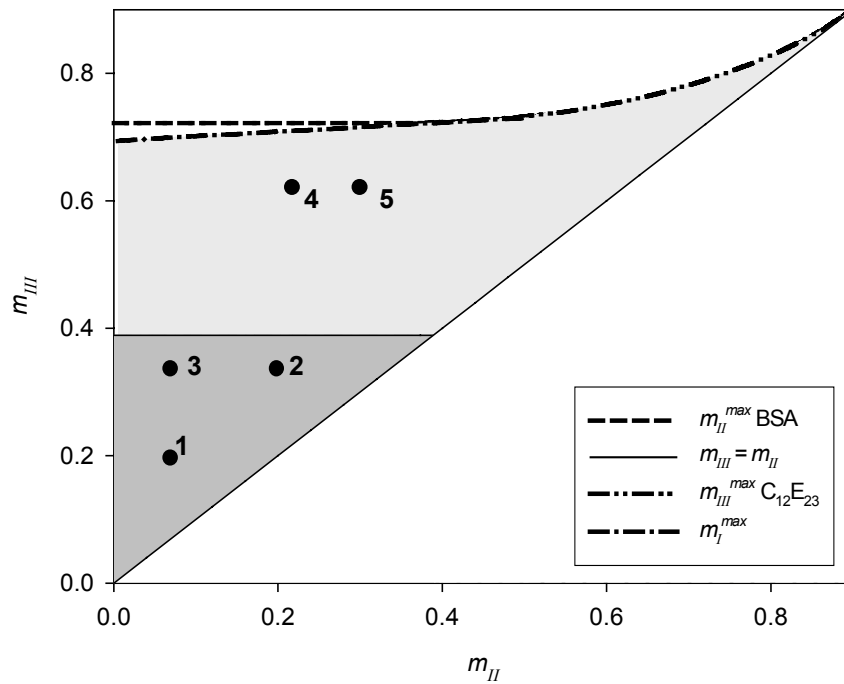
Figure 4.6.   *Area of separation for BSA and ϕ29 in SEC-SMB (dark gray area) and area of separation in SASEC-SMB (light and dark gray area). The dots give the m-values of the experiments*

The *m*-values chosen for the experiments are also given in figure 4.6. Table 4.4 also gives these *m*-values together with the flow rates and switch times of the experiments. The feed flow has been kept constant in each experiment for ease of comparison.

Table 4.4.   Parameters used during the SMB experiments

Exp.	m_I	m_{II}	m_{III}	Φ_D [ml/min]	Φ_E [ml/min]	Φ_F [ml/min]	τ [sec]	c_D [%, w/w]
1	0.40	0.05	0.20	7.0	2.2	1.0	180	0
2	0.40	0.20	0.35	7.0	1.3	1.0	180	0
3	0.40	0.05	0.35	3.8	1.2	1.0	330	0
4	0.54	0.20	0.60	3.2	0.9	1.0	450	9.5
5	0.60	0.30	0.60	4.3	1.0	1.0	345	9.5

4.4.3   SEC-SMB

Log reduction

The measured concentration profiles in the SMB are given in figure 4.7. From this figure it can be seen that the extent of viral clearance is mainly determined by the value of m_{II}. An increase of m_{II} causes the ϕ29-concentration profile to move more towards the right. A better clearance is thus achieved. The phages are too large to enter the pores of the gel material and will thus only move with the mobile phase. At larger flows this movement is faster and more ϕ29 is removed with the waste stream. The dynamic model describes the concentration profiles very well. The model has been used to determine the log reduction that can be achieved in the extract (product) flow. These log reductions are given in table 4.5.

Table 4.5.   Performance of the SMB experiments

Exp. #	LRV [-]	Y [-]	PR [g BSA/10^{-3} m³ (gel)/d]	CS [l/g BSA]	c_{BSA} [c/c_F]
1	2.7	0.92	22.0	1.5	0.41
2	11.1	0.88	21.0	1.6	0.68
3	3.8	0.95	22.7	0.79	0.79
4	12.3	0.98	23.3	0.65	1.1
5	16.9	0.96	23.0	0.93	0.96

BSA concentration

The maximal possible concentration of BSA is determined by:

$$c_{BSA,E}^{max} = \frac{m_{III} - m_{II}}{m_I - m_{II}} \cdot c_{BSA,F} \tag{4.16}$$

This can only be achieved when the yield on BSA is 1. Concentrating the product is therefore only possible when m_I has a lower value than m_{III}. This is however not possible in isocratic SMB due to the constraints of the m-values (see table 4.3). An m_I-value close to the m_{III} value will thus give the highest possible concentration. In the first 3 experiments the m_I - value has been kept constant. It can be seen from the figures that the concentration in the extract is indeed increasing when m_{III} is increased. Concentration of the product is, however, not possible in an isocratic mode.
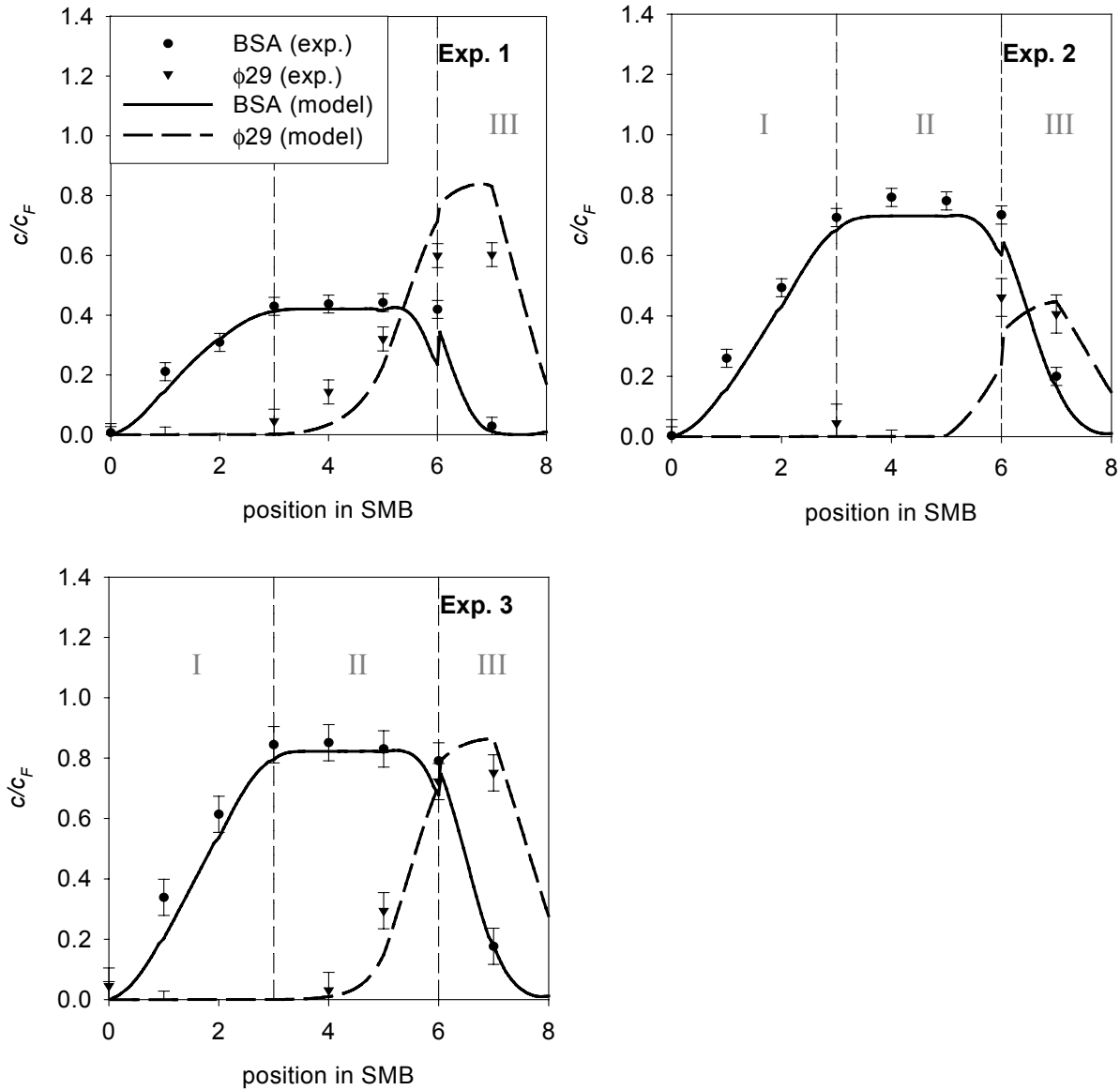
Figure 4.7. *Concentration profiles of BSA and $\phi29$ in the SEC-SMB experiments 1, 2 and 3.*

4.4.4   SASEC-SMB

Log reduction

In the isocratic surfactant-free experiments, it was found that an increase in m_{II} results in an increase in log reduction. When surfactants are introduced in the desorbent flow, higher m_{II} -values can be chosen (figure 4.6). Two experiments have been performed at $c_D = 9.5\%$ (w/w), the results can be seen in figure 4.7. The model predicts a better clearance compared to SEC-SMB and the experimental results confirm this to a limited

extent. In the fixed bed experiments no influence of surfactant was found on the distribution behavior of ϕ29. The bacteriophage cannot enter the pores of the gel and will thus be moved with liquid flow. The experimental results in the SASEC experiments, however, seem to show a larger deviation from the model prediction than the other experiments. This can be explained by several reasons. The concentration of ϕ29 in the last two experiments was twice as low as in the first three experiments. In the figures a relative concentration is given. The concentration of ϕ29 in section II was thus in the lower range of the detection limit and the error is larger in this range. It is also possible that the signal was the results of naked DNA from phages broken apart. Finally, the presence of surfactant can also influence the fluorescence measurements, which was not taken into account.

BSA concentration

Due to the surfactant gradient, it is now possible to choose an m_I that is equal to or even lower than m_{III}. This means that concentration of BSA should be possible. This is indeed the case in our experiments as can be seen in figure 4.8.

Solvent consumption

In all experiments the feed flow has been kept constant at 1 ml/min. This makes it easy to compare the desorbent flows of each experiment. In experiment 2 and 4 the same m_{II} value has been used. Besides the increase of the BSA concentration, the advantage of the SASEC experiment is also the decrease of the desorbent flow with almost a factor 2.

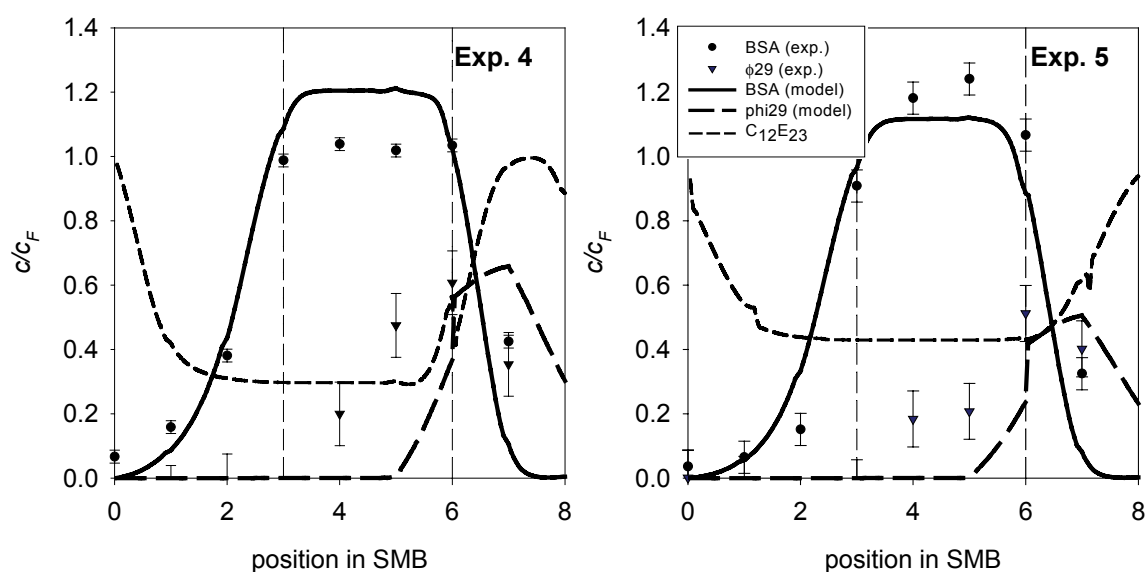**Figure 4.8.** *Concentration profiles of BSA and ϕ29 in the SASEC-SMB experiments 4 and 5.*

Productivity

The productivity does not seem to change much using SASEC-SMB instead of SEC-SMB. The reason is that for all experiments the same amount of gel and the same flow has been used. The productivity is thus only depending on the yield of the process (see equation 4.14). In experiment 2 the yield is significantly lower than in the SASEC-experiments, because BSA is lost via the waste stream. To prevent this loss, more column length is needed in section III. This will negatively influence the productivity. In experiments 1 and 3, the yield is about the same as in the SASEC experiments, but the achieved *LRV*-values are much lower. To get the same *LRV*-values as in the SASEC experiments, more column length is needed in section II. This will also result in lower productivity. The SASEC experiments, however, show both high yield and high *LRV*-values. Probably, in practice, lower *LRV*-values are already sufficient which means that a smaller bed length in section II can be used. In that case even higher productivity can be achieved with SASEC-SMB.

4.5   Conclusion

The separation of BSA and ϕ29 is performed using traditional SEC and using surfactant-aided SEC, i.e. SASEC. Pulse experiments in fixed bed chromatography showed that with SASEC the protein BSA was more distributed towards the solid phase than compared to using SEC. The micelles had no influence on the distribution behavior of ϕ29. Therefore, higher resolution could be achieved when using SASEC. The experimental results were in good agreement with the dynamic model, presented in this paper. This model uses the excluded volume theory to describe the distribution behavior of solutes between the mobile phase and solid phase in the presence of (non-ionic) micelles. Experiments and model showed that when using SASEC, larger LRV-values could be achieved than with SEC without loss of productivity or increase in solvent consumption.

Even larger *LRV*-values and lower solvent consumption can be achieved using the SASEC principle in simulated moving bed chromatography. The SMB-experimental results were in good agreement with the model. Evaluation of the results showed that higher productivity could be achieved with SASEC-SMB compared to SEC-SMB based on resin volume. Another advantage of SASEC-SMB is the absence of product dilution. It is even possible to concentrate the product, which is not possible with normal SEC-SMB. The complete validation of SASEC and its practical implications for GMP operation is matter for future research. This paper however shows the potential and advantages of SASEC in viral clearance.

Acknowledgements

Nomenclature

$c_{i,k}$	concentration of solute i in phase k
CS	solvent consumption
D	diffusion coefficient
D_{ax}	dispersion coefficient
d_p	particle diameter
H_i	integral of mean curvature of component i
K_i	distribution coefficient of component i
k_L	mass transfer coefficient at liquid side
$k_o a$	overall mass transfer coefficient
k_s	mass transfer coefficient at solid side
LRV	log reduction value
m_j	flow ratio in section j
PR	productivity
r_i	radius of component i
R	resolution
S_i	surface area of component i
t	time
U_{ij}	excluded volume between components i and j
v	interstitial velocity
V_e	elution volume
V_i	volume of component i
V_{inj}	injected volume
V_{out}	collected volume
W_i	peak width
x_i	number concentration of component i
Y	yield
z	distance
Φ	flow
ε	column void fraction
ϕ_i	volume fraction of component i
γ_{ij}	steric interaction parameter between components i and j
$\eta_m r_m$	semi-axis of oblate micelle

Δt_{cycle} cycle time

Sub and superscripts

D   desorbent
E   Extract
eq   equilibrium
F   feed
f   gel fiber
L   liquid phase
m   micelle
s   solid phase
I,II,III   section number in SMB

References

Adcock WL, MacGegor A, Davies JR, Hattarki M. Anderson DA Goss NH. 1998. Biotechnol. Appl. Biochem. 28: 85-94

Anderson DL, Hickman DD, Reilly BE. 1966. J of bacteriology. 91: 2081-2089.

Bosma JC, Wesselingh JA. 2000. J. Chromatogr. B 743: 169-180

Burnouf T, Radosewich M. 2003. Haemophilia 9: 24-37

Burnouf T, Griffiths E. Padilla A. Seddik S. Stephano MA, Gutiérrez JM. 2004. Biologicals 32:115-128.

Evans DF, Wennerström H. 1994. The Colloidal Domain, VCH publ., New York

FDA, Guidance on viral safety evaluation of biotechnology products derived from cell lines of human or animal origin, 1998

Guiochon GS, Golshan-Shirazi S, Katti AM. 1994. Fundamentals of Preparative and Nonlinear Chromatography, Academic Press, Boston

Hagel L, Ostberg M, Andersson T. 1996. J. Chromatogr. A. 743:33-42.

Horneman DA, Wolbers M, Zomerdijk M, Ottens M, van der Wielen LAM. J.Chromatogr. B. 2004; 807: 39-45.

Horneman DA, Ottens M, van den Broeke LJP, van Roosmalen D, Keurentjes JTF, van der Wielen LAM. 2004a. Patent EP1491246

Horneman DA, Ottens M, van der Wielen LAM, Keurentjes JTF. 2006. J. Chromatogr. A. 1113: 130-139

Houwing J, Billiet HAH, van der Wielen LAM. 2003. AICHE J. 49: 1158-1167

Jansons KM, Phillips CG. 1990. J Colloid Interface Sc. 137: 75-91

Kalyanpur M. 2002. Molecular Biotech. 22: 87-98

Lazzara MJ, Blankschtein D, Deen WM. 2000. J. Colloid Interface Sc. 226: 112-122

Levy RV, Phillips M, Lutz H. 1998. Filtration in biopharmaceutical Industry, Marcel Dekker, New York

Meijer WJJ, Horcajada JA, Salas M. 2001. Microbiology and Molecular Biology Reviews. 65:261-287

Ogston G. 1958. Trans Faraday Soc 54:1754-1757

Sober H.A. (ed.). 1970. CRC Handbook of Biochemistry: Selected Data for Molecular Biology (2nd ed.), The Chemical Rubber Co., Cleveland, Ohio

van Regenmortel *et al.* (eds). 2000. The Seventh Report of The International Committee on Taxonomy of viruses, Academic Press.

van Roosmalen D, Lazzara MJ, van den Broeke LJP, Keurentjes JTF, Blankschtein D. 2004. Biotech and Bioeng. 87: 695-703

Vonk P. 1994. Ph.D. Thesis, University of Groningen, Groningen

5

Surfactant-aided size-exclusion chromatography for the purification of IgG

Abstract

This paper shows the purification of monoclonal IgG from its heavy chain contaminant. The heavy chain fragment is simulated experimentally using BSA, which has approximately the same molecular weight. The purification is performed using traditional size-exclusion chromatography (SEC) and using surfactant-aided SEC, i.e. SASEC, testing two different surfactants ($C_{12}E_{23}$ and Tween20) and two different gels (Sephacryl^{TM} S200HR and Sephacryl^{TM} S300 HR).

Pulse experiments show that with SASEC both BSA and IgG are more distributed towards the solid phase than compared to using SEC. This effect is larger on IgG, the largest component than on BSA. As a consequence, azeotropes will be formed at a specific surfactant concentration. Above this concentration the selectivity is reversed and increased to values higher than obtained with conventional SEC. These experiments further show that when using SASEC larger productivity, higher yields and lower solvent consumption can be achieved without loss of purity of IgG when compared to conventional SEC.

Mathematical simulation of the separation of BSA and IgG using simulated moving bed (SMB) chromatography indicates a large increase in productivity when applying a surfactant gradient in SASEC-SMB compared to conventional isocratic SEC-SMB. Furthermore, solvent consumption reductions with a factor 15 prove possible as well as the concentration of the IgG by a factor 2.

*Keywords: monoclonal antibodies, surfactants, size-exclusion chromatography, protein purification, azeotrope, simulated moving bed chromatogra*phy.

5.1   Introduction

Monoclonal Antibodies have become a major tool in biological and medical research. They are used in nonclinical and clinical assays, for purification of other biological molecules and for treating diseases in humans and animals. The market of monoclonal antibodies is growing very fast and development of large scale manufacturing of monoclonal antibodies is therefore very important (Reuveny *et al.*, 1989). Antibodies consist of two heavy chains and two light chains (figure 5.1), which are linked by noncovalent and SS bonds. After the production of the monoclonal antibody, the separate chains of the antibody are often also present in the mixture as well as other contaminating proteins. These components should be removed from the whole antibodies. Affinity chromatography with a protein A coupled affinity matrix is often used in the purification of the monoclonal antibody IgG. Protein A binds selectively to the Fc-sites (Fragment crystallisable) on IgG (Das *et al*, 1985). This Fc-site is located on the heavy-chain of IgG (figure 5.1). Protein A can therefore be used to remove other proteins and chain fragments that do not contain this Fc-site. Single heavy chains contain this Fc-site and cannot be removed with protein A from the whole IgG molecule. Size-exclusion chromatography (SEC) can be an option to remove these heavy chain fractions. The main disadvantages of SEC, however, are the low selectivity and resolution, which can only be increased by increasing the column length or decreasing the sample load. Recently it has been shown that the selectivity and thus the resolution of size-exclusion chromatography can be changed in-situ, by using non-ionic surfactants in the mobile phase (Horneman *et al.,* 2004; Roosmalen *et al*., 2004; Horneman *et al.,* 2004a). Non-ionic surfactants form micelles at very low concentration. The extent to which biomolecules and bioparticles partition towards a phase containing "inert" micelles, depends on the volume fraction of the micelles and the diameter ratio of the solute versus the micelles. These parameters and thus the selectivity can be changed in-situ by varying the solution conditions, such as concentration and type of surfactants, temperature, and the addition of salts (Evans *et al.*, 1994; Horneman *et al.,* 2004; Roosmalen *et al*., 2004).

This paper demonstrates the application of surfactant-aided size-exclusion chromatography (SASEC) in the purification of IgG from its heavy chain fragments. IgG is a monoclonal antibody with a molecular size of about 150 kDa. A single heavy chain will have a molecular weight of about 50 kDa. BSA has a molecular weight of about 67 kDa and is taken as a model for this heavy chain. The potential of using SASEC in the purification of IgG is shown in both fixed bed and simulated moving bed chromatography.
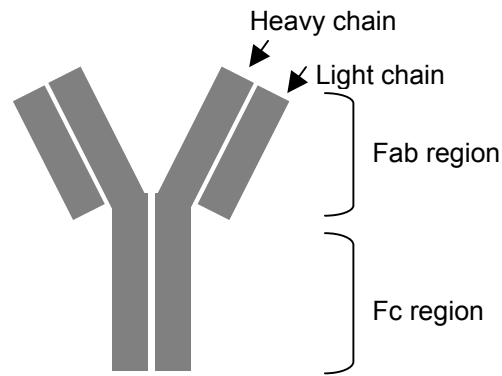
Figure 5.1. *A schematic representation of a monoclonal antibody.*

5.2 Theory

5.2.1 Distribution coefficients in size-exclusion chromatography

The elution of solute *i* is characterized by its distribution coefficient, K_i, which is defined as the ratio of the solute concentration in the solid phase, $c_{i,s}$ over the solute concentration in the liquid phase, $c_{i,L}$ at equilibrium. Throughout this paper, the solid phase is defined as the total gel volume, including the fibers and the pores of the gel particles.

$$K_i = \frac{c_{i,s}}{c_{i,L}}$$

(5.1)

Relatively large solutes cannot diffuse into the pores and have a *K*-value close to 0, whereas relatively small solutes can diffuse into the pores relatively easily and have higher *K*-values. K_i can be experimentally evaluated by the determination of the experimental elution volume, V_e of a given solute by means of pulse experiments in a chromatographic column. The elution volume is then normalized to a column-independent distribution coefficient by (Fisher, 1980):

$$K = \frac{V_e - V_0}{V_t - V_0}$$

(5.2)

where V_0 is the volume of the mobile phase in the column and V_t is the total volume of the column.

In size-exclusion chromatography the distribution coefficient can be described by an excluded volume model that describes the steric interactions among the solutes and the

fibers (Horneman *et al.*, 2004; Bosma *et al.,* 2000; Ogston, 1958). In this model, all volumes excluding a solute due to the presence of all types of fibers and solutes, including the solute itself, are calculated in each phase. The general equation (Lazarra *et al.,* 2000) is given by:

$$K_i = exp\left(-\sum_j \chi_{ij,s} + \sum_j \chi_{ij,L}\right)$$

(5.3)

where the dimensionless number $\chi_{ij,k}$ is the total excluded volume of solute *i* and a set of objects *j* per volume of phase *k*.

In conventional SEC, the second term on the right hand side of equation 5.3 will be zero at low concentration of the solute. In surfactant-aided SEC (SASEC), micelles are added to the mobile phase. The excluded volume of the solute and these micelles should be taken into account in the calculation of *K*. This excluded volume interaction between the solute and the micelles will increase the distribution of the solute to the solid phase. Previous papers show that the distribution coefficient is indeed increased at increasing surfactant concentrations (Horneman *et al.* 2006; van den Broeke *et al.* 2006; van Roosmalen *et al.*, 2004; Horneman *et al.* 2004)

5.2.2   Separation performance

The performance of the separation is described in terms of purity (*Pu*), Yield of product (*Y*), Productivity (*PR*), product concentration (c_{BSA}) and solvent consumption (*CS*). In the fixed bed experiments, productivity and solvent consumption are defined as:

$$PR = \frac{c_{BSA\_in} V_{inj} Y}{\Delta t_{cycle} V_s}$$

(5.4)

$$CS = \frac{\Delta t_{cycle} \Phi}{c_{BSA\_in} V_{inj} Y}$$

(5.5)

where V_{inj} is the volume of the sample injected to the column, Δt_{cycle} is the time between two sample injections and Φ is the flow rate.

In the SMB these terms are defined as:

$$PR = \frac{c_{BSA,F} \Phi_F Y}{V_s}$$

(5.6)

$$CS = \frac{\Phi_D}{c_{BSA,F} \Phi_F Y}$$
(5.7)

Where the subscripts *D* and *F* stand for desorbent and feed respectively.

5.3   Materials and methods

5.3.1   Determination distribution coefficient IgG and BSA

Columns

Two Omnifit glass columns (SigmaAldrich) with an internal diameter of 10 mm were used in an FPLC Äkta Explorer (GE Healthcare). One column was packed with Sephacryl™ S300 HR (GE Healthcare, cat no. 17-0599-01) up to a height of 9.4 cm. The other column was packed with Sephacryl™ S200 HR (GE Healthcare, cat no. 17-0599-01) up to a height of 8.7 cm. The dead volume of the system, which is the total volume between injection point and spectrophotometer minus the column volume itself, is determined by pulses of dextran blue and BSA. The void volume of the packed column is determined by dextran blue pulses.

Experiments

Pulses of 0.1 ml containing 1 g/l BSA (Sigma, cat no A 7906) or 0.1 g/l IgG (kindly supplied by Organon) in a surfactant-buffer solution were injected. In all experiments, a 10 mM phosphate buffer at pH 6.8 containing 0.1 M NaCl and a known concentration of surfactant was used as eluent. The flow was kept constant at 1 ml/min. The surfactants used in these experiments were the non-ionic surfactant $C_{12}E_{23}$ (Acros organics, cat no 228345000) and the non-ionic surfactant Tween20 (Sigma, cat. no. P1379). Various surfactant concentrations between 0 and 20% (w/w) were used in the eluent.

5.3.2   Separation of IgG and BSA

For the separation of IgG and BSA, a pre-packed XK 16/60 column S300HR (GE Healthcare) was used. Pulses of 0.5 ml containing 0.75 g/l fluorescent BSA (Sigma, cat no A9771) and 0.66 g/l IgG in a surfactant-buffer solution were injected. In all experiments, a 10 mM phosphate buffer, pH 6.8 containing 0.1 M NaCl and a known concentration of surfactant was used as eluent. The flow was kept constant at 0.7 ml/min. In these separation experiments only the non-ionic surfactant $C_{12}E_{23}$ (Acros organics, cat no 228345000) was used. The experiments were performed at 0 and 7.5% (w/w) surfactant in the eluent.

Analyses

The concentration of IgG and BSA at the outlet of the column was determined on-line by a spectrophotometer at 280 nm. In the separation experiments, fluorescent BSA was used which was detected at 280 and 495 nm.

5.3.3 Modeling of the separation in SMB chromatography

The separation of IgG and BSA using an open loop SMB is simulated using a dynamic model as described below. In this model the concentration profiles were simulated by numerical integration of the mass balance equations on the liquid and solid phase (Guiochon *et al.,* 1994):

$$\frac{\partial c_{i,L}}{\partial t} = -u\frac{\partial c_{i,L}}{\partial z} + D_{ax}\frac{\partial^2 c_{i,L}}{\partial z^2} - \frac{1-\varepsilon}{\varepsilon}\frac{\partial c_{i,s}}{\partial t} \tag{5.8a}$$

$$\frac{\partial c_{i,s}}{\partial t} = k_0 a\left(c_{i,s}^{eq} - c_{i,s}\right) \tag{5.8b}$$

where u is the interstitial velocity, ε is the void fraction in the column, $k_o a$ is the overall mass transfer coefficient, calculated by:

$$\frac{1}{k_o a} = \frac{d_p}{6}\left(\frac{K}{k_L} + \frac{1}{k_s}\right) \tag{5.9}$$

where k_L and k_s are the mass transfer coefficients at the liquid side and solid side respectively. These can be calculated from the Sherwood number. For the Sherwood number on the solid side a value of 10 is used (Bosma *et al.*, 2000). K is the distribution coefficient, which depends on all actual volume fractions as is shown in equation 5.3. The liquid diffusion coefficient of BSA is $D_{BSA} = 6\cdot10^{-11}$ m^2/s (Sober *et al.,* 1970). The diffusion coefficient of IgG is calculated from the Stokes-Einstein relation, which gives $D_{IgG} = 3\cdot10^{-11}$ m^2/s. The intraparticle diffusion coefficient, D_s was calculated from these liquid diffusion coefficients by (Vonk, 1994):

$$D_s = D_L\ exp\left(-\phi_f^{0.5}\frac{r_i}{r_f}\right) \tag{5.10}$$

For spatial discretization of the convection term, a second order backward discretization scheme was used. The axial dispersion was approximated by numerical dispersion (Guiochon *et al.,* 1994). The resulting system of ODE's is solved in time by a fourth order Runga-Kutta method.

5.4   Results and discussion

5.4.1   Distribution coefficient of IgG and BSA

$C_{12}E_{23}$ and S200HR

The distribution coefficient of IgG and BSA was determined from the pulse experiments. From the two gel materials tested, S200 is considered as the best gel material to use in conventional SEC for the separation of BSA and IgG (Hagel *et al.,* 1989). Therefore this gel material was first tested. Figure 5.2 shows the results of these experiments. IgG is the larger component has a lower K-value than BSA in conventional SEC. The distribution coefficient of both components increases with increasing surfactant concentration. Figure 5.2 also shows that this increase is larger for IgG than for BSA. As a result the selectivity first decreases at increasing surfactant concentration. At approximately 8% (w/w) the *K*-values of both components are equal and the mixture will form an azeotrope. Above this concentration, the selectivity is reversed and increases to values larger than obtained in conventional SEC.
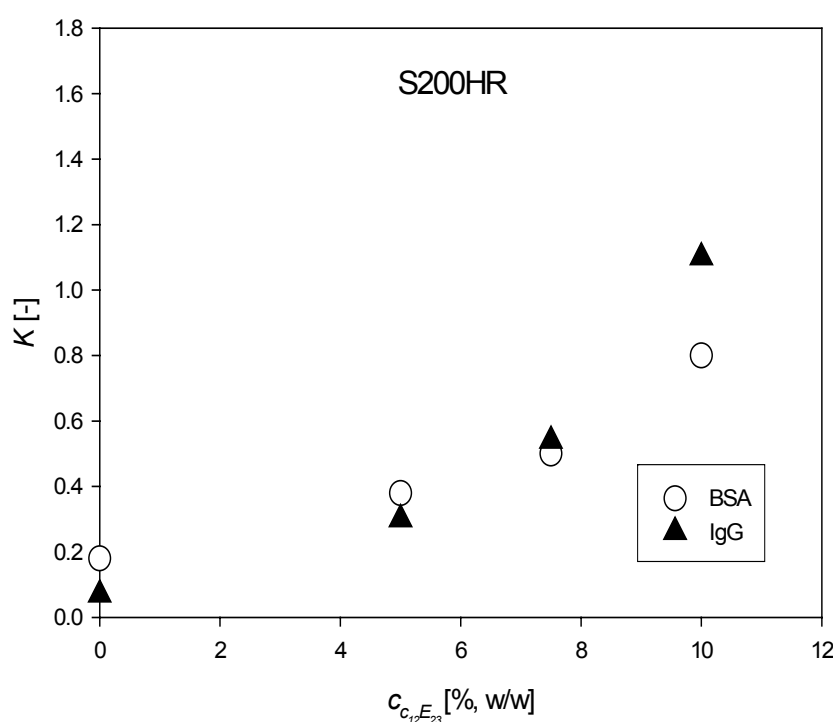

Figure 5.2.   *Distribution coefficient of BSA and IgG as function of the concentration of $C_{12}E_{23}$ using Sephacryl^{TM} S200HR*

$C_{12}E_{23}$ and S300HR

The main difference between S200 and S300 is the size of the pores. S200 has smaller pores than S300 (Hagel *et al* 1996). In conventional SEC S300 will give lower selectivity in the separation of BSA and IgG. This is however beneficial for SASEC in which the selectivity first needs to be reversed before it can be increased. The lower the selectivity at 0% (w/w) the lower the concentration at which this reversion point or azeotrope is reached. Figure 5.3 shows that with S300 this azeotrope is already reached at 5% (w/w). Above this concentration better selectivity can be reached than compared to conventional SEC using S300 or S200. The data further shows that introducing micelles in the mobile phase increases the distribution coefficients of the proteins beyond the normal range found in SEC, i.e. between 0 and 1. At 10% (w/w) IgG has a distribution coefficient of 1.6.

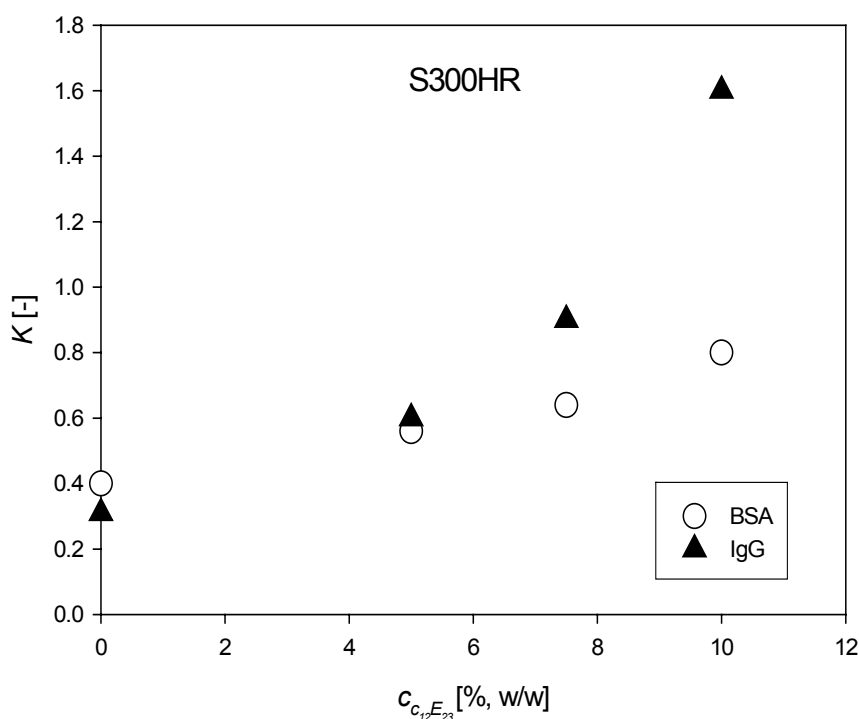***Figure 5.3.*** *Distribution coefficient of BSA and IgG as function of the concentration of $C_{12}E_{23}$ using Sephacryl^{TM} S300HR*
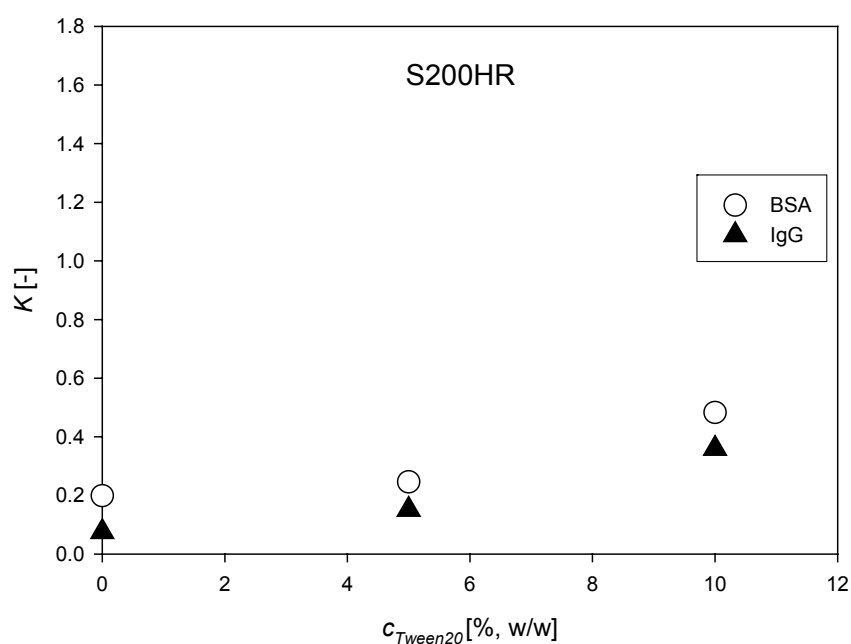
Figure 5.4. *Distribution coefficient of BSA and IgG as function of the concentration of Tween20 using Sephacryl^TM S200HR*
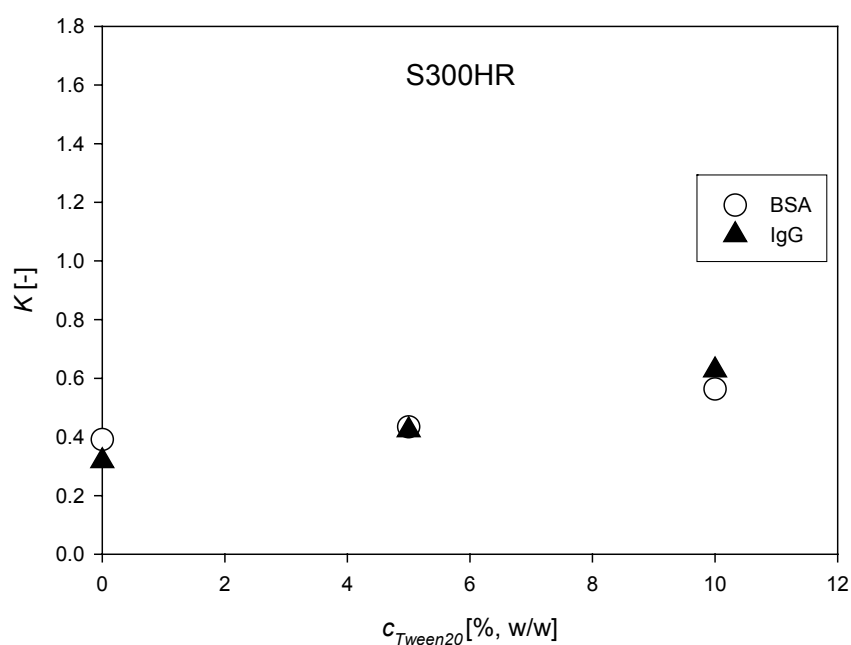

Figure 5.5. *Distribution coefficient of BSA and IgG as function of the concentration of Tween20 using Sephacryl^TM S300HR*

Tween20

The same experiments have been performed with Tween20. Tween20 is a non-ionic surfactant that forms spherical micelles with a radius of 2.5 nm (Mahajan *et al.,* 2004). These micelles are smaller than the micelles formed by $C_{12}E_{23}$, which have a radius of about 4 nm (Tanford *et al.,* 1977). In previous studies it was shown that smaller micelles will have a larger effect on the distribution coefficient (Liu *et al.*, 1998; van Roosmalen *et al.,* 2004; Horneman *et al.,* 2004). Figures 5.4 and 5.5 show the distribution coefficient as function of the concentration of Tween20. For both gel materials an increase in distribution coefficient is seen at increasing concentration although no inversion of the selectivity is seen when S200HR is used. The increase is not as large as seen with $C_{23}E_{23}$. This can be explained by the fact that the concentrations are expressed in weight fractions of the surfactant, while the distribution coefficient is depending on the volume fraction of the micelles (Liu *et al.*, 1998; van Roosmalen *et al.,* 2004; Horneman *et al.,* 2004). The following conversion can be used:

$$x_{vol} = Ax_{wt} \tag{5.11}$$

with:

$$A = \frac{\rho N_{av}}{Mw_{surf}N} V_m \tag{5.12}$$

Where ρ is the density of the solution, N_{av} the Avogadro number, Mw_{surf} the molecular weight of the surfactant and N the aggregation number of the micelle. For Tween20 the conversion factor A is 1.067 while for $C_{12}E_{23}$ the conversion factor is 2.629. This means that the volume fraction of Tween20 is almost the same as the weight fraction, while for $C_{12}E_{23}$ the volume fraction is 2.6 times the weight fraction of the surfactant.

The effects of the smaller Tween20 micelles might be larger on the basis of the volume fraction of the micelles. But higher surfactant concentrations are needed to reach the same volume concentration of micelles as with $C_{12}E_{23}$.

5.4.2   Separation of IgG and BSA

For the separation of BSA and IgG the XK16/60 column was used, which was packed with S300HR. In the first experiment no surfactant was used. Figure 5.6 shows that IgG, the larger component, elutes before BSA. The resolution of this separation is very low. In the second experiment, a concentration of 7.5% (w/w) $C_{12}E_{23}$ is used. At this concentration K_{IgG} is larger than K_{BSA}. Figure 5.7 shows that now indeed BSA is eluted

before IgG. At this concentration the selectivity should also be increased (see figure 5.2). The peaks are indeed more separated and a better resolution is obtained.
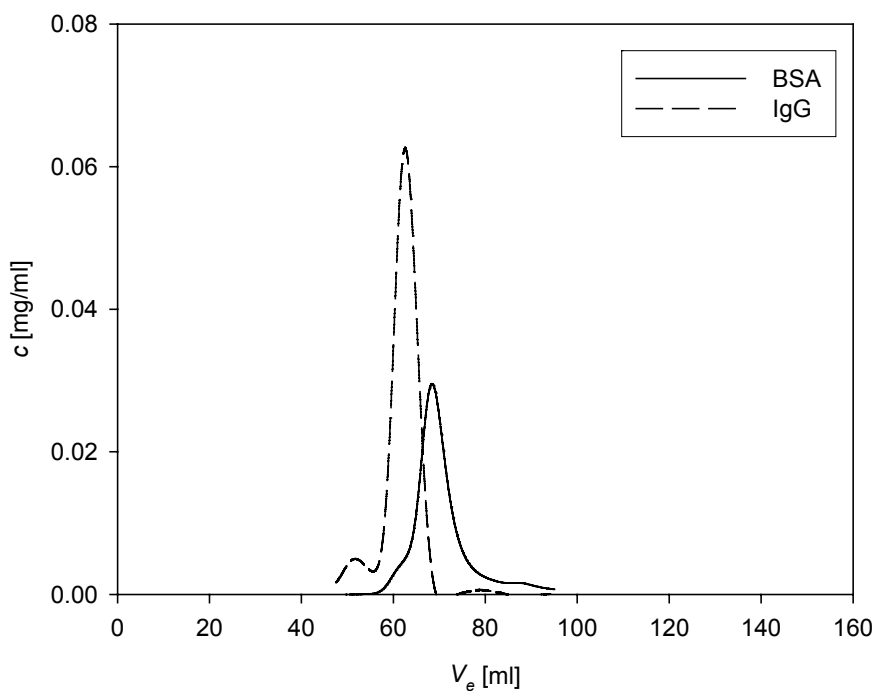

Figure 5.6.   *Separation of IgG and BSA using S300HR. No surfactants are added*
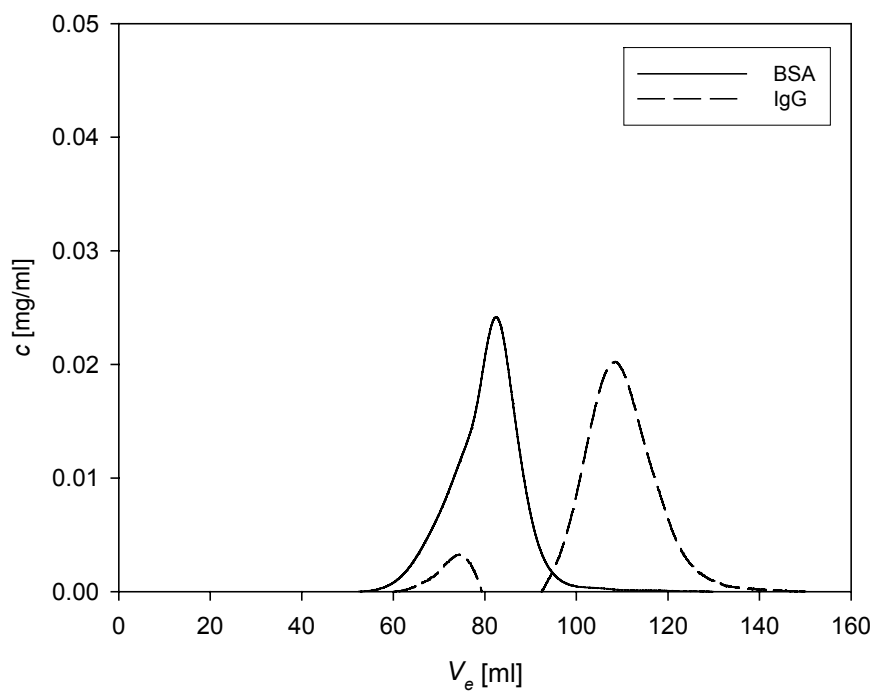

Figure 5.7.   *Separation of IgG and BSA using S300HR, 7.5% (w/w) surfactant $C_{12}E_{13}$ is added to the eluent.*

In both separations an extra peak appears, with unknown identity, which was absent in the small scale pulse experiments of each separate component. One possible cause may be the interaction between BSA and IgG, although the concentrations of both components are very low. Another possibility is interaction between $C_{12}E_{23}$ and BSA or IgG. This was not seen in the pulse experiments on the small columns, but has become visible in these experiments due to the longer contact time. This however does not explain the extra peak in the first separation in which no surfactant has been used. Due to the very low concentrations it is however also possible that the extra peak is the result of a measurement error, or a sample impurity, not visible in the small scale pulse experiments.

The performance of both separations is expressed in terms of productivity, solvent consumption and purity. For the comparison of the two methods the purity of IgG was fixed at 99%. The results are shown in table 5.1. To reach this purity in conventional SEC, only a small fraction of IgG can be collected resulting in a very low yield of 11%. Using 7.5% (w/w) of $C_{12}E_{23}$ in SASEC the resolution is increased and a larger fraction of IgG can be collected. The yield is increased to 76% while the productivity is increased with a factor of 4. The increase in productivity is not as large as the increase in the yield, which can be explained by the increase in cycle time due to the longer residence time in the column. The solvent consumption is decreased with more than a factor of 4 in SASEC.

Table 5.1. Comparison of yield (Y), productivity (PR), solvent consumption (CS), and purity (Pu) using SEC and SASEC.

	SEC	SASEC
$c_{C_{12}E_{23}}$ [%, w/w]	0	10
Y	0.11	0.76
PR [g IgG/m^3 /d]	3.5	15.7
CS [l/g IgG]	2664	595
Pu [%]	**99**	**99**

The performed separations are not optimized. In both cases it is possible to increase the yield without lowering the purity by, for example, increasing the column length. Increasing the column length will improve the resolution by the following relation:

$$R_s \propto \sqrt{L}$$ (5.13)

When both methods have the same resolution, the yield and purity will be about the same for SEC and SASEC. Table 5.2 shows the results of this calculation when a resolution of 1 is aimed for. In conventional SEC the column length has to be increased with a factor 3 while for SASEC the length only has to be increased with a factor 1.5. The cycle time will be increased with about the same factor as the length of the column. It is assumed that in both cases a yield of 90 % will be possible at this resolution at the same purity as in the experimental results. Using equation 5.7 to 5.8 the productivity and solvent consumption are calculated. Also in this more optimized situation, SASEC gives higher productivity and lower solvent consumption.

Table 5.2. Comparison of column length (L), productivity (PR), solvent consumption (CS), and purity (Pu) using SEC and SASEC at a resolution of 1.

	SEC	SASEC
$c_{C_{12}E_{23}}$ [%, w/w]	0	10
Rs	1	1
L [cm]	180	90
PR [g IgG/m^3 /d]	3.1	7.7
CS [l/g IgG]	921	758

5.4.3   Prediction of the distribution coefficients of BSA and IgG

In previous papers (Horneman *et* al, 2004, 2006*)* it was shown that the distribution coefficient of proteins in SASEC can be described by the excluded volume model given by equation 5.3. BSA can be assumed as a spherical protein and the micelles formed by $C_{12}E_{23}$ as oblate shaped micelles. For dilute BSA solutions equation 5.3 then becomes (Jansons *et al.*, 1989; Lazarra *et al.*, 2000; Horneman et al 2004):

$$K_i = exp\left(\frac{-ln\left(\frac{1}{1-\phi_f}\right)\left(1+\frac{r_i}{r_f}\right)^2 - \left(ln\left(\frac{1}{1-\phi_{m,s}}\right) - ln\left(\frac{1}{1-\phi_{m,L}}\right)\right) \cdot}{\left(1+\frac{1}{\eta_m}\left(\frac{r_i}{r_m}\right)^3 + \frac{3}{2}\left(\frac{r_i}{r_m}\right)^2 \frac{g(\eta_m)}{\eta_m} + \frac{3}{2}\left(\frac{r_i}{r_m}\right)\frac{f(\eta_m)}{\eta_m}\right)} \right) \qquad (5.14)$$

with:

$$f(\eta_m) = 1 + \eta_m^2 \left(1 - \eta_m^2\right)^{-1/2} \cosh^{-1}\left(\eta_m^{-1}\right)$$

$$g(\eta_m) = \eta_m + \left(1 - \eta_m^2\right)^{-1/2} \cos^{-1}\left(\eta_m\right)$$

Where r is the radius, ϕ is the volume fraction. The subscripts f and m indicate the gel fiber and the micelle. An oblate micelle is defined by three semi-axes r_m, r_m and $\eta_m r_m$ where $\eta_m < 1$. The concentration of micelles in the solid phase can be calculated using the distribution coefficient of the micelle itself. This distribution coefficient can again be calculated using equation 5.3 (Horneman *et al.*, 2004).
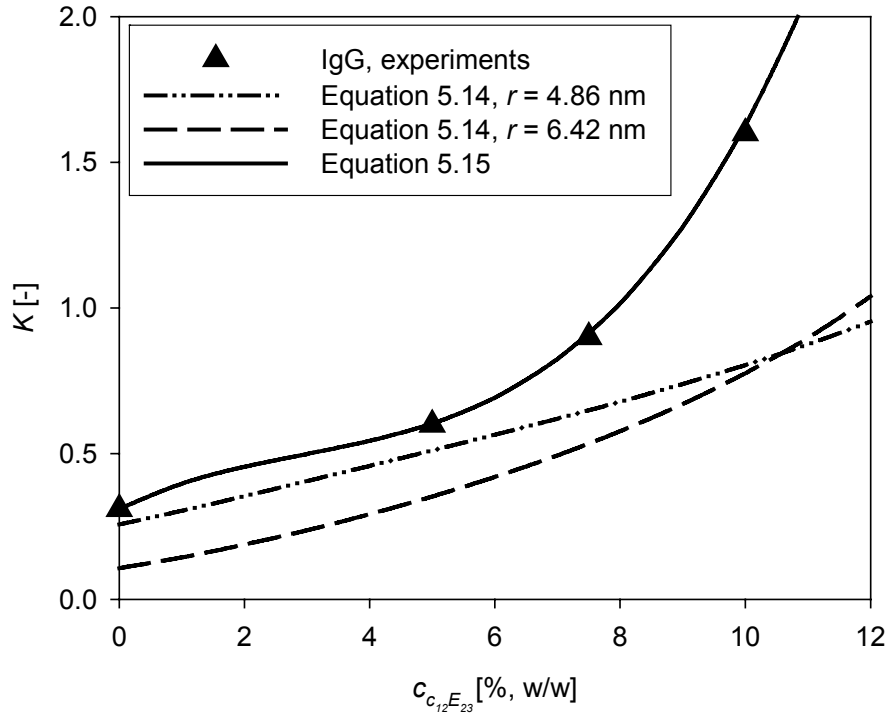

Figure 5.8. *Distribution coefficient of IgG as function of the surfactant concentration. The triangles give the experimental values the broken lines the excluded volume model with two different assumption of the radius of IgG. The solid line gives a polynomial function fitted through the data points.*

The same relation can be used for IgG, assuming IgG to be a spherical protein. If IgG is assumed as a solid sphere, the radius of this sphere will be approximately 4.8 nm (Harris *et al.*, 1998; Tessier *et al.*, 2002). IgG can also be seen as a tetrahedron inside a sphere with a circumradius of approximately 6.5 nm (Harris *et al.*, 1995). Both assumptions for the radius are used to predict the distribution coefficient of IgG. Figure 5.8 shows that neither assumption gives a good prediction. Of course IgG is not spherical and therefore also other shapes are considered. A cylinder oblate, prolate and tetrahedron are the shapes that have been used to calculate the excluded volume in equation 5.3. None of these shapes gave good results. Therefore, in this paper, a polynomial is fitted through the data points. This gave the following relation for the distribution coefficient:

$$K_{IgG} = 0.31 + 10.57(c_{surf}) - 214(c_{surf})^2 + 2400(c_{surf})^3 \qquad (5.15)$$

This relation, however, does not have a physical meaning but can be used for the prediction of the distribution coefficient of IgG as function of the concentration of $C_{12}E_{23}$.

5.4.4   Separation of BSA and IgG in Micellar Gradient SMB

Area of separation

The optimal way to use the SASEC concept in an SMB is by using a surfactant gradient. (Jensen *et al.,* 2000; Horneman *et al.,* 2006). The gradient should have a low surfactant concentration in the first two sections and a high concentration in sections III and IV (see figure 5.9). In this way the loading capacity of BSA and IgG will be increased in sections III and IV while a low surfactant concentration in sections I and II facilitates the elution of BSA and IgG in these sections.
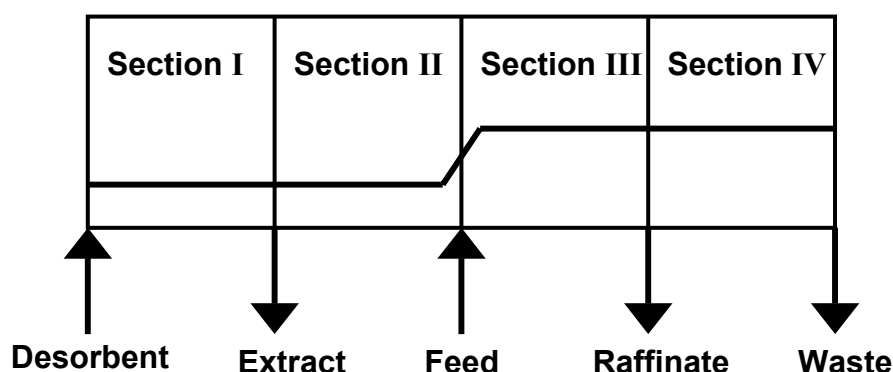
Figure 5.9.   *The preferred micellar gradient in a four section SMB.*

Two types of gradients can be formed: an upward gradient, in which the surfactants are predominantly transported with the liquid flow, or a downward gradient in which the surfactant is predominantly transported with the solid phase (Houwing *et al.,* 2003). In this paper, the surfactant used in the simulations is $C_{12}E_{23}$. For this separation, an upward gradient is chosen because of the relative high distribution coefficients of BSA and IgG compared to that of the micelles (Horneman *et al.,* 2004). The formed micelles have a concave curved isotherm. This type of isotherm results in a shock front during loading of the column with a solution with increased surfactant concentration and a diffuse front during elution with a solution with a decreased surfactant concentration. To avoid

problems with a possible azeotrope the surfactant concentration should be above 5% (w/w) in all sections. The constraints for the separation are:

$$\left(\frac{\Delta q}{\Delta c}\right)_{c_{III}-c_D}, K_{IgG}(c_D) \quad < \quad m_I$$

$$\left(\frac{\Delta q}{\Delta c}\right)_{c_{III}-c_D}, K_{BSA}(c_D) \quad < \quad m_{II} \quad < \quad K_{IgG}(c_D)$$

$$\left(\frac{\partial q}{\partial c}\right)_{c_{III}}, K_{BSA}(c_{III}) \quad < \quad m_{III} \quad < \quad K_{IgG}(c_{III})$$

$$\left(\frac{\partial q}{\partial c}\right)_{c_{III}} \quad\quad\quad < \quad m_{IV} \quad < \quad K_{BSA}(c_{III})$$

The derivation of these constraints is given elsewhere (Horneman *et al.*, 2006).
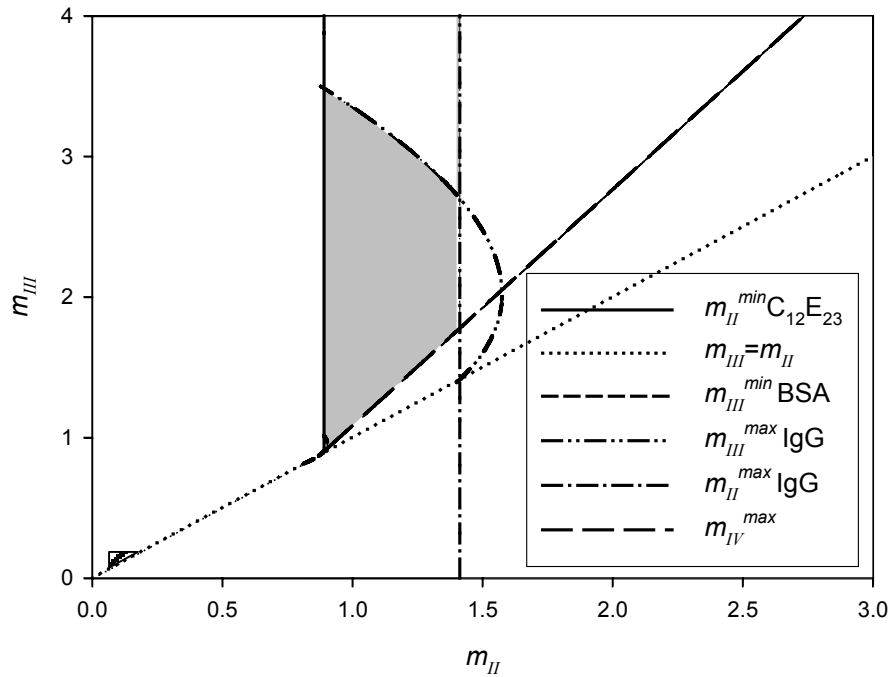

Figure 5.10. *Area of separation for the separation of IgG and BSA using an upward micellar gradient in SASEC-SMB, with c_D=7.5% (w/w) and c_F = 13% (w/w). The small triangle in the left bottom corner gives the area of separation in case of conventional SEC-SMB.*

In the simulation 7.5% (w/w) is added to the desorbent and 13% (w/w) to the feed. The area of separation is given in figure 5.10. The line $m_{IV}{}^{min}$ gives the m_{III} and m_{II} values at which the concentration of surfactant in section III becomes such that $K_{BSA} = \partial q/\partial c$. Below this line the constraint for m_{IV} cannot be fulfilled. The performance of SASEC-SMB will be compared with normal SEC-SMB using Sephacryl™ S200. Figure 5.10 also shows the area of separation in case of conventional SEC-SMB using S200, using the K-values found in the pulse experiments at 0% (w/w). From comparison of these two areas it can already be seen that a higher productivity is possible in SASEC-SMB compared to SEC-SMB.

5.4.5   Comparison SASEC-SMB and SEC-SMB

For all simulations a 4 section SMB was used which 10 columns of 15 cm length and a diameter of 2 cm. In both the SEC-SMB and SASEC-SMB the best configuration was to have 2 columns in sections I and IV and 3 columns in sections II and III.

Table 5.3 gives all parameters used in the calculations. The flows in the different sections are calculated with (Migliorini *et al.*, 1999):

$$\Phi_i = \frac{mV_c(1-\varepsilon)+V_c\varepsilon+V_d}{\tau} \tag{5.16}$$

Where V_c is the column volume and V_d is the dead volume per column

Table 5.3.   Parameters used in the simulation of the separation of IgG and BSA in conventional SEC-SMB and in SASEC-SMB

	SEC-SMB	SASEC-SMB
m_I	0.3	2
m_{II}	0.1	0.95
m_{III}	0.15	3
m_{IV}	0.05	0.95
c_D [%, w/w]	0	9.5
c_F [%, w/w]	0	13
τ [s]	90	90
c_{IgG_F} [g/l]	1	1
c_{BSA_F} [g/l]	1	1

Productivity

In both simulations the same number of columns of the same size is used. Also the switch time was kept constant at 90 sec. The results of both simulations are given in table 5.5. In both simulations a recovery of 99.9% was achieved as well as purity of IgG of more than 99%. The productivity that can be reached with SASEC is almost 40 times higher than compared to the productivity reached with SEC. This is due to the higher feed flow that is possible in SASEC.

Solvent consumption

Although the desorbent flow is larger in SASEC the solvent consumption per unit product is decreased with a factor 15. This is due to the high productivity that is obtained with SASEC-SMB.

Concentration

The maximal possible concentration of IgG is determined by:

$$c_{IgG}^{max} = \frac{m_{III} - m_{II}}{m_{I} - m_{II}} \cdot c_{IgG,F} \tag{5.17}$$

This can only be achieved when the yield on IgG is 1. Concentrating the IgG can only occur when $m_I < m_{III}$ which is not possible in isocratic SMB due to the constraints of the *m*-values. In SEC-SMB the product will therefore always be diluted. Applying a micellar gradient in SASEC-SMB makes it possible to choose m_I equal to or even lower than m_{III}. That means that concentration of IgG should be possible. This is indeed the case in our simulation experiments as can be seen in table 5.4. IgG is concentrated with almost a factor 2.

Table 5.4. Comparison of yield (Y), productivity (PR), solvent consumption (CS), purity (Pu) and concentration (c_{IgG}) using SEC-SMB (first column) and SASEC-SMB (second column)

	SEC-SMB	SASEC-SMB
Y	0.99	0.99
PR [kg IgG/m^3 /d]	3.1	129
CS [l/g BSA]	19.7	1.3
Pu [%]	99	99
c_{IgG} [g/l]	0.50	1.95

5.5   Conclusions

The separation of BSA and IgG is performed using traditional SEC and using surfactant-aided SEC, i.e. SASEC. Pulse experiments showed that with SASEC both BSA and IgG were more distributed towards the solid phase than compared to using SEC. This effect was larger on IgG, the largest component than on BSA. As a consequence an azeotrope will be formed at a specific surfactant concentration. Above this concentration the selectivity is reversed and increased to values higher than obtained with conventional SEC.

Two surfactants have been tested, $C_{12}E_{23}$ and Tween20. The effects of $C_{12}E_{23}$ seem to be larger than that of Tween20 when compared on bases of weight fractions of surfactant.

Also two gel materials have been tested; Sephacryl^{TM} S200 HR and Sephacryl^{TM} S300 HR. In conventional SEC, S200HR would be the best choice. In SASEC S300 HR is the best choice. Due to the lower selectivity without surfactant the selectivity is reversed at lower concentrations than in S200HR. Higher selectivity is therefore obtained at lower surfactant concentrations.

The separation experiments have shown that with SASEC reversion of the selectivity is indeed possible. At 7.5% (w/w) of $C_{12}E_{23}$ BSA was eluted before IgG. These experiments further show that when using SASEC larger productivity, higher yields and lower solvent consumption can be achieved without the loss of purity of IgG when compared to conventional SEC.

Simulation of the separation of BSA and IgG in SMB chromatography showed that applying a surfactant gradient in a SMB results in a large increase in productivity compared to what is possible with conventional isocratic SEC-SMB. Further, the solvent consumption was decreased substantially with a factor 15. Another positive outcome is that the product is not diluted during this separation, but concentrated with almost a factor 2.

Acknowledgements

Nomenclature

c_i	concentration of solute i
CS	solvent consumption
D	diffusion coefficient
D_{ax}	dispersion coefficient
d_p	particle diameter
D_s	intraparticle diffusion coefficient
K_i	distribution coefficient of component i
k_L	mass transfer coefficient at liquid side
$k_o a$	overall mass transfer coefficient
k_s	mass transfer coefficient at solid side
L	length
m_j	flow ratio in section j
Mw	molecular weight
N	aggregation number
N_{av}	Avogadro number
PR	productivity
Pu	purity
r_i	radius of component i
R_s	resolution
t	time
U_{ij}	excluded volume between components i and j
v	interstitial velocity
V	volume
V_c	column volume
V_d	dead volume per column
V_e	elution volume
V_{inj}	injection volume
V_o	void volume
x_i	number concentration of component i
x_{vol}	volume fraction
x_{wt}	weight fraction
Y	yield
z	distance
ε	column void fraction
ρ	density
Φ	flow
τ	switch time

ϕ_i	volume fraction of component *i*
$\chi_{ij,k}$	steric interaction parameter between components *i* and *j in phase k*
$\eta_m r_m$	semi-axis of oblate micelle
Δt_{cycle}	cycle time

Sub and superscripts

D	desorbent
eq	equilibrium
F	feed
f	gel fiber
L	liquid phase
m	micelle
s	solid phase
surf	surfactant
I,II,III,IV	section number in SMB

References

Bosma JC, Wesselingh JA. 2000. J. Chromatogr. B 743: 169-180

Das C, Mainwaring R, Langone JJ, 1985. An. Biochem. 45: 27-36

Evans DF, Wennerström H. 1994. The Colloidal Domain, VCH publ., New York

Fisher L. 1980. Gel filtration Chromatography, Elsevier/North-Holland, Amsterdam

Guiochon GS, Golshan-Shirazi S, Katti AM. 1994. Fundamentals of Preparative and Nonlinear Chromatography, Academic Press, Boston

Horneman DA, Wolbers M, Zomerdijk M, Ottens M, Keurentjes JTF, van der Wielen LAM. 2004. J. Chromatogr. B 807: 39-45

Horneman DA, Ottens M, van den Broeke LJP, van Roosmalen D, Keurentjes JTF, van der Wielen LAM. 2004a. Patent EP1491246

Horneman DA, Ottens M, van der Wielen LAM, Keurentjes JTF. 2006. J. Chromatogr. A. 1113: 130-139

Houwing J, Billiet HAH, van der Wielen LAM. 2003. AICHE J. 49: 1158-1167

Jansons KM, Phillips CG. 1990. J Colloid Interface Sc. 137: 75-91

Lazzara MJ, Blankschtein D, Deen WM. 2000. J. Colloid Interface Sc. 226: 112-122

Liu C, Kamei DT, King JA, Wang DIC, Blankschtein D. 1998. J. Chromatogr. B, 711: 127-138

Migliorini C, Mazzotti M, Morbidelli M. 1999. AIChE J 45: 1411-1421

Ogston G. 1958. Trans Faraday Soc 54:1754-1757

Reuveny S, Lazar A. 1989. Adv. in biotech proc, 11: 45-80.

Van den Broeke LJP, van Roosmalen D, Dohmen-Speelmans MPJ, Dietz CHJT, van der Wielen LAM, Keurentjes JTF. 2006. Biotech and Bioeng., 93: 355-360

van Roosmalen D, Lazzara MJ, van den Broeke LJP, Keurentjes JTF, Blankschtein D. 2004. Biotech and Bioeng. 87: 695-703

Vonk P. 1994. Ph.D. Thesis, University of Groningen, Groningen

6

Concentration effects in size-exclusion chromatography

This chapter has been submitted for publication in J. Chromatogr. A, 2006

Abstract

Size-exclusion chromatography of high protein concentrations leads to non-linear distribution behavior. Break-through experiments with high concentrations of BSA clearly show that this is the case. Two models are used to describe the experimental results. A thermodynamic equilibrium model for the prediction of the distribution coefficient, taking into account various interactions, is able to describe the experimentally obtained values accurately. The second virial coefficient is 65% of the value calculated using a model based on steric interactions only. The concentration effects of non-linearity in size-exclusion chromatography are discussed for the application in fixed bed chromatography as well as in SMB chromatography.

Keywords: BSA, non-linear isotherms, size-exclusion chromatography, simulated moving bed, protein purification.

6.1   Introduction

Size-exclusion chromatography (SEC) is a method that is commonly applied in the final purification of biopharmaceutical proteins. The separation is based on the difference in size and shape of the components to be separated in relation to the network structure of the stationary phase. Size-exclusion chromatography is often considered as linear chromatography. This means that the concentration in the solid phase is always proportional to the concentration in the mobile phase (Sofer *et al.,* 1997). However, some concentration effects have been described in theoretical studies in literature. (Fanti *et al.,* 1990; Shearwin *et al.,* 1990; Bosma and Wesselingh, 2000; Lazzarra *et al.*, 2000). The models used in these studies were based on excluded volume interactions and show the possible existence of non-linear isotherms in SEC.

Furthermore, other publications show that in SEC hydrodynamic instability of elution zones will occur before this non-linearity will play a role. This is often referred to as viscous fingering (Czok *et al.,* 1991; Guiochon *et al.,* 1994; Sofer *et al.,* 1997). This is mainly a problem in fixed bed chromatography when only small sample volumes are migrating through the column. When the sample volumes are increased hydrodynamic instability is less significant. The front of the sample volume stays hydrodynamicly stable since the viscosity increases. Only the rear front might show some instability or fingering (Czok *et al.,* 1991). In SEC-SMB no small sample volumes are migrating through the column and therefore hydrodynamic instability will probably play no significant role while non-linearity might play a more important role in the separation.

This paper will show that an increase in solute concentration results in non-linear chromatography in SEC for a model protein Bovine Serum Albumin (BSA). This will be illustrated both by experiments and a mathematical model developed in the next section. Breakthrough experiments of BSA were performed in order to study the influence of protein concentration on the mass transfer rate and on the distribution behavior. The possible consequences of this concentration depending behavior will be discussed for SEC separations in both FB and SMB mode.

6.2   Theory

Concentration profiles in chromatography can be described by the mass balance equations of the liquid and solid phase (Guiochon *et al.,* 1994):

$$\frac{\partial c_{i,L}}{\partial t} = -u\frac{\partial c_{i,L}}{\partial z} + D_{ax}\frac{\partial^2 c_{i,L}}{\partial z^2} - \frac{1-\varepsilon}{\varepsilon}\frac{\partial c_{i,s}}{\partial t}$$

(6.1a)

$$\frac{\partial c_{i,s}}{\partial t} = k_0 a \left(c_{i,s}^{eq} - c_{i,s}\right)$$

(6.1b)

where u is the interstitial velocity, ε is the void fraction in the column, $c_{i,s}^{eq}$ is the concentration in the solid phase in equilibrium with the concentration in the liquid phase, $c_{i,L}$. The axial dispersion coefficient, D_{ax}, can be described by the following relation: (Van Deemter *et al.,* 1956):

$$D_{ax} = \lambda_1 D_L + \lambda_2 d_p u$$

(6.2)

where λ_1 and λ_2 are geometrical constants, d_p is the particle diameter and D_L is the diffusion coefficient in the liquid phase. The first term on the right hand side describes the molecular diffusivity and the second term the eddy dispersion. In size-exclusion chromatography, the first term can be neglected (Hagel *et al.,* 1996; Sofer *et al.,* 1997). The geometrical constant, λ_2 is near unity in size-exclusion chromatography (Hagel, 1989).

The overall mass transfer coefficient, $k_o a$ can be calculated by:

$$\frac{1}{k_o a} = \frac{d_p}{6}\left(\frac{K}{k_L} + \frac{1}{k_s}\right)$$

(6.3)

where K is the distribution coefficient and k_L and k_s are the mass transfer coefficients at the liquid side and solid side respectively. The mass transfer coefficients at the liquid side can be calculated from the Sherwood number (Guiochon *et al.,* 1994).

$$Sh_L = \frac{d_p k_L}{D_L} = \frac{1.09}{\varepsilon}Re^{0.33}Sc^{0.33}$$

(6.4)

For the Sherwood number on the solid side a value of 10 is used (Bosma and Wesselingh, 2000). The intraparticle diffusion coefficient, D_s is calculated from the liquid diffusion coefficient using the relation given by Vonk (Vonk, 1994):

$$D_s = D_L \exp\left(-\phi_f^{0.5}\frac{r_i}{r_f}\right)$$

(6.5)

where ϕ_f is the volume fraction of fibers in the gel particles and r_i and r_f are the radius of the solute i and the gel fiber, respectively.

6.2.1   Concentration effects on the mass transfer rate

The diffusion coefficient depends on the viscosity of the mobile phase:

$$D = D_{c=0} \left(\frac{\eta}{\eta_{c=0}} \right)^n \tag{6.6}$$

where n is 1 at low concentration and between 0.5 and 1 at higher concentrations (Reid *et al.,* 1987; Guiochon *et al.,* 1994; Miyabe *et al.,* 2000).

6.2.2   Concentration effects on the distribution coefficient

The distribution coefficient in SEC can be predicted by the Ogston model (Ogston, 1958). This model is based on the available space fraction for a rigid spherical solute in a random distribution of long fibers.

$$K_i = \exp\left(-\phi_f \left(1 + \frac{r_i}{r_f} \right)^2 \right) \tag{6.7}$$

In this model, the overlap of fibers is neglected. Bosma and Wesselingh (Bosma and Wesselingh, 2000) extended this model by including the overlap of the fibers:

$$K_i = \exp\left(-\ln\left(\frac{1}{1-\phi_f} \right) \left(1 + \frac{r_i}{r_f} \right)^2 \right) \tag{6.8}$$

This relation, however, does not take into account concentration effects of the mobile species.

Lazzarra (Lazzarra *et al.*, 2000) developed a generalized excluded volume model for membrane partitioning. In this model, all volumes excluded to a solute due to the presence of all types of fibers and solutes, including the solute itself, are calculated in each phase. The following general equation was derived:

$$K_i = \exp\left(-\sum_j \chi_{ij,s} + \sum_j \chi_{ij,L} \right) \tag{6.9}$$

where the dimensionless number $\chi_{ij,k}$ is the total excluded volume of solute i and a set of objects j per volume of phase k and is defined as:

$$\chi_{ij,s} = x_{j,s}U_{ij,s}$$

$$\chi_{ij,L} = x_{j,L}U_{ij,L}$$

(6.10)

Where $x_{j,k}$ is the number concentration of component j in phase k $(\#/m^3)$ and $U_{ij,k}$ is the excluded volumes between i and j in phase k. The excluded volume of two convex particles can be calculated by the following general expression (Jansons and Phillips, 1989; Lazzarra *et al.*, 2000):

$$U_{ij} = V_i + \frac{S_iH_j + S_jH_i}{4\pi} + V_j$$

(6.11)

where V_i, S_i and H_i are the volume, the surface area and the integral of the mean curvature of component i, respectively. With this expression, it is possible to calculate the excluded volume between two convex objects of any shape or size. This model has been used successfully for the prediction of the distribution coefficients in size-exclusion chromatography and surfactant-aided size-exclusion chromatography (Horneman *et al*, 2004, 2006).

The distribution coefficient of a single spherical solute in SEC with only one type of fiber can now be calculated using equations 6.9 to 6.11. Assuming that the length of the fibers is substantially larger than the fiber radius, i.e. $l_f \gg r_f$, the distribution coefficients becomes:

$$K_i = \exp\left(-\phi_f\left(1+\frac{r_i}{r_f}\right)^2 - (\phi_{i,s} - \phi_{i,L})\left(1+\frac{r_i}{r_i}\right)^3\right)$$

(6.12)

where ϕ_i is the volume fraction of the solute i. The first term in the exponent on the right hand side of equation 6.12 describes the steric interactions between the fiber and the protein in the gel phase. The second term describes the steric self-interaction among the protein molecules themselves in the gel and mobile phase. For dilute protein solutions, the second term can effectively be neglected and equation 6.12 equals the well-known Ogston relation (eq. 6.7).

This model described above is only based on steric interactions. Another approach to take concentration effects into account is a thermodynamic equilibrium model using a

virial expansion to calculate the chemical potential of a solute in the liquid and in the solid phase (Wills *et al*, 1995):

$$\mu_{i,L} = \mu_{i,L}^0 + RT \ln \gamma_{i,L} c_{i,L}$$
$$\mu_{i,S} = \mu_{i,S}^0 + RT \ln \gamma_{i,s} c_{i,s}$$

(6.13)

Where γ_i is the activity coefficient of solute *i*, $\mu_{i,L}^0$ is the chemical potential of solute *i* in the liquid reference state and $\mu_{i,s}^0$ is the chemical potential of solute *i* in the solid reference state. The reference state is an infinitely dilute solution of the solute. In dilute solutions the activity coefficients will become unity and the distribution coefficient in dilute solutions will thus read:

$$K_i^0 = \frac{c_{i,s}}{c_{i,L}} = \exp\left[\frac{\mu_{i,L}^0 - \mu_{i,s}^0}{RT}\right]$$

(6.14)

When the concentration increases or other solutes are involved, the activity coefficient can be calculated by:

$$\ln \gamma_i = 2B_{ii}c_i + \sum_j B_{ij}c_j$$

(6.15)

Where B_{ii} is the second virial coefficient for two-body interaction of identical solutes and B_{ij} is the second virial coefficient of dissimilar solutes. Excluded volume effects and other interactions are combined in this coefficient. The contribution from the excluded volume, B_{ij}^{ex} for a spherical solute is given by:

$$2B_{ij}^{ex} = \frac{4}{3}\pi N_{av}(r_i + r_j)^3$$

(6.16)

If only one solute is present at high concentration the distribution coefficient of this solute now becomes:

$$K_i = \frac{c_{i,s}}{c_{i,L}} = K_i^0 \exp\left[2B_{ii}(c_{i,s} - c_{i,L})\right]$$

(6.17)

When for B_{ii} only the contribution of the excluded volume effects is taken and the Ogston relation for K_i^0 is used the same relation as equation 6.12 will be obtained. When only steric interactions are involved, both models are identical. If other interactions besides the

steric interactions are involved, these can be combined in the second virial coefficient. This makes this model a more generally applicable model.

6.3   Materials and method

6.3.1   Column

An XK16 column from GE Healthcare was used in an FPLC system (GE Healthcare). The column was packed with Sephacryl^{TM} S300 HR (GE Healthcare, cat no. 17-0599-01) up to a height of 8.8 cm. The volume fraction of the gel fibers, ϕ_f, was determined with salt pulses (Horneman *et al.,* 2004). Small salt molecules (NaCl) can diffuse into all the pores of the gel. The difference between the elution volume of NaCl and the geometrical volume of the column gives the volume of the gel fibers. A value of 0.08 was found for this gel, the radius of the gel fiber, r_f was assumed to be 1.5 nm (Horneman *et al.,* 2004). The dead volume of the system (total volume between injection point and spectrophotometer minus the column volume itself) is determined by pulses of dextran blue and BSA. The void volume of the packed column is also determined by dextran blue pulses.

Table 6.1.   Concentrations and sample volumes used in the breakthrough experiments

c_{BSA} [g/l]	V_{sample} [ml]
9.6	24
18.1	24
36.4	24.5
63.9	24.5
94.6	24
198.8	23

6.3.2   Experiments

BSA (Sigma, cat no A 7906) was dissolved in a 10 mM phosphate buffer, pH 6.8 containing 0.1M NaCl. All solutions were filtrated and sonicated in an ultra-sonic bath for 20 minutes. Before each experiment the column was equilibrated with 2 column volumes of phosphate buffer. After equilibration the feed was changed to the BSA solution for about 2 column volumes. This step was followed again by 2 volume columns of phosphate buffer. The flow was equal to 1 ml/min in all experiments. The exact concentration and sample volumes used in the experiments are given in table 6.1.

6.3.3 Analyses

The density of each BSA solution was measured by the density meter DMA 480 (Anton Paar) The viscosity of BSA solutions was determined using a rotational viscometer (Haake Visco Tester 550, sensor NV). The concentration of BSA at the outlet of the column was determined on-line by a spectrophotometer at two different wavelengths (280 nm and 305 nm).

6.3.4 Numerical methods

The concentration profiles were simulated using the partial differential equations 6.1a and 6.1b. For spatial discretization of the convection term a second order backward discretization scheme was used while for the discretization of the dispersion term a central difference method was used. The resulting system of ODE's is solved in time by a fourth order Runga-Kutta method.

6.4 Results and Discussion

6.4.1 Breakthrough curves

Figure 6.1 shows the results of the breakthrough experiments at different concentrations of BSA, varying from 10 to 200 g/l.
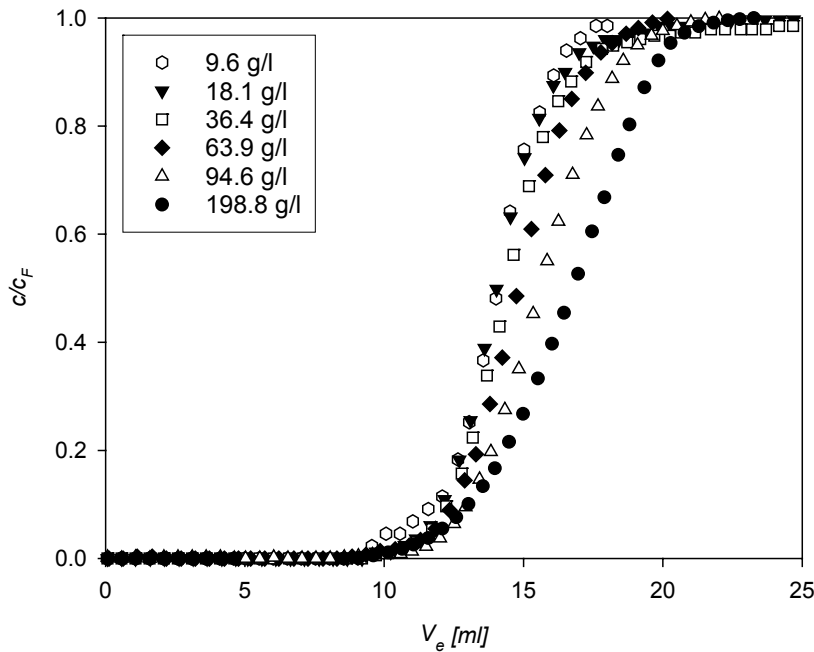

Figure 6.1. *Results of breakthrough experiments of BSA at different concentrations of BSA.*

From the experiments it is evident that the concentration of BSA substantially influenced the elution of BSA in SEC. At increased concentrations BSA eluted later. This can already be seen at a feed concentration of 36.4 g/l. No instability of the loading front was seen at the concentrations used.

6.4.2   Mass transfer effects

First the possible changes in mass transfer are examined. Increasing the BSA concentration in a solution means a change in density and viscosity. Both will have an effect on the overall mass transfer rate. Figure 6.2a shows the experimental results for the density as a function of the concentration BSA. A linear relation is fitted through the experiments:

$$\rho = 1003.6 + 0.3c_{BSA} \tag{6.18}$$

The viscosity of the BSA-solution can be described by the generalized Arrhenius formula (Monkos, 1996):

$$\eta_{r,i} = \frac{\eta}{\eta_0} = \exp\left[\frac{c}{\alpha - \beta c}\left(-(B_i - B_w) + (F_i - F_w)T + \frac{\Delta E_i - \Delta E_w}{RT}\right)\right] \tag{6.19}$$

with:

$$\alpha = \rho_w \frac{M_i}{M_w} \tag{6.20}$$

and

$$\beta = \alpha v - 1 \tag{6.21}$$

Where v is the specific volume of BSA, ΔE is the activation energy and B and F constants. The values for these parameters are taken from the paper of Monkos (Monkos, 1995) and given in table 6.2. Figure 6.2b shows that this model predicts the experimentally obtained values very well.

Table 6.2.   Values of parameters used to calculate the relative viscosity

	water	BSA
B [-]	25.94	$3.891 \cdot 10^5$
F [K^{-1}]	0.02	648.8
ΔE [KJ/mol]	32.01	$5.374 \cdot 10^5$
v [m^3/kg]		$1.417 \cdot 10^{-3}$

With these relations for the density and the viscosity, the diffusion coefficient and finally the overall mass transfer coefficient are calculated as a function of the concentration as shown in figures 6.2C and 6.2D. The overall mass transfer coefficient decreases at increasing BSA concentrations. The axial dispersion coefficient doesn't change with a varying BSA concentration and therefore only a change in the overall mass transfer coefficient can give a change in the elution profile. Simulations, however, show that the decrease in the overall mass transfer coefficient only results in a small change in elution profile. Almost no band broadening takes place (figure 6.3). Literature shows that even when band broadening is larger than predicted, the elution time will remain almost the same (Sajonz *et al.,* 1996).
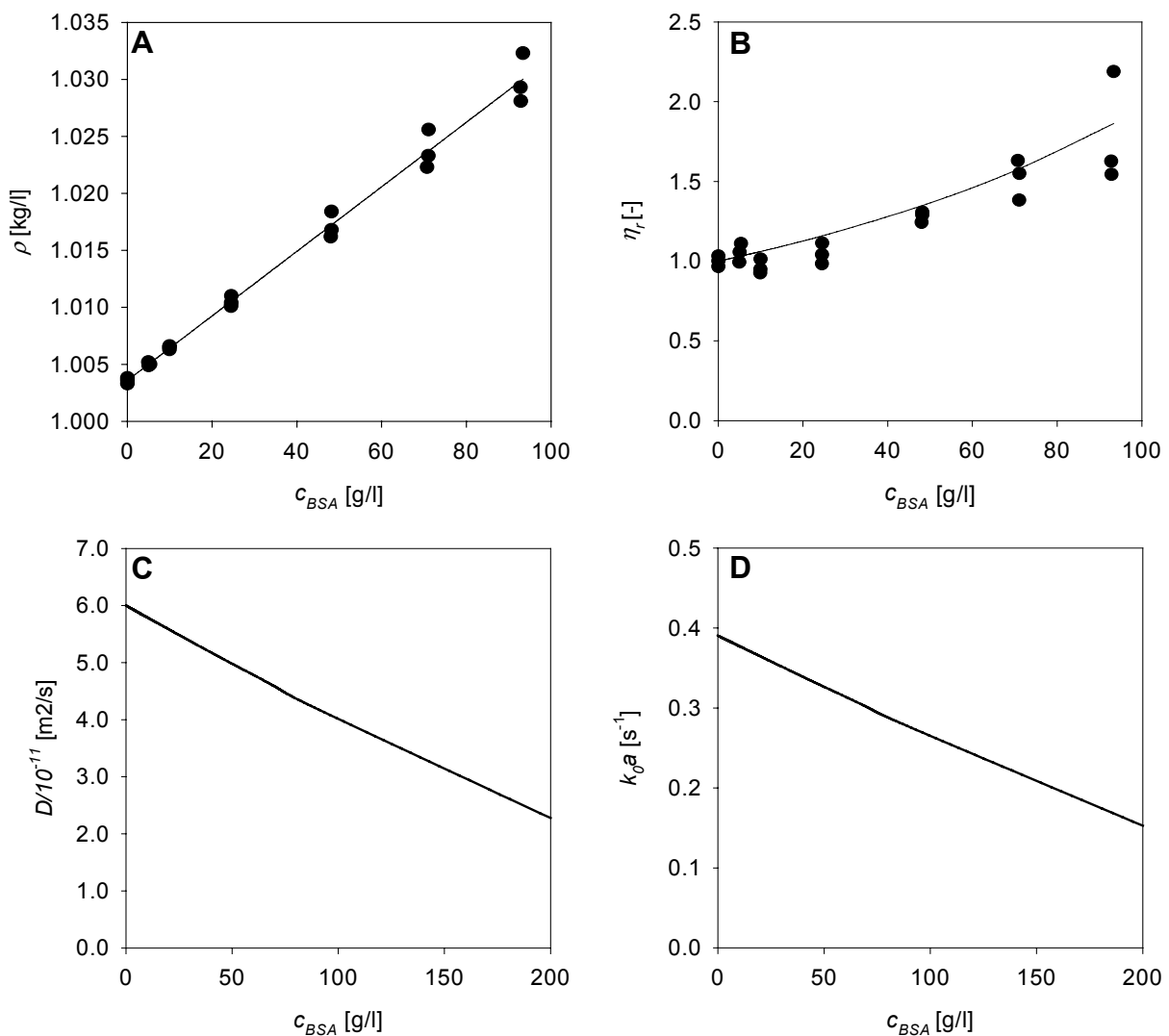

Figure 6.2. *Influence of concentration on A: density, B: viscosity, C: estimated diffusivity (equation 6.6, n=0.6) and D: estimated overall mass transfer coefficient (equation 6.3). Symbols represent the experimental results and the lines the model results*
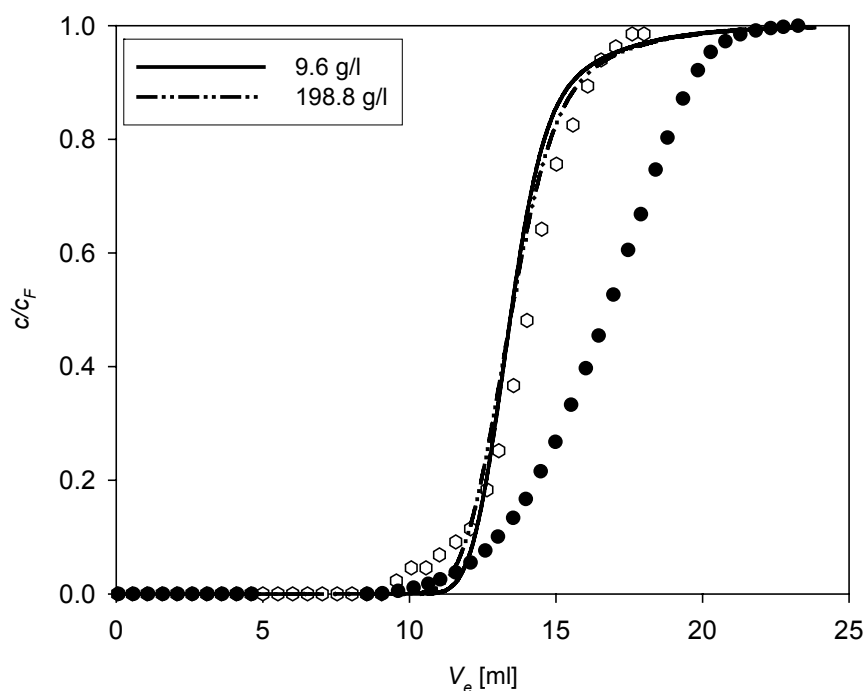
Figure 6.3. *Simulation of concentration profiles using a linear isotherm and taking the concentration effects in the mass transfer into account. The symbols are the experimental results. For explanation of these symbols see Figure 6.1.*

6.4.3 Influence of the distribution coefficient

The observed changes in elution volumes must therefore be caused by a change in distribution coefficient. A first assumption is that only steric interactions play a role in this distribution behavior (equation 6.12). Figure 6.4 shows that this assumption does indeed shift the profiles to the right but to a higher extent that was seen in the experiments. It seems that the influence of protein interaction is not as large as expected from the excluded volume theory.

The modeling results in figure 6.4 are obtained by using equation 6.12. The same results are obtained with equation 6.16 using only the excluded volume contribution of B_{ii} ($B_{ii}=B_{ii}^{ex}$). This value seems to be too large therefore the B_{ii}-value was decreased until the simulated profiles described the experimentally obtained profiles accurately. A B_{ii}-value of 65% of B_{ii}^{ex} resulted in the best agreement between the experimental and the model results. This is shown in figure 6.5. Apparently other interactions play a role in the distribution behavior of BSA in SEC. It was shown in literature that for example salts lower the activity coefficient of BSA (Moon *at al.,* 2000, Haynes *et al.*, 1993, Vilker *et al.,*

1981). It should be noted that in this paper the effects of buffer and salt are not included in the calculation of B_{ii}.
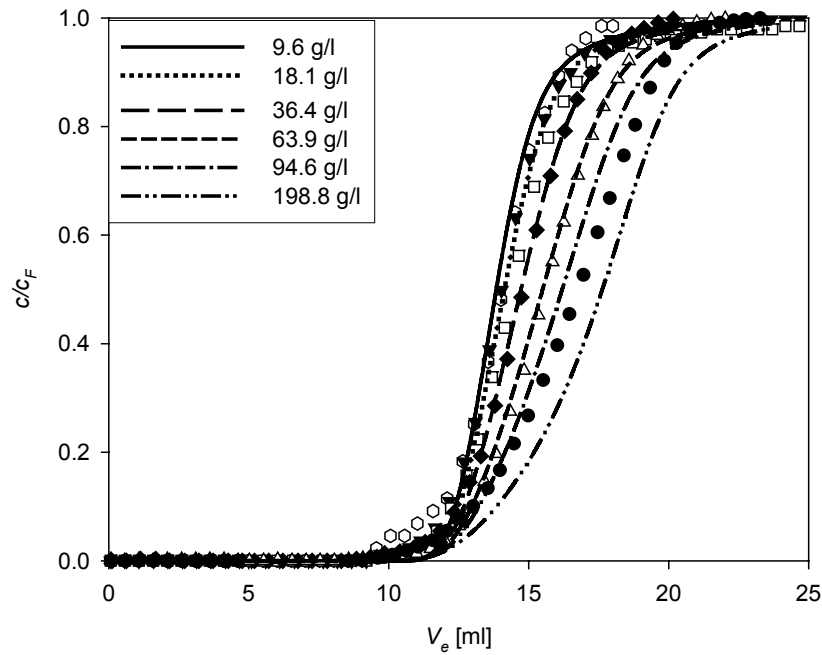

Figure 6.4. *Simulation of concentration profiles using equation 6.12. The symbols are the experimental results. For explanation of these symbols see Figure 6.1.*
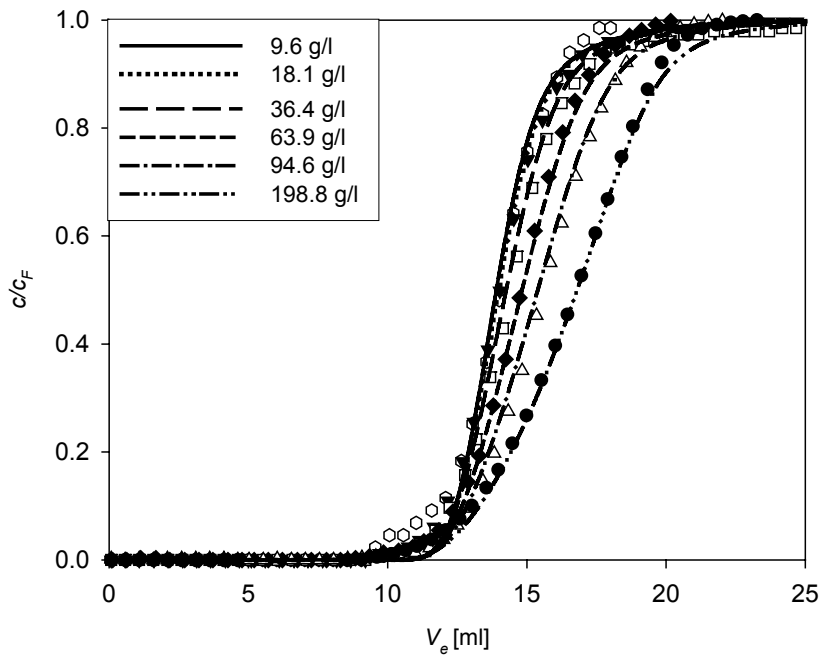

Figure 6.5. *Simulation of concentration profiles using equation 6.17 with $B_{ii} = 0.65\ B_{ii}^{ex}$. The symbols are the experimental results. For explanation of these symbols see Figure 6.1.*

6.4.4 Viscous fingering

Hydrodynamic instability can occur when the difference in viscosity of the mobile phase and the sample plug becomes too large. This hydrodynamic instability can appear at the boundary from low viscosity to high viscosity. In case of a high viscosity sample in a low viscosity mobile phase, the front of the low viscosity mobile phase can finger into the high viscosity sample plug. For small sample volumes this fingering can cause the separation of the sample plug into smaller plugs. This will cause at least band broadening but in the worst case the formed plugs will elute separately (Guiochon *et al.,* 1994; Czok *et al.,* 1991). For BSA it is recommended to use a concentration below 70 g/l in SEC to prevent viscous fingering (Sofer *et al.,* 1997). In general it is recommended to keep the viscosity of the sample below twice the mobile phase viscosity (Guiochon *et* al., 1994). For BSA this would be around 100 g/l (figure 6.2b). During the breakthrough experiments described in this paper, the sample volume was too large to be separated in smaller plugs. Only instability of the rear front is expected where the mobile phase can finger into the sample plug. Figure 6.6 shows that up to 36.4 g/l no instability of the rear front was observed. At 63.9 g/l and 94.6 g/l some instability is visible while only at 200 g/l real deformation of the front is observed.
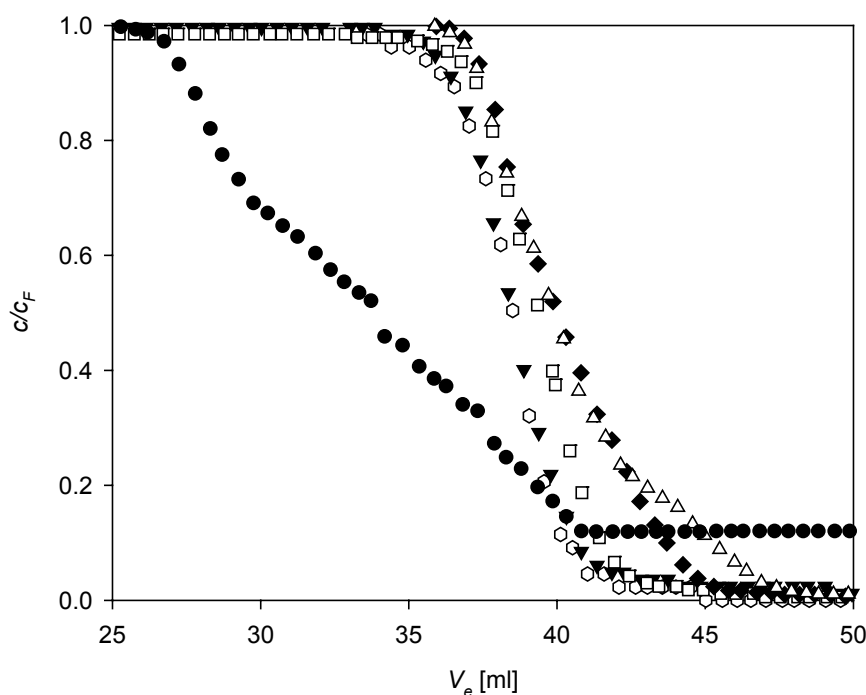

Figure 6.6. *The rear boundary of the concentration profiles during the breakthrough experiments. For explanation of the symbols see Figure 6.1.*

6.4.5   Effect on chromatography design

Fixed bed

The distribution coefficient of BSA is calculated using equation 6.16 with $B_{ii} = 0.65 \cdot B_{ii}^{ex}$. The distribution coefficient is increasing at increasing BSA concentrations as is shown in figure 6.7. Although SEC is considered as linear chromatography, this figure clearly shows that this is not the case. Already at 50 g/l K is increased from 0.39 to almost 0.5. At this concentration hydrodynamic instability is not expected to occur and therefore this non-linearity should be taken into account when designing SEC. Further it should be noticed that in SEC this change in K can be considered as a relative large change as all K-values are between 0 and 1. It is expected that a high concentration of one component will also affect the distribution behavior of the other components in the mixture. An increase of concentration of one of the components can therefore positively or negatively affect the selectivity.
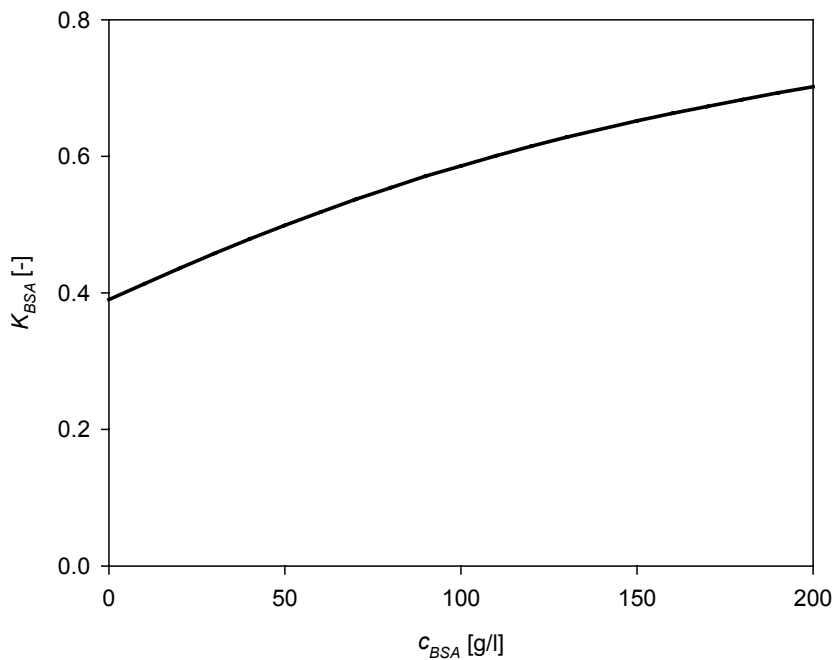
Figure 6.7.   *Distribution coefficient as function of the concentration of BSA using equation 6.17 with $B_{ii} = 0.65 \cdot B_{ii}^{ex}$.*

SMB

In SMB based separations, higher protein concentrations can be reached compared to FB separations. As a consequence, the change in distribution coefficient becomes more significant. A satisfactory performance of the SMB can only be achieved after proper selection of the flow rates. The procedure to determine the proper flow rates is based on

the isotherms of the components to be separated. This procedure for non-linear isotherms is described in literature (Migliorini *et al.,* 2000, Houwing, 2003). Figure 6.8 shows the area of separation for a mixture of concentrated BSA (50 g/l) and an impurity of Myoglobine (5 g/l). The distribution coefficients were calculated using equation 6.18. The BSA-BSA, BSA-Myo and Myo-Myo interactions were taken into account. All second virial coefficients were taken as 0.65 times the coefficient based on steric-interactions. Figure 6.7 shows that the boundary for m_{II} is shifted to the right while m_{III} is shifted upwards. The change of boundaries is significant and flow rates outside the correct m_{II} - m_{III} area might be chosen when the concentration effects are not taken into account which can lead to incomplete separations.
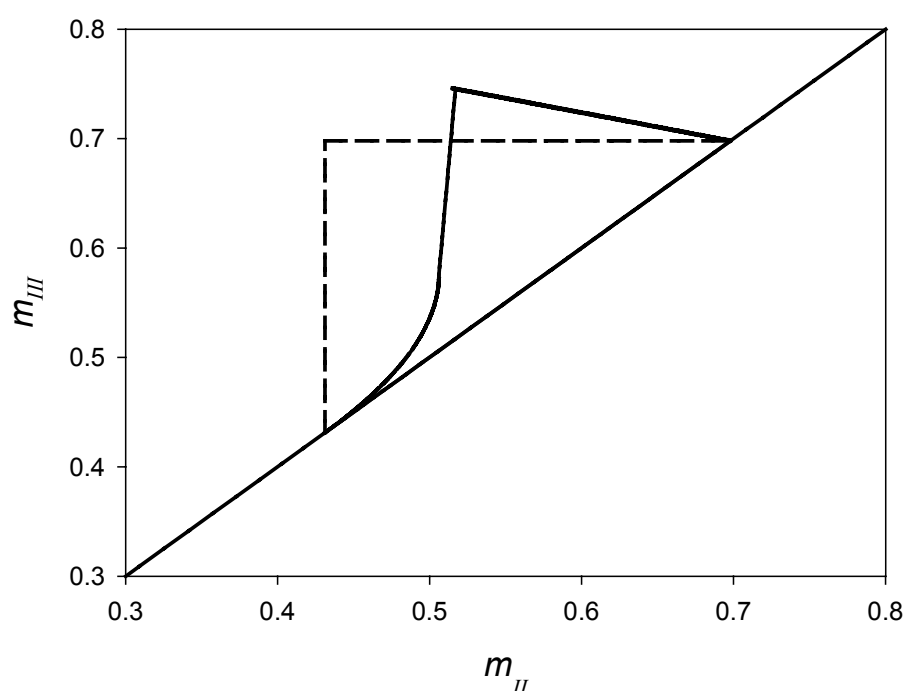
Figure 6.8. *Area of separation for diluted mixture of BSA and Myo (dashed line) and area of separation for a mixture with 50 g/l BSA and 5 g/l Myo (solid line).*

6.5 Conclusion

This paper clearly shows that SEC cannot always be considered as linear chromatography. Breakthrough experiments of BSA showed that BSA elutes later at increasing BSA concentrations. This increase in elution time can only be explained by an increase in the distribution coefficient of BSA. A thermodynamic equilibrium model is used to predict the distribution coefficient. Good agreement between experimental and model results is found when a virial coefficient of 65% of the value of the virial coefficients that only takes steric interaction between the BSA molecules into account.

The non-linear behavior in SEC at high concentrations will have an effect on the separation of different components. In fixed bed experiments the concentration is kept normally relatively low to prevent hydrodynamic instability. The results in this paper however show that even when BSA is below the recommended concentration, non-linearity can be observed.

In SMB chromatography higher concentrations of the components to be separated can be reached. Therefore non-linear behavior in SEC plays a significant role in designing and operating an SMB.

Acknowledgements

Nomenclature

ΔE	activation energy
B	parameter
B_{ij}	second virial coefficient of solute i and j
$c_{i,k}$	concentration of component i in phase k
D_{ax}	axial dispersion
D_L	diffusivity in the liquid phase
D_p	intraparticle diffusion coefficient
d_p	particle diameter
F	parameter
H_i	integral of the mean curvature of component i
K_i	distribution coefficient of component i
k_L	mass transfer coefficient at liquid side
$k_o a$	overall mass transfer coefficient
k_s	mass transfer coefficient at solid side
L	length of column
m_i	flow rate ratio in SMB section i
M_w	molecular weight
n	constant
N_{av}	Avagadro number
Pe	Peclet number
R	gas constant
Re	Reynolds number

r_i	radius of component i
S_i	surface area of component i
Sh	Sherwood number
T	temperature
t	time
u	interstitial velocity
U_{ij}	excluded volume between components i and j
V_e	elution volume
V_{sample}	sample volume
x_i	number concentration of component i
z	distance

α	parameter
β	parameter
μ	chemical potential
ε	column porosity
λ	constant
ρ	density
τ	switch time
η	viscosity
γ_i	activity coefficient
ϕ_i	volume fraction of component i
χ_{ij}	steric interaction parameter between components i and j
Φ_L	volumetric flow rate

Sub and superscripts

f	gel fiber
s	solid phase
L	liquid or mobile phase
w	water

References

Bosma JC, Wesselingh JA. 2000. J. Chromatogr. B 743: 169-180

Czok M, Katti AM, Guiochon G. 1991. J. Chromatogr. 550: 705-719

Van Deemter JJ, Zuiderweg FJ, Klinkenberg A. 1956. Chem. Eng. Sci. 5: 271-289

Fanti LA, Glandt ED. 1990. J. Colloid Interface Sc. 135: 385-395

Guiochon GS, Golshan-Shirazi S, Katti AM. 1994. Fundamentals of Preperative and Nonlinear Chromatography, Academic Press, Boston

Hagel L, Ostberg M, Andersson T. 1996. J. Chromatogr. A. 743: 33-42.

Hagel L. 1989 Gel Filtration. In: Protein purification, Principles, High Resolution Methods and Applications (Eds Janson, J.C., Rydén, L.), VCH, New York

Haynes CA, Benitez FJ, Blanch HW, Prausnitz JM. 1993. AICHE J. 39: 1539-1557

Horneman DA, Wolbers M, Zomerdijk M, Ottens M, Keurentjes JTF, van der Wielen LAM. 2004. J. Chromatogr. B 807: 39-45

Houwing, J. 2003. Separation of Proteins by Simulated Moving Bed Chromatography, Ph.D. thesis, Delft University of Technology, Delft

Jansons KM, Phillips CG. 1990. J Colloid Interface Sc. 137: 75-91

Lazzara MJ, Blankschtein D, Deen WM. 2000. J. Colloid Interface Sc. 226: 112-122

Migliorini C, Mazzotti M, Morbidelli M. 2000. AIChE J. 46: 1384-1399

Miyabe K, Guiochon G. 2000. J. Chromatogr. A. 890: 211-223

Monkos K. 1996. Int.J. Biol. Macromol. 18: 61-68

Moon YU, Curtis RA, Anderson CO, Blanch HW, Prausnitz JM. 2000.,J. Sol. Chem. 29: 699.

Ogston G. 1958. Trans Faraday Soc 54:1754-1757

Reid RC, Prausnitz JM, Poling BE. 1987. The Properties of Gases & Liquids (4th edition). McGraw-Hill Book Company, New York

Sajonz P, Zong G, Guiochon G. 1996 J. Chromatogr. A 728: 15-23

Shearwin KE, Winzor DJ. 1990. Eur. J. Biochem. 190: 523-529

Sofer G. Hagel L. 1997. Handbook of Process Chromatography, Academic Press.

Vilker VL, Colton CK, Smith KA. 1981. J Colloid Interface Sc. 79: 548-566

Vonk P. 1994. Ph.D. Thesis, University of Groningen, Groningen

Wills PR, Georgalis Y, Dijk J, Winzor DJ. 1995. Biophysical Chem 57: 37-46

7

Outlook

7.1 Introduction

The results presented in this thesis show that surfactant-aided size-exclusion can be used for the purification of relevant biomolecules. Better selectivity, productivity and more efficient eluent use can be achieved than compared with conventional size-exclusion chromatography. This was especially shown in the examples described in chapters 4 and 5. Although the micelle-gel systems in these examples gave good results, it is not necessarily the most optimal system. Another choice of surfactant or gel material could have resulted in other and even better results.

In this final chapter, the choice of micelle-gel system will be discussed. Therefore the influence of different parameters on the selectivity will be studied on a theoretical base. The theoretical optimal conditions will be compared with existing conditions in real micelle-gel system. Finally other considerations that can play a role in using SASEC will be discussed.

7.2 Theoretical limits to the micelle-gel system

The selectivity factor of the separation of two solutes A and B is defined as:

$$\alpha = \frac{max(K_A, K_B)}{min(K_A, K_B)} \qquad (7.1)$$

Where K_i, is the distribution coefficient of component i. The distribution coefficient in SASEC and thus the selectivity is depending on the volume fractions of the gel fibers and the micelles, the radius ratio of the solutes versus the gel fibers and the radius ratio of the micelle versus the gel fibers (Horneman et al., 2004):

$$K_i = \exp\left(\frac{-\ln\left(\frac{1}{1-\phi_f}\right)(1+R_{i/f})^2}{-\left(\frac{1}{1-\phi_m} - \frac{1}{1-K_m\phi_m}\right)\left(1+\frac{R_{i/f}}{R_{m/f}}\right)^n}\right) \qquad (7.2)$$

with:

$$R_{i/f} = \frac{r_i}{r_f} \qquad (7.3)$$

$$R_{m/f} = \frac{r_m}{r_f} \qquad (7.4)$$

where ϕ_f and ϕ_m are the volume fractions of the gel fibers and the micelles respectively, r_i, is the radius of the solute, r_f the radius of the gel fiber and r_m the radius of the micelles. The exponent n equals 3 in case of spherical micelles and 2 in case of cylindrical micelles, K_m is the distribution coefficient of the micelles. In the calculations it is assumed that cylindrical micelles are too large to enter the pores of the gel material ($K_m = 0$). For spherical micelles the distribution coefficient is calculated by:

$$K_m = \exp\left(\frac{-\ln\left(\dfrac{1}{1-\phi_f}\right)\left(1+R_{m/f}\right)^2}{-\left(\dfrac{1}{1-\phi_m} - \dfrac{1}{1-K_m\phi_m}\right)\left(1+\dfrac{r_m}{r_m}\right)^3} \right) \qquad (7.5)$$

The selectivity is thus depending on three ratios: $R_{A/f}$, $R_{B/f}$ and $R_{m/f}$. Figure 7.1 gives the selectivity as function of the micelle concentration for different values of $R_{m/f}$. The figure on the left is for cylindrical micelles ($n = 2$) and the figure on the right is for spherical micelles. The ratio's $R_{A/f}$ and $R_{B/f}$ have been kept constant at 1 and 2 respectively. Both figures show that the selectivity first decreases with increasing micelle concentration until an azeotrope is formed at a specific micelle concentration. Above this concentration the selectivity is reversed and increases to values higher than obtained with conventional SEC.

The excluded volume between two equal spheres is larger than between a sphere and a cylinder with the same diameter. Higher selectivity might therefore be expected using spherical micelles. At the other hand, spherical micelles are able to diffuse into the pores of the gel particle. This will lower the concentration difference of the micelles over the two phases and will therefore have a negative effect on the selectivity. Figure 7.1 shows indeed higher selectivity's for cylindrical micelles. The difference becomes smaller at decreasing values of $R_{m/f}$. To have a high selectivity at relative low surfactant concentration, $R_{m/f}$ should be as low as possible.

Figure 7.1. *The selectivity as function of the micellar volume fraction at different values of $R_{m/f}$. Left: cylindrical micelles. Right: Spherical micelles. $R_{A/f} = 2$, $R_{B/f} = 1$ and $\phi_f = 0.1$*

Figure 7.2. *The selectivity as function of the micellar volume fraction at different values of $R_{A/f}$ and $R_{B/f}$. Left: cylindrical micelles. Right: Spherical micelles. $R_{m/f} = 1$ and $\phi_f = 0.1$*

In figure 7.2 $R_{A/f}$ and $R_{B/f}$ are varied while r_A/r_B have been kept constant. A decrease in $R_{A/f}$ and $R_{B/f}$ results in a higher distribution of the solutes A and B towards the solid phase. This effect is larger for the larger component and therefore the selectivity is decreased with these decreasing ratios in conventional SEC. In the calculations the value of $R_{m/f}$ has been kept constant, which means that the concentration difference of the micelles over the two phases is only depending on the volume fraction of the micelles in the liquid phase and not on the values of $R_{A/f}$ and $R_{B/f}$. The effect of the micelles on the components to be separated is thus only related to the excluded volume between the micelles and these components. This excluded volume is increased at increasing values of $R_{A/f}$ and $R_{B/f}$, which will result in higher distribution coefficients. This effect is again larger on larger components and as a consequence, the selectivity increases faster at higher values of $R_{A/f}$ and $R_{B/f}$ above the reversion point as can be seen in figure 7.2.
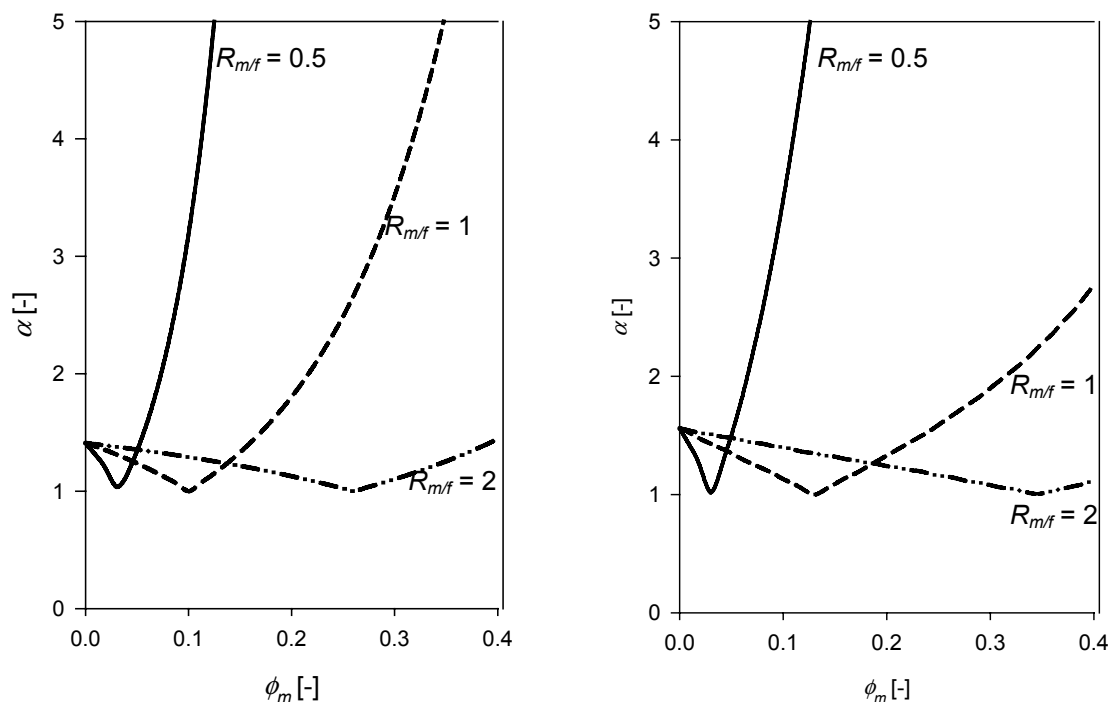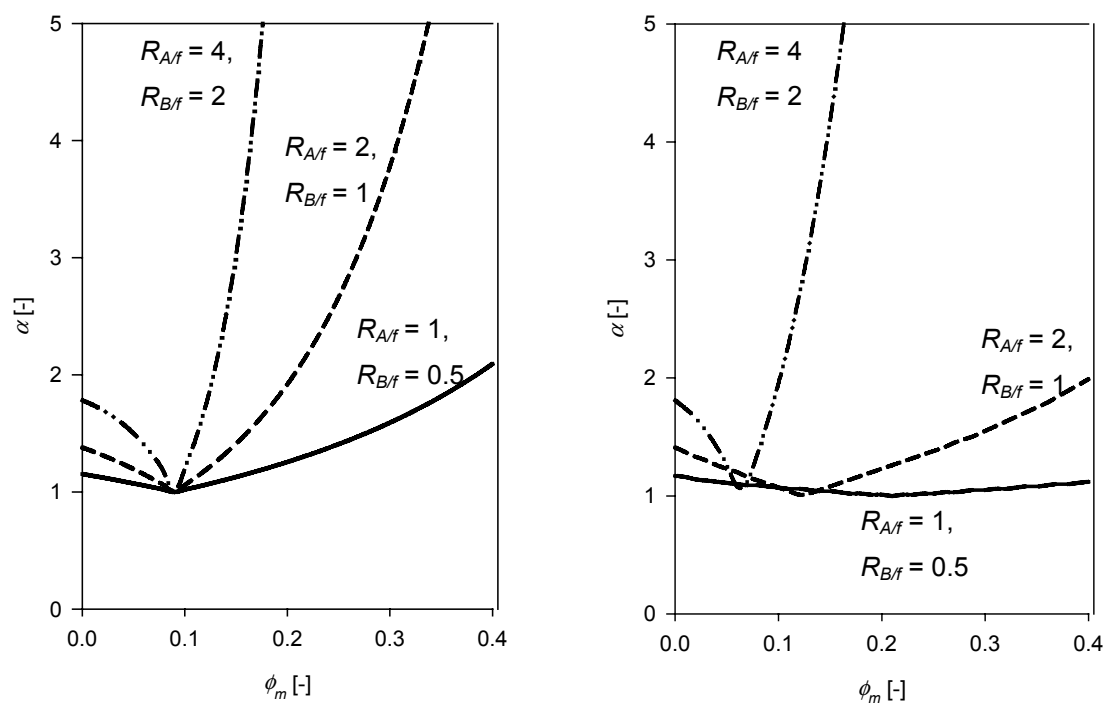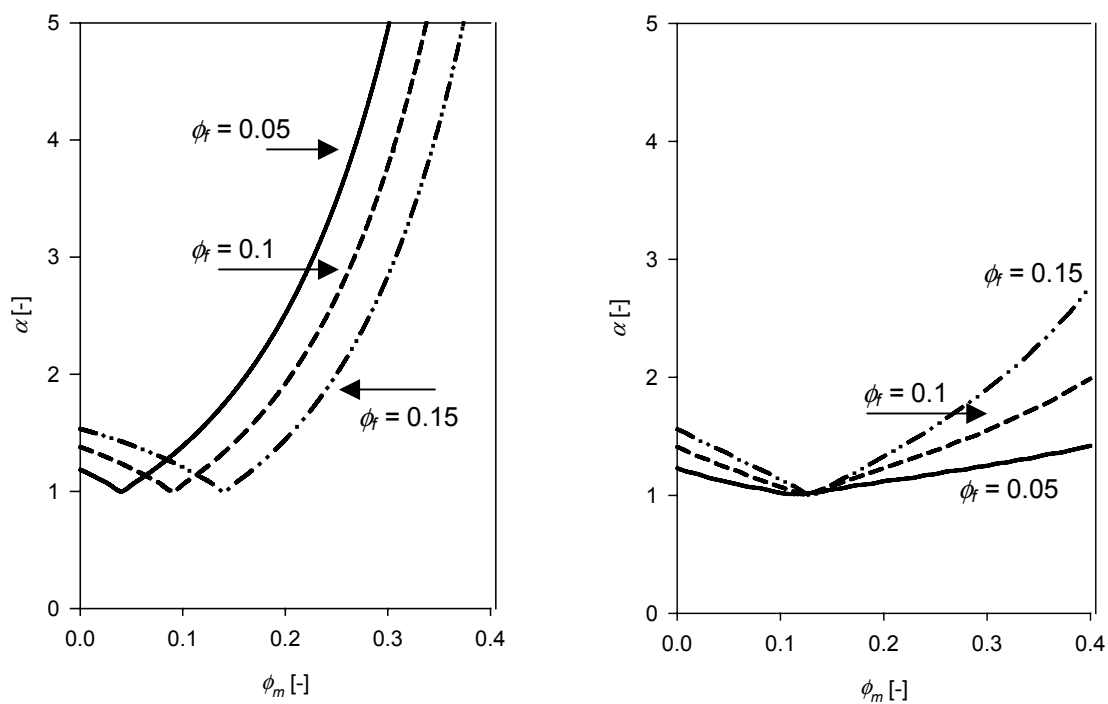

Figure 7.3. *The selectivity as function of the micellar volume fraction at different values of ϕ_f. Left: cylindrical micelles. Right: Spherical micelles. $R_{m/f}$ = 1, $R_{A/f}$ =2 and $R_{B/f}$ = 1.*

All calculations above have been done using a constant concentration of gel fibers. The concentration of gel fibers will also have an effect on the selectivity. This is shown in figure 7.3. This time the effect is different for the different shaped micelles. When cylindrical micelles are used, the concentration of gel fibers only affects the distribution behavior of the components to be separated. An increase in ϕ_f will results in lower distribution coefficients of the solutes A and B. This effect is larger on the larger

component. In conventional SEC this will therefore result in an increasing selectivity while in SASEC the selectivity is decreased above the reversion point. When spherical micelles are used the concentration of gel fibers will also influence the distribution behavior of the micelles. When this concentration is increased the micelles will be less distributed towards the solid phase. The concentration difference of the micelles over the two phases will be decreased which will lead to an increase in selectivity. Cylindrical micelles, therefore, perform best at relative low concentrations of the fibers while spherical micelle perform better at relative high concentrations.

7.3 Constraints to real micelle-gel systems

Figures 7.1 to 7.4 have shown that the highest selectivity can be reached by minimizing $R_{m/f}$ and maximizing $R_{A/f}$ and $R_{B/f}$. The possible values of this ratio's in real micelle-gel systems are limited by the characteristics of the available gel materials and micelles.

7.3.1   Micelles

Table 7.1 gives an overview of a (small) selection of available non-ionic surfactants and their properties. Of most micelles, however, the information on the size and shape cannot directly be obtained from literature. To get some insight on these characteristics other information of the micelles can be used.

Table 7.1.   Properties of some of the available non-ionic surfactants

Trade name	Chemical composition	Mw [g/mol]	N[1,3,4,5] [-]	Shape[2,6]	Size[2,6] [nm]
Tween 20	POE(20) sorbitan monolaurate	1228	31	Oblate	2.1/3.4
Tween 40	POE(20) sorbitan palminate	NA	NA	NA	NA
Tween 80	POE(20) sorbitan monooleate	1310	58-60	Oblate	4.1/2.3
Brij 35	POE(23) lauryl ether	1198	20-50	Oblate	3.7/4.1
Brij 58	POE(20) cetyl ether	1122	70	Oblate	3.8/4.8
Igepal CA-630	-	617	149	NA	NA
-	Octyl-β-glucopyranoside	292	27	NA	NA
-	n-dodecyl-β-D-maltoside	511	98	NA	NA
Triton X100	t-octylphenoxypoly ethoxyethanol	626	120-140	NA	NA
Triton X-114	t-octylphenoxypoly ethoxyethanol	537	NA	NA	NA

1. Hinze et al, 1993, 2. Tanford et al., 1977, 3. Acharya et al., 1997, 4. Sigma Aldrich, 5. Berthod et al., 2000, 6. Mahajan *et al.,* 2004.

Micellar shape

The aggregation number, *N* gives the number of surfactant molecules in a micelle. Only a limited number of hydrophobic chains can form a spherical core. When this number is exceeded, the volume and asymmetry of this core will be increased leading to a non-spherical shape. The surfactant Brij35 ($C_{12}E_{23}$) has a hydrocarbon chain with 12 carbon atoms that form the hydrophobic core. Only less than 20 hydrocarbon chains can fit into a spherical core (Tanford *et al*, 1977). The aggregation number found for this surfactant is larger than 20 and the micelles formed are indeed not spherical but more oblate (disc like). Cylindrical micelles will only be formed at very large aggregation number. From table 7.1 it is clear that most surfactants mentioned in this table will probably from globular and not cylindrical micelles.

Another method to get some insight in the shape of a micelle is the surfactant number, N_s, which is defined as:

$$N_s = \frac{v}{la_0}$$ (7.6)

where *v* and *l* are the volume and length of the hydrocarbon chain and a_0 is the area per head group. The surfactant number relates the properties of the surfactant molecule to the aggregate structure. Depending on this surfactant number the following shapes occur (Evans *et al.,* 1994):

Spherical micelles	$N_s = 0.33$
Infinite cylinders	$N_s = 0.5$
Planar bilayer	$N_s = 1$
Inverted cylinders and micelles	$N_s > 1$

The maximum length of a hydrocarbon chain (l_{max}) and the volume of the hydrocarbon core of a hydrocarbon chain can be estimated by the following approximations (Tanford et al, 1977; Evans et al, 1994):

$$l_{max} = 0.15 + 0.127(n_c - 1)$$ (7.7)
$$v = 0.027(n_c + n_{me})$$ (7.8)

Where n_c is the number of carbon atoms in the hydrocarbon tail and n_{me} is the number of methyl groups. The maximum length gives the length of the fully extended hydrocarbon chain. Hydrocarbon chains in the liquid state are not fully extended and the length of the

hydrocarbon tail will therefore always be smaller than this maximum length (Tanford*, 1980*). Unfortunately, there is no standard method to calculate the area per polar group.

Micellar size

When the hydrophilic group is small compared to the length of the hydrocarbon chain, the length of this hydrocarbon chain can be a first estimation of the micellar size. Otherwise also the size of the hydrophilic group has to be taken into account.

7.3.2 Real values for $R_{m/f}$, $R_{A/f}$ and $R_{B/f}$

The size of the gel fibers can be found by fitting existing data with the Ogston relation (Bosma *et al.* 2000*, Horneman *et al.* 2004). Bosma found fiber sizes in the range of 0.7 nm for polyacrylamide tot 2.2 nm for agarose. The sizes of the micelles mentioned in table 7.1 are assumed to be in the range of 1 to 5 nm. For (globular) proteins, the radius ranges from approximately 1 to 10 nm. In figure 7.4 the gray area gives approximately the area of $R_{m/f}$ and $R_{A/f}$ and $R_{B/f}$ in real micelle-gel systems. The area above the dashed line indicates the conditions that can lead to improved separation when using SASEC instead of SEC.
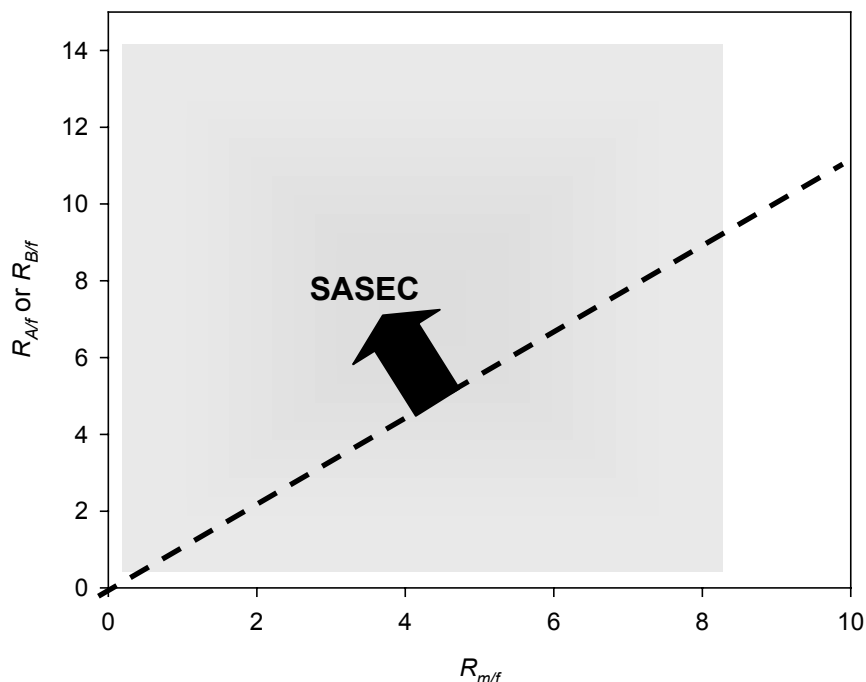

Figure 7.4. *The gray area indicates the conditions possible in real micelle gel systems. The area above the dashed line gives the conditions at which SASEC can lead to improved separation compared to conventional SEC.*

Figure 7.4 shows that it is possible to select a micelle-gel system that can improve the selectivity. It also shows that the choice should be made carefully and that not all systems will result in improvement of the separation.

7.4 Practical considerations using surfactant-aided size-exclusion chromatography

With the available gel materials and micelles, it is possible to design a purification step using SASEC with higher selectivity than conventional SEC. Still some other practical issues need to be considered.

7.4.1 Viscosity

The viscosity of a micellar solution is depending on the size, shape and concentration of the micelles (Evans et al, 1994). The viscosity is related to these parameters by the Einstein relation:

$$\eta = \eta_s (1 + [\eta]\phi_m)$$ (7.9)

where η_s is the viscosity of the solvent, $[\eta]$ is the intrinsic viscosity of the micelles.

For spheres $[\eta] = 2.5$, when the symmetry of the micelle changes, the intrinsic viscosity will change. For stiff rods with length L and radius r the intrinsic viscosity is given by:

$$[\eta] = \frac{L^2}{\pi r^2}$$ (7.10)

These relations indicate that solutions with cylindrical micelles will have higher viscosities than solution with spherical micelles at equal volume concentrations.

The pressure over a chromatographic column is depending on the flow rate and the viscosity of the solution. For most gel material a maximum allowed pressure is given. Exceeding this pressure may cause the medium to compress and may reduce the resolution of the separation. This can limit the use of highly concentrated micellar solutions.

7.4.2 Fixed bed versus SMB

The selectivity is a key parameter in fixed bed chromatography. The higher the selectivity the better the resolution will be and the better the performance. In SASEC, the selectivity needs first to be reversed before it is increased. This means that SASEC should be

performed at a micelle concentration above this reversion point. In SMB, the selectivity is also one of the key parameters. Complete separation can be reached if the following constraints are fulfilled:

$$K_A(c_I), K_B(c_I) < m_I$$

$$K_A(c_{II}) < m_{II} < K_B(c_{II})$$

$$K_A(c_{III}) < m_{III} < K_B(c_{III})$$

$$m_{IV} < K_A(c_{IV}), K_B(c_{IV})$$

The productivity in an SMB is defined by:

$$PR = \frac{c_{i\_F}\Phi_F Y}{V_s} \tag{7.11}$$

where Y is the yield. The feed flow is defined as:

$$\Phi_F = \frac{(m_{III} - m_{II}) \cdot V_s}{\tau} \tag{7.12}$$

Combining these two equations gives:

$$PR = \frac{c_{i\_F}(m_{III} - m_{II}) \cdot Y}{\tau} \tag{7.13}$$

To maximize the productivity, the difference between m_{III} and m_{II} should be maximized. This is reached at the minimum boundary of m_{II} and maximum boundary of m_{III}. In isocratic SMB this optimal point is fixed. In gradient SASEC-SMB the concentration of micelles in section III is higher than the concentration in section II. The boundary of m_{III} will thus be moved upwards and higher productivity can be obtained (figure 7.4). Note that for gradient SMB this can already be achieved at micelle concentrations before the selectivity is reversed. Concentrations below the reversion point can thus be used in gradient SASEC-SMB. It should however be noted that the concentration of micelles in the SMB should be either below or above the reversion point in the whole SMB to avoid formation of azeotropes. Mass transfer limitations are not taken into account in this 'optimal' point and a more robust point away from the boundaries needs to be chosen (Houwing *et al.*, 2003). Nevertheless, a decrease in the boundary of m_{II} or an increase in the boundary of m_{III} indicates a possibility for a higher productivity.
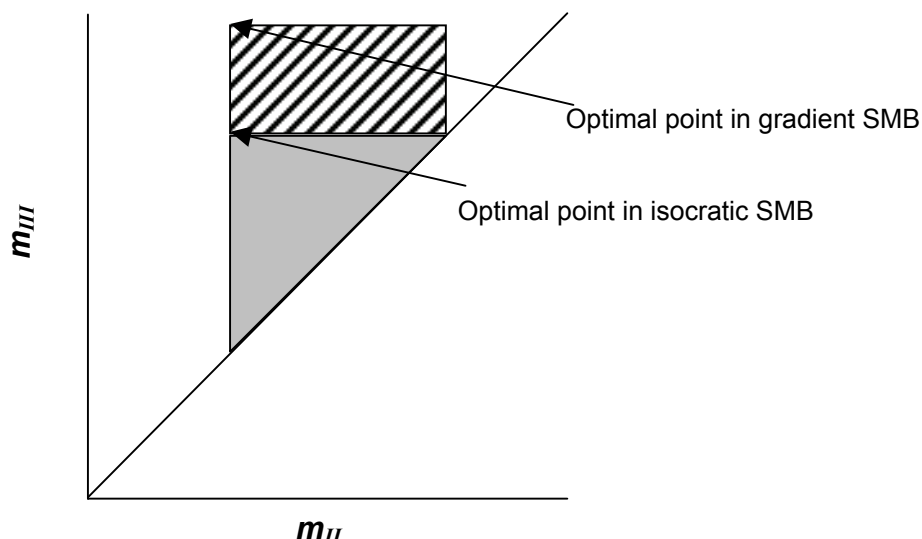
Figure 7.5. *Schematic representation of the area of separation in isocratic SMB (gray area) and micellar gradient SMB (striped area). In gradient SMB the boundary of m_{III} is shifted upwards*

7.4.3 Removal of surfactants

Most non-ionic surfactants are considered as non-toxic and classified as edible by the U.S. FDA (Quina *et al.,* 1998*)*, but for pharmaceutical more stringent regulations are applied. Some non-ionic surfactants like Tween are used for formulation and can therefore be applied in the process. Table 7.1 shows which surfactants have FDA clearance and some of the applications of the surfactants at this moment.

Table 7.2. Applications of some of the available non-ionic surfactants

Trade name	Chemical composition	FDA[1] clearance	Application[2]
Tween 20	POE(20) sorbitan monolaurate	Yes	A, C, D, E, G, H
Tween 40	POE(20) sorbitan palminate	Yes	A, C, D, E, G, H
Tween 80	POE(20) sorbitan monooleate	Yes	A, C, D, E, G, H
Brij 35	POE(23) lauryl ether	Yes	A, C, D, E, G
Brij 58	POE(20) cetyl ether	Yes	A, C, D, E, G
Igepal CA-630	-	NA	A, B, C, D, E, F, G, H
-	Octyl-β-glucopyranoside	NA	A, C, D, E, F, G
-	n-dodecyl-β-D-maltoside	NA	A, C, D, E, F, G
Triton X100	t-octylphenoxypoly ethoxyethanol	NA	A,B,C and D
Triton X-114	t-octylphenoxypoly ethoxyethanol	NA	D and E

1.Uniquema, 2. Sigma Aldrich, A=diagnostic application, B=molecular biology C= electrophoreses/chromatography, D= membrane protein solubilization, E= enzymology, F= antigen/vaccine preparation, G= drug delivery/liposomes, H=cell culture

Depending on the product and the allowed surfactant concentration in the product, removal of surfactant might be necessary. In those cases removal of the surfactant should be implemented in the process. Several options are possible. Aqueous two-phase separation is a simple method to remove the micelles from the product. Increasing the temperature will result in phase separation. The product will go to the micellar poor phase while it is possible to recycle the micellar rich phase. This is already applied in cloud point extractions (Persson *et al*, 1999). It is also possible to add an extra chromatography step. Size-exclusion can be used when the micelles are of different size than the product. Ion-exchange is also mentioned for the removal of surfactants (Baihri, 2001). These options will give an extra step in the process but at the other hand, the micelles can also be recycled which will reduce the costs. When SMB is used for the separation it might also be possible to the design the SMB in such a way that a micellar free product can be obtained.

7.5   Final Conclusions

In this thesis it is shown that SASEC can be used for the separation of biomolecules and bioparticles on bases of the difference in size of the components to be separated. These kinds of separations are now usually done with SEC. An advantage of this new separation method is the higher flexibility of the method as the selectivity can be tuned in-situ. Other advantages are the increased productivity and the decrease in eluent consumption that can be obtained with SASEC relative to conventional SEC. SASEC can be applied for the separation of components with a relative small difference in size as was shown in the separation of IgG and BSA but can also be applied for the separation of components with a larger difference in size as was shown in the viral clearance of BSA. This indicates that SASEC can be applied for a wide range of separations.

Of course only a few examples have been given and only a few micelle-gel systems have been tested. This final chapter however gives some insight in how to choose an appropriate micelle-gel system for a specific application. The selectivity is mainly depending on the diameter ratios in the system. Relative low values of $R_{m/f}$ in combination with relative high values of $R_{i/f}$ will give the best results. Looking at the characteristics of the existing micelles and gel materials there seems to be enough choice for micelle-gel systems for many specific separations.

Most calculations and experiments were done with diluted protein mixtures. In chapter 6 it was however demonstrated that concentrated protein mixtures have non-linear isotherms in SEC. It is therefore expected that an increase in protein concentration will also have an effect on the separation in SASEC and on the design of such a separation, which should be included in future research.

The choice of surfactant is not only depending on its ability to improve the existing separation step but also on the acceptance of this surfactant in the production process. In many processes it is probably required that the surfactant is (partly) removed from the final product. In future research of the application of SASEC, more attention should be paid to the use of this new technique including the possibility of the removal of the surfactants either by using a separate step or implemented in the same step by for example the use of a SMB chromatography system.

Nomenclature

a_o	area of the head group
c_i	concentration of component i
K_i	distribution coefficient of component i
l	length of hydrocarbon chain
L	length of micelle rod
m_i	flow ratio in section i
N_s	surfactant number
PR	productivity
r	radius
v	volume of hydrocarbon chain
V	volume
Y	yield

α	selectivity factor
Φ	flowrate
ϕ	volume fraction
τ	switch time
η	viscosity
η_s	viscosity of solvent
$[\eta]$	intrinsic viscosity

Sub and superscripts

m	micelle
f	fiber
s	solid phase
F	feed

References

Baihri SM. 2001. Detergents: A guide to the properties and uses of detergents in biological systems, Calbiochem-Novabiochem Corporation.

Berthod A, Garcia- Alvarez-Coque C. 2000. Micellar Liquid Chromatography, Marcel Dekker, New York.

Bosma JC, Wesselingh JA. 2000. J. Chromatogr. B 743: 169-180

Evans DF, Wennerström H. 1994. The Colloidal Domain, VCH, New York.

Hinze WL, Pramauro, E. 1993. Crit. Rev. An. Chem. 24: 133-177

Horneman DA, Wolbers M, Zomerdijk M, Ottens M, Keurentjes JTF, van der Wielen LAM. 2004. J. Chromatogr. B 807: 39-45

Mahajan RK, Chawla Y, Bakshi MS, Kaur G, Aswal VK, Goyal PS. 2004. Colloid Polym Sci. 283: 164-168

Quina FH, Hinze WL. 1999. Ind. Eng. Chem. Res. 38: 4150-4168

Tanford C, Nozaki Y, Rohde MF. 1980. J. Phys. Chem. 81: 1555-1560

Tanford C. 1980. The Hydrophobic Effect Formation of Micelles and Biological Membranes, Wiley, New York

Persson J, Nyström L, Ageland H, Tjerneld F. 1999. Biotech and Bioeng. 65: 371-381

http://www.uniqema.com/fibers/lit/fibres6.pdf

http://www.sigmaaldrich.com/img/assets/15402/Detergent_Selection_Table.pdf

Appendix A: Separation method

for bioparticles

Patent: EP1491246-A1; WO2004112935-A1 (Removal of bioparticles e.g. virus by subjecting aqueous solution or dispersion of biological materials containing the bioparticles to gel permeation chromatography in presence of micelles of ionic or non-ionic surfactant in mobile phase)

(19) **Europäisches Patentamt**
European Patent Office
Office européen des brevets

(11) **EP 1 491 246 A1**

(12) **EUROPEAN PATENT APPLICATION**

(43) Date of publication:
29.12.2004 **Bulletin 2004/53**

(51) Int Cl.[7]: **B01D 15/08**

(21) Application number: **03076960.8**

(22) Date of filing: **23.06.2003**

(84) Designated Contracting States:
**AT BE BG CH CY CZ DE DK EE ES FI FR GB GR
HU IE IT LI LU MC NL PT RO SE SI SK TR**
Designated Extension States:
AL LT LV MK

(71) Applicant: **STICHTING VOOR DE TECHNISCHE
WETENSCHAPPEN**
3527 JP Utrecht (NL)

(72) Inventors:
 • **Homeman, Danielle Amanda**
  2728 GK Zoetermeer (NL)
 • **Ottens, Marcel**
  2313 RC Leiden (NL)

 • **Van der Wielen, Lucas Antonius Maria**
  2665 AR Bleiswijk (NL)
 • **Van Roosmalen, Dick**
  5621 HR Bleiswijk (NL)
 • **Van den Broeke, Leo Jacques Pierre**
  1076 VR Amsterdam (NL)
 • **Keurentjes, Johannes Theodorus Faustinus**
  5708 EH Helmond (NL)

(74) Representative:
**Prins, Adrianus Willem, Mr. Ir. et al
Vereenigde,
Nieuwe Parklaan 97
2587 BN Den Haag (NL)**

(54) **Separation method for bioparticles**

(57)   The present invention relates to a method for the removal of bioparticles, including biomolecules from an aqueous solution or dispersion of biological materials containing said bioparticles, using gel permeation chromatography using a mobile and a stationary phase, said method comprising subjecting the said aqueous solution or dispersion of biological material containing said bioparticles, to gel permeation chromatography in the presence of micelles of a ionic or non-ionic surfactant, whereby the said surfactant has substantially no interaction with the bioparticles.

EP 1 491 246 A1

(12) INTERNATIONAL APPLICATION PUBLISHED UNDER THE PATENT COOPERATION TREATY (PCT)

(19) World Intellectual Property
Organization
International Bureau

(43) International Publication Date
29 December 2004 (29.12.2004)

PCT

(10) International Publication Number
WO 2004/112935 A1

(51) International Patent Classification[7]: **B01D 15/08**

(21) International Application Number:
PCT/NL2004/000445

(22) International Filing Date: 22 June 2004 (22.06.2004)

(25) Filing Language: English

(26) Publication Language: English

(30) Priority Data:
03076960.8   23 June 2003 (23.06.2003)   EP

(71) Applicant *(for all designated States except US)*: **STICHT-ING VOOR DE TECHNISCHE WETENSCHAPPEN** [NL/NL]; Van Vollenhovenlaan 661, NL-3527 JP Utrecht (NL).

(72) Inventors; and
(75) Inventors/Applicants *(for US only)*: **HORNEMAN, Danielle, Amanda** [NL/NL]; Dijkmanschans 116, NL-2728 GK Zoetermeer (NL). **OTTENS, Marcel** [NL/NL]; Bakhuis Roozenboomstraat 9, NL-2313 RC Leiden (NL). **VAN DER WIELEN, Lucas, Antonius, Maria** [NL/NL]; Margrietlaan 4, NL-2665 AR Bleiswijk (NL). **VAN ROOSMALEN, Dick** [NL/NL]; Edison-straat 68, NL-5621 HR Eindhoven (NL). **VAN DEN BROEKE, Leo, Jacques, Pierre** [NL/NL]; Olympiaweg 71 D, NL-1076 VR Amsterdam (NL). **KEURENTJES,**

Johannes Theodorus Faustinus [NL/NL]; Gerwenseweg 27, NL-5708 EH Helmond (NL).

(74) **Agent: WINCKELS, J.H.F.**; Nieuwe Parklaan 97, NL-2587 BN Den Haag (NL).

(81) Designated States *(unless otherwise indicated, for every kind of national protection available)*: AE, AG, AL, AM, AT, AU, AZ, BA, BB, BG, BR, BW, BY, BZ, CA, CH, CN, CO, CR, CU, CZ, DE, DK, DM, DZ, EC, EE, EG, ES, FI, GB, GD, GE, GH, GM, HR, HU, ID, IL, IN, IS, JP, KE, KG, KP, KR, KZ, LC, LK, LR, LS, LT, LU, LV, MA, MD, MG, MK, MN, MW, MX, MZ, NA, NI, NO, NZ, OM, PG, PH, PL, PT, RO, RU, SC, SD, SE, SG, SK, SL, SY, TJ, TM, TN, TR, TT, TZ, UA, UG, US, UZ, VC, VN, YU, ZA, ZM, ZW.

(84) Designated States *(unless otherwise indicated, for every kind of regional protection available)*: ARIPO (BW, GH, GM, KE, LS, MW, MZ, NA, SD, SL, SZ, TZ, UG, ZM, ZW), Eurasian (AM, AZ, BY, KG, KZ, MD, RU, TJ, TM), European (AT, BE, BG, CH, CY, CZ, DE, DK, EE, ES, FI, FR, GB, GR, HU, IE, IT, LU, MC, NL, PL, PT, RO, SE, SI, SK, TR), OAPI (BF, BJ, CF, CG, CI, CM, GA, GN, GQ, GW, ML, MR, NE, SN, TD, TG).

Published:
— *with international search report*

For two-letter codes and other abbreviations, refer to the "Guidance Notes on Codes and Abbreviations" appearing at the beginning of each regular issue of the PCT Gazette.

(54) Title: SEPARATION METHOD FOR BIOPARTICLES

(57) Abstract: The present invention relates to a method for the removal of bioparticles, including biomolecules from an aqueous solution or dispersion of biological materials containing said bioparticles, using gel permeation chromatography using a mobile and a stationary phase, said method comprising subjecting the said aqueous solution or dispersion of biological material containing said bioparticles, to gel permeation chromatography in the presence of micelles of a ionic or non-ionic surfactant, whereby the said surfactant has substantially no interaction with the bioparticles.

WO 2004/112935 A1

P65147EP00

Title: Separation method for bioparticles

The invention relates to a method for the removal of bioparticles from an aqueous solution or dispersion of biological materials containing said bioparticles, using gel permeation chromatography using a mobile and a stationary phase.

One of the critical steps in the manufacturing of biological materials is the isolation and purification of the desired material from a complex medium. For example, in the cases of protein inclusion bodies, organelles or virus particles produced or generated through fermentation, separation or concentration of the desired material from contaminating materials in large-scale manufacturing is always necessary. In addition, preparation of purified bioparticles extracted from natural materials also requires purification or concentration steps that are often complex, time consuming, and costly. Purification of biological fluids, such as blood or blood products is also very complex, especially as the valuable components are susceptible to degradation and/or denaturation as a consequence of the treatment.

Commonly used separation and purification methods include centrifugation, chromatography, and membrane filtration. However, centrifugation, which utilizes a density gradient, may disrupt the structure of bioparticles, and the capability of scaling up the centrifugation operation is limited.

Membrane filtration is easy to operate, but it may involve the application of pressure, which may be detrimental to certain materials. Membrane filtration also is limited in terms of the degree of separation of biological particles, which may provide a hazard if the said bioparticles are viruses, bacteria or other infectous biological materials.

Other separation methodologies include two-phase liquid-liquid extraction methods. The traditional liquid -liquid extraction method utilizes two partially immiscible phases formed by contacting an organic phase with an aqueous phase. The disadvantage of this approach follows from the possible adverse effects of an organic solvent on the conformations and functions of

biological molecules. An alternative liquid-liquid extraction method utilizes two-phase aqueous systems formed by using water-soluble polymers. Certain aqueous solutions containing two types of water-soluble polymers will separate into two coexisting phases, with each phase containing predominantly only one type of polymer. The most commonly used polymers are dextran and poly(ethylene oxide). The use of this type of systems is exemplified by Harrison et al. who reported the concentration of spermatozoa by these means. The main disadvantages of this method are (1) the necessary separation of the water soluble polymers and the particulate product, because of the high viscosity of the resulting solution and (2) the high consumption of these polymers per unit of desired product separated.

Another approach using a two-phase aqueous system is mentioned by Blankschtein et al. (WO-A 9705480), which relies on the ability of surfactants to form micelles. Surfactants are molecules composed of a hydrophilic moiety, which is soluble in water, and a hydrophobic moiety, which is not. This duality towards an aqueous environment leads to a broad spectrum of complex self-association phenomena which simple solutes do not exhibit in water. In order to avoid contact of the hydrophobic moieties with water, the individual surfactant molecules self-associate to form aggregate structures known as micelles. Whereas these micelles are hydrophilic on the exterior surface, they possess a hydrophobic and non-aqueous core. Typically, micellization, that is, the formation of micelles, occurs beyond a threshold surfactant concentration, known as the critical micelle concentration (CMC), below which surfactant molecules are predominantly dispersed as monomers and above which they begin to form micelles. The dual hydrophobic / hydrophilic environment provided by micelles has been exploited to separate and concentrate biological molecules according to their hydrophobicity using an aqueous solution of the non-ionic surfactant Triton X-114, which, under certain conditions, separates into two phases.

In this system, the biological materials are concentrated in the phase containing a high concentration of micelles with the more hydrophobic analytes being separated from the contaminants by incorporation into the cores of the micelles. In order to further purify the hydrophobic material separated in this way, a series of extraction steps may be required to extract the analyte which

has been incorporated within the micelles. Based on the principles laid out by Bordier (J. Biol. Chem., 256, 1604-1607, 1981) in which the hydrophobic proteins may be incorporated into the core of micelles in the micelle-rich phase of a two-phase aqueous system, a method was developed for retrieving hydrophilic proteins in the micelle-rich phase by causing the hydrophilic proteins to be retained by ligands on the surface of micelles. In all the above systems, the experimental conditions are driven by the theory that a material of interest be separated according to its degree of hydrophobicity. Accordingly, hydrophobic materials are concentrated in the micelle-rich phase, and the remainder of the material, considered to be waste, passes into the second phase of the two-phase aqueous system, identified in the above references as the aqueous phase.

This theory is substantially different from that disclosed by Nikas et al. (Macromolecules, 25, 4797-4806, 1992,); and Liu et al. (AIChE J., 41, 991-995, 1995), who identified a principle of separation that relies on volume exclusion and not on the degree of hydrophobicity, where the analyte could be partitioned into the second phase of the two-phase aqueous system, identified as micelle-poor. According to Nikas et al. and Liu et al., the volume exclusion of molecules from the micelle-rich phase could be using preselected micelle shapes. Nikas et al. and Liu et al. supported their theory of volume exclusion by describing the partitioning behavior of preparations containing single hydrophilic proteins in aqueous micellar phases containing cylindrical micelles.

In WO-A 9705480 a method for size separating a mixture of reagents including an analyte and at least one contaminant of different size is described, said method comprising:

(a) providing at least one surfactant, the surfactant being capable under selected conditions of forming a two-phase aqueous micellar system having a micelle-rich phase and a micelle-poor phase;

(b) forming the two-phase aqueous micellar system containing surfactant as specified in (a) in the presence of the mixture of reagents; and

(c) permitting the analyte and the contaminant to partition unevenly between the two phases so as to cause at least partial separation of the analyte from the contaminant on the basis of size.

This method does provide some degree of separation of, for example viruses, however, the degree of separation is still insufficient for most purposes.

Accordingly, there is still a need for identifying effective methods of separating or concentrating an analyte from a mixture where the methods are simple to implement, do not involve denaturing steps, are applicable to a wide range of materials, and can be easily scaled up.

In addition, in case of viruses and other infectious bioparticles, surfactants are commonly used to disrupt them or otherwise chemically destroy them and to substantially increase the safety of the final product (Harrison R.G. et al, Bioseparations Science and Engineering, Oxford Univ. Press, 2003). These socalled 'surfactant steps' are usually time consuming, add negatively to the process economy and may cause degradation and/or denaturation of the biotechnological product. In other cases, surfactants and comparable molecules are also used in the formulation of biopharmaceutical products, such as octanoate in the formulation of human serum albumin. Hence, surfactants are a common class of chemicals in bioprocesses, that must be used with the lowest possible amount.

The invention has as one of the objects to provide a method for the decrease in contaminants in biological fluids, said contaminants being bioparticles, including biomolecules having a size between 5 nm and 10 μm, more in particular viruses. More in particular, the invention has as an object to reduce the amount of such contaminants, more in particular viruses, bacteria and other infectous bioparticles to a degree of at least a factor 1000, preferably up to a factor 1,000,000.

More in particular the invention is concerned with a situation where a desired bioproduct (biomolecules or bioparticles), are to be separated from undesired bioparticles such as viruses, bacteria and other infectous bioparticles

The invention is accordingly directed to a method for the removal of bioparticles, including biomolecules from an aqueous solution or dispersion of biological materials containing said bioparticles, using gel permeation chromatography using a mobile and a stationary phase, said method comprising subjecting the said aqueous solution or dispersion of biological material containing said bioparticles, to gel permeation chromatography in the presence

of micelles of a ionic or non-ionic surfactant, whereby the said surfactant has substantially no interaction with the bioparticles.

More in particular the invention is concerned with the removal of bioparticles having a size of between 5 nm en 10 µm, such as those ranging in size from viruses to bacteria and other micro organisms. The present invention is based on the effect of the micelles in the mobile phase that improves the selectivity and/or effectivity and/or productivity of the removal of the bioparticles from the aqueous solution or dispersion of biological materials. These micelles do not interact with the bioparticles, which i.a. means that the micelles do not take up the biomolecules in their interior and/or bind the biomolecules to either the polar or apolar part of the surfactant and/or that the surfactant deactivates or destroys the bioparticles, more in particular the viruses.

The micelles are present in the mobile phase of the gel permeation chromatography system (which term includes gel filtration and size-exclusion chromatography as equivalent methods). The micelles are formed from the surfactant, once the concentration thereof is above the CMC, as defined hereinabove.

Most surfactant micelles have a hydrophobic core and a hydrophilic 'mantle'. The (smallest) radius of the hydrophobic core is about 70-80 % of the extended hydrocarbon tail of the surfactant. The radius of the hydrophilic mantle is depending on the length of the hydrophilic tail.

The aggregation number is an indication of the shape of micelles. Aggregation numbers can vary between 5-5000. A micelle with a low aggregation number will form spherical micelles. The higher the aggregation number the more stretched (cylindrical) the surfactant will be.

The aggregation number is depending on the ratio of the hydrophilic and hydrophobic part of the surfactant molecule. An increase in hydrophobicity leads to an increase in the aggregation number.

Depending on the nature and concentration of the surfactant, as well as components in the aqueous medium, the shape of the micelles may be different, such as cylindrical, round, ellipsoidal and the like.

The shape can become more complex at high surfactant concentration. Also additives can have an influence on the size and shape of the micelles. An

increase in temperature gives an increase in aggregation numbers. The shape of the micelles is important for the effect on the treatment, as well as the volume of the micelles in the mobile phase is. The influence of the shape of the micelles, particularly their dimensions, is important, as many tiny micelles provide a much larger 'excluded' volume then a few (let's say a single) at the same volume fraction.

The micelles are preferably small and spherical. Preferably their volume is between 0.1 and 50vol.%, preferably 1-30 vol.%.

The amount of surfactant is an important factor in determining the volume of the micelles in the aqueous system and may vary considerably, dependent on the various variables playing a role therein. The amount exceeds the CMC, preferably it is at least 1.01 times the CMC and may be up to $7*10^6$ times the CMC. In practice the amount of surfactant in the mobile (aqueous phase) will be between the CMC, or slightly above that and about 50 wt.%, more preferred 5 to 25 wt.% more in particular 5 to 15 wt.%.

The micelles have the function of improving the separation in selectivity and effectivity, more in particular when the removal of the bioparticles is combined with another treatment or separation of the biological material.

Suitable surfactants are non-ionic, cationic, anionic and zwitterionic surfactants. Preferred surfactants are the non-ionic surfactants, as these surfactants have a minimal interaction with the bioparticles and solutes except for the volume exclusion interaction. Examples thereof are the various polymers and copolymers of ethylene oxide and propylene oxide, and derivatives thereof, preferably having a molecular weight of at least 150, preferably up to 10,000. Specific examples are polyoxyethylene glycol monoethers, polyoxyethylene methyl-n-alkylethers, the various copolymers of EO and PO, t-octylphenoxy polyoxyethylene ethers, polyoxyethylene nonyl phenyl ethers, polyoxyalkylene derivatives of sorbitan or of fatty acids.

As most of these surfactants are also used in processes of treating biological materials, as defined above, their presence in the purified product is not a great problem. Further, it is to be noted that especially in case of the application of the process of the invention in combination with gradient simulated moving bed technology, the amount of surfactants in either the

purified biological material and the raffinate (bioparticle flow) may be kept very low.

The method of the invention is suitably carried out in conventional GPC methods, such as fixed bed, simulated moving bed, gradient simulated moving bed (SMB) or true moving bed systems, such as known in the art. The stationary phase of the systems is preferably selected from cross-linked or entangled polymers such as agarose, dextran and acrylamides, and derivatives thereof.

In a preferred embodiment of the invention, the removal of the undesired bioparticles from the biological fluid is combined with the separation of at least some of the other components of the biological fluid, such as proteins, DNA, and peptides.

It is preferred to use a simulated moving bed system or a gradient simulated moving bed system, such as described in Houwing et al., AIChE J, 2002 or in WO-A 0033934.

In a simulated moving bed, a feed stream can be separated into two fractions by the simulated countercurrent movement of an adsorbent and a liquid stream. Many known SMB systems consist of 4 sections with one feed stream, one desorbent stream and two product streams. By correct selection of the ratio of liquid to solid flow rates in each of the sections, weakly retained components (B) move towards the raffinate outlet and strongly retained components (A) move towards the extract outlet.

This SMB device contains a (non functionalized) gel material and has at least one inlet for the feed stream, one inlet for the desorbent stream. The two outlet streams are the extract stream containing component A and the raffinate stream containing component B. At least one of the feed streams or the desorbent stream contains a non-ionic surfactant at such concentration and temperature that it has formed micelles. A third outlet stream is the waste stream, which can (partly) be recycled to the desorbent stream. In each section m is defined as the ratio of the liquid flow and the sorbent flow in this section.

The separation in a SMB device mainly takes place in the two sections around the inlet of the feed stream containing component A and B. Component B should move upstream with respect to the liquid flow in the SMB and

component A should move downstream with respect to the liquid flow in the SMB.

The embodiment of the invention including the gradient simulated moving bed provides a method that minimises the contact between the undesired particles (say viruses) and the stationary phase, thereby reducing the risk of product contamination, batch-to-batch carry over, while being integrated in one single chromatographic step (instead of having both steps). This integrated chromatographic separation – viral clearance step - simultaneously may also be used to purify the desired bioproduct from a third component such as a protein.

An advantage of the combined use of such an SMB method and the method of the invention resides therein the integration enables one to dispense with one process step and that the amount of contaminating surfactant in the target solute, generally a protein solution, is kept low.

In this system two different separation aspects of treating biological materials are solved, namely the separation of the bioparticles from the biological materials and the separation of components of the biological materials from each other (generally proteins).

In such a situation it is to be noted that the size of the micelles to be used in the mobile phase is preferably in the same range (order of magnitude) as the size of the biological materials (proteins) to be separated from each other in the SMB system. This will also be optimal from a viral clearance point of view.

EXAMPLE 1

Viral clearance of Human Serum Albumin (HSA) using gradient, surfactant-aided size-exclusion SMB chromatography.

In this example a 5-section SMB is used for the separation as shown in figure 1.

For this separation a 5-section SMB is used, with two columns per section, as shown in figure 1.A feed stream with HSA and parvovirus having a size of 10 nm is introduced into the SMB between section 2 and 3. This virus is very difficult to remove using conventional methods due to its small size. A feed

stream with surfactant is introduced between section 3 and 4. An extract stream with HSA is discharged between section 1 and 2 and a raffinate stream with surfactant and virus is discharged between section 4 and 5. A desorbent stream without surfactant is introduced at section 1 and a waste stream is discharged from section 5.. Each section has 2 columns with a length of 10 cm and a diameter of 1 cm.

The concentration of HSA in the feed stream was 5 g/l, the concentration of virus particles was 10^{12} particles/ml. The surfactant concentration in the second feed stream was 20 vol.% of $C_{12}E_{23}$ (Brij35)

The following flow ratio's have been chosen:

m_1 = 0.53

m_2 = 0.2

m_3 = 0.55

m_4 = 0.85

m_5 = 0.9

Figure 2 gives the average relative concentration profile, with respect to the concentration in feed, when the system is in steady state. It clearly shows a separation of HSA and the virus. The virus is removed by a log reduction of 6.8, the recovery of HSA is 97 %, and the enrichment of HSA is 105 %.

EXAMPLE 2

Viral clearance of Human Serum Albumin (HSA) using gradient, surfactant-aided size-exclusion 4 section SMB chromatography.

In this example a 4-section SMB is used for the separation as shown in figure 3. A feed stream with HSA and parvovirus having a size of 10 nm is introduced into the SMB between section 2 and 3. In this case the surfactant A desorbent stream with surfactant is introduced at section 1. An extract stream with HSA is discharged between section 1 and 2 and a raffinate stream with surfactant and virus is discharged between section 3 and 4. The numbers of columns in section 1, 2, 3 and 4 are 3, 4, 3 and respectively. Each column has

a length of 10 cm and a diameter of 1 cm. Although not done in this example, it is possible to (partly) recycle the waste stream to the desorbent stream.

The concentration of HSA in the feed stream was 10 g/l, the concentration of virus particles was 10^{12} particles/ml. The surfactant concentration in the second feed stream was 20 Vol% of $C_{12}E_{23}$ (Brij35)

The following flow ratio's have been chosen:

m_1 = 0.53

m_2 = 0.2

m_3 = 0.55

m_4 = 0.3

Figure 4 gives the average relative concentration profile, with respect to the concentration in feed, when the system is in steady state. It clearly shows a separation of HSA and the virus. The virus is removed by a log reduction of 5.7, the recovery of HSA is 96 %, and the enrichment of HSA is 102 %.

Claims

1.   Method for the removal of bioparticles, including biomolecules from an aqueous solution or dispersion of biological materials containing said bioparticles, using gel permeation chromatography using a mobile and a stationary phase, said method comprising

5   subjecting the said aqueous solution or dispersion of biological material containing said bioparticles, to gel permeation chromatography in the presence of micelles of a ionic or non-ionic surfactant, whereby the said surfactant has substantially no interaction with the bioparticles.

10   2.   Method according to claim 1, wherein the volume of the micelles in the mobile phase is between 0.1 and 30 vol.%, preferably between 1.0 and 20 vol.%.

3.   Method according to claim 1 or 2, wherein the said bioparticles are selected from the group of bioparticles having a size between 5 nm

15   and

10 µm, preferably from the group consisting of viruses, bacteria, cells and cell debris.

4.   Method according to claim 1-3, wherein the said surfactant is a non-ionic surfactant, which is preferably selected from the group of

20   polyethers and polyether derivatives.

5.   Method according to claim 4, wherein the said non-ionic surfactant is selected from the group of polyethylene glycol, polypropylene glycol, copolymers of propylene glycol and ethylene glycol and derivatives thereof,.

25   6.   Method according to claim 1-5, wherein the concentration of the non-ionic surfactant is at least 1.01 times the critical micelle concentration and preferably at most $7*10^6$ times the critical micelle concentration.

7.   Method according to claim 1-6, wherein the concentration of

30   surfactant is between 1 and 50 wt.% of the mobile phase, preferably 1-30 wt.%.

8. Method according to claim 1-7, wherein the said removal is combined with a separation treatment of the said biological material.

9. Method according to claim 1-8, wherein the said biological material is selected from the group of blood, blood derived products, protein containing aqueous systems and fermentation products.

10. Method according to claim 1-9, wherein the gel permeation chromatography is performed using a simulated moving bed system.

11. Method according to claim 10 including a gradient simulated moving bed system.

12. Method according to claim 1-11, wherein the gel material for the gel permeation chromatography is selected from the group consisting of hydrophillic polymers such as dextran (derivates), agarose (derivates) and acrylamide (derivates).

13. Method for producing an aqueous solution or dispersion of biological materials having a reduced content of bioparticles compared to the feed material containing said bioparticles, the method comprising removing the said bioparticles, using the process of any one of the claims 1-12.

14. Use of micelles of surfactants in improving the selectivity and/or the effectivity of gel permeation chromatography for the removal of bioparticles from an aqueous solution or dispersion of biological materials containing said bioparticles.

Title: Separation method for bioparticles

Abstract

The present invention relates to a method for the removal of bioparticles, including biomolecules from an aqueous solution or dispersion of biological materials containing said bioparticles, using gel permeation chromatography using a mobile and a stationary phase, said method comprising subjecting the said aqueous solution or dispersion of biological material containing said bioparticles, to gel permeation chromatography in the presence of micelles of a ionic or non-ionic surfactant, whereby the said surfactant has substantially no interaction with the bioparticles.
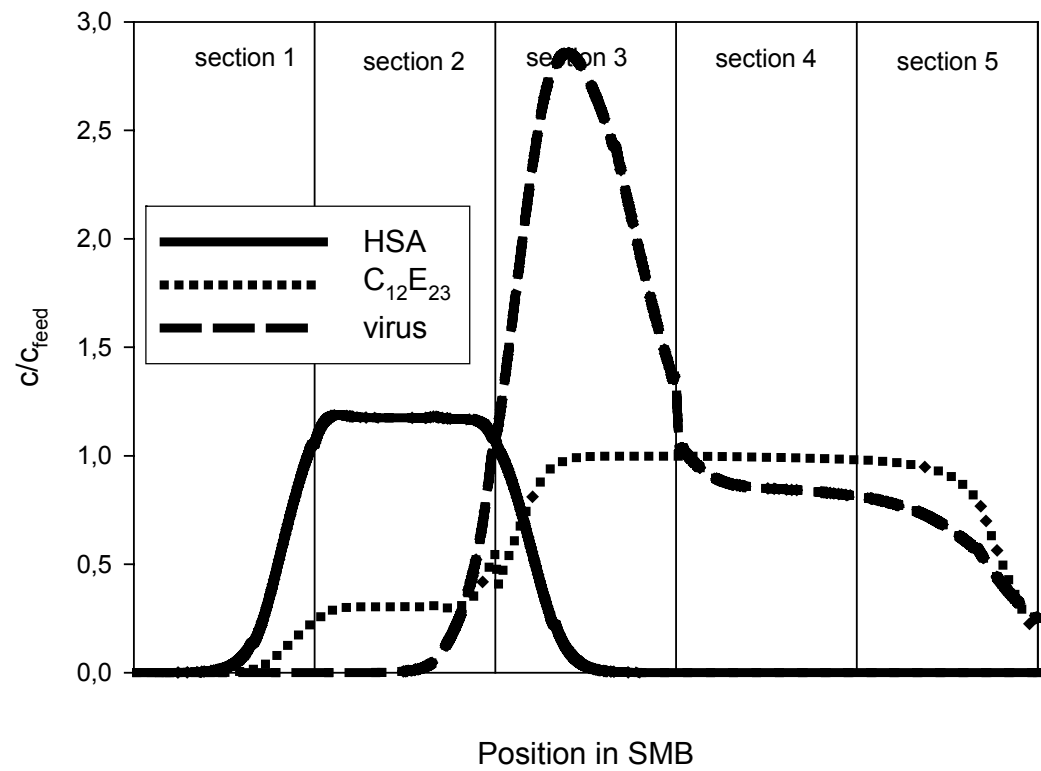
*sorbent
recycle*

W

| 5 |

R
[B]+[S]

| 4 |

F2
[S]

| 3 |

F1
[A]+[B]

| 2 |

E
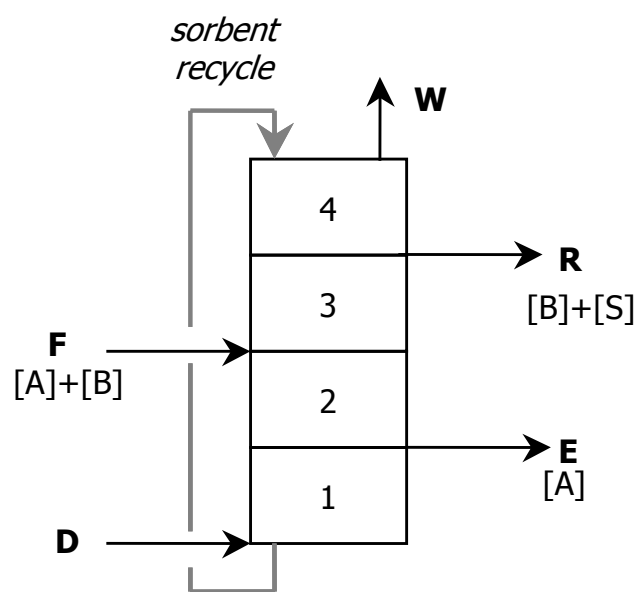[A]

| 1 |

D
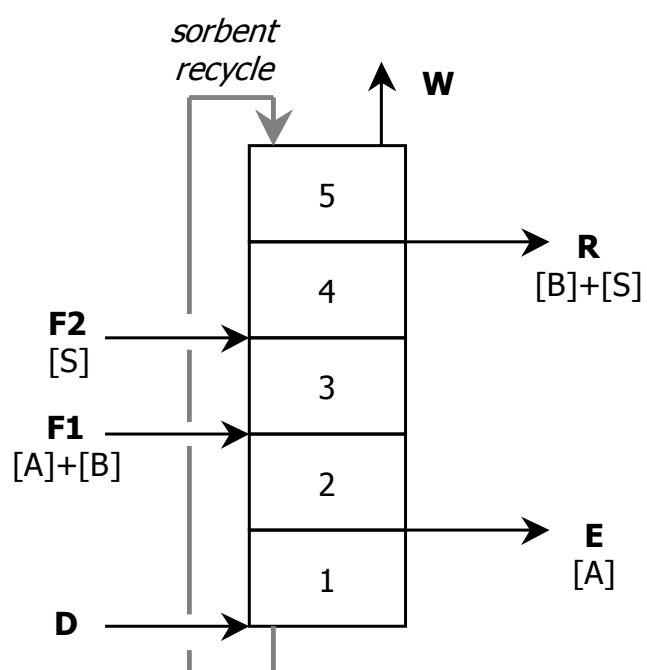
Figure 1
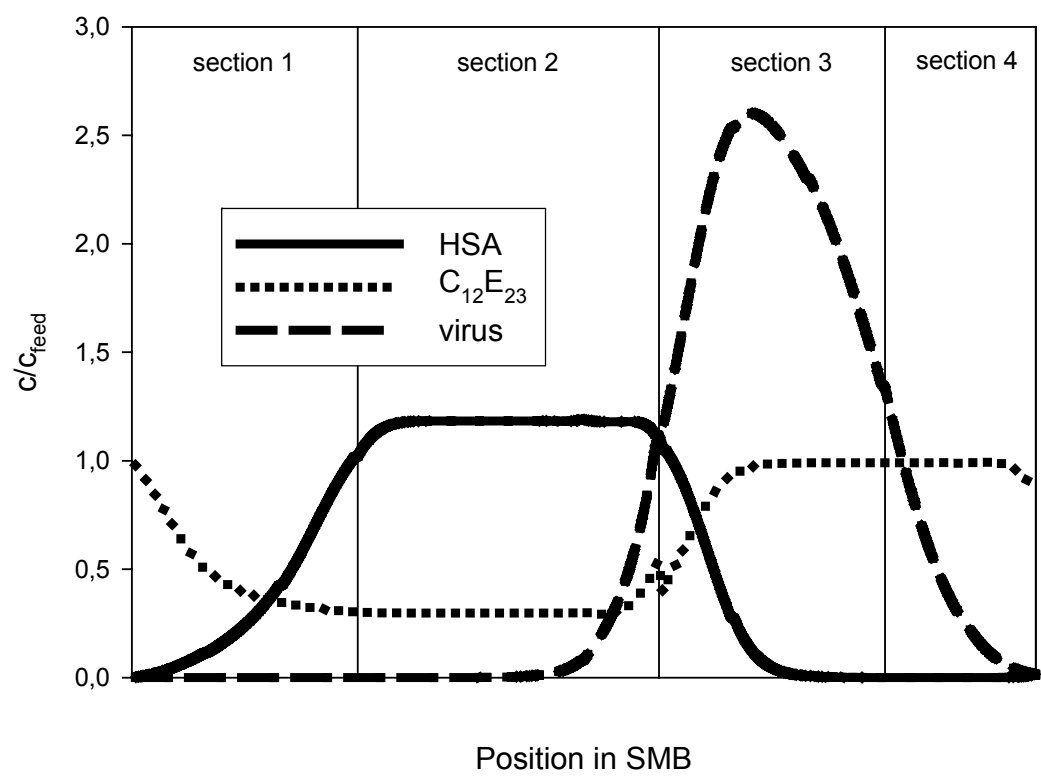
Figure 2

Figure 3

Figure 4

Summary

Bioseparations using Surfactant-Aided Size-Exclusion Chromatography

In most bioprocesses one or more chromatographic steps are used in the purification of the product. Size-exclusion chromatography (SEC) is often one of these chromatographic steps. It is based on the difference in size and shape of the components to be separated and is used for the separation of molecules with a near identical chemical composition such as dimer or oligomers from monomeric products. In SEC, the selectivity only depends on the characteristics of the gel material: the volume of the gel fibers and the diameter ratio of the pores versus the components to be separated. These parameters cannot be changed in-situ and each specific separation therefore requires a specific gel. Beside this low flexibility, SEC is characterized by a low efficiency due to the limited selectivity of the gel material. High resolution is possible but will result in high eluent and resin consumption, diluted products and high process times, which all have a negative effect on the costs of the production process. This indicates that there is a need for improvements or alternative concepts for this polishing step. This thesis describes an alternative method which is based on the integration of SEC and a selective mobile phase containing non-ionic micelles.

Chapter 2 gives a detailed description of this new alternative method: surfactant-aided size-exclusion chromatography (SASEC). The way in which biomolecules and bioparticles partition towards a mobile phase containing "inert" micelles of nonionic surfactants, depends on the same type of parameters as in size-exclusion chromatography: the volume fraction of the micelles and the diameter ratio of the solute and the micelles. In SASEC, the larger component will be excluded to a higher extent from the micellar mobile phase than the smaller component. In theory, the gel matrix should act as a practically non-selective "storage" phase for the components to be separated but selectively exclude micelles. Small species elute first, thereby reversing the "normal" chromatographic behavior. In chapter 2 a proof of principle is given with the model proteins Bovine Serum Albumin (BSA) and Myoglobine (Myo). Pulse experiments have been performed using the nonionic surfactants $C_{12}E_{23}$ or $C_{16}E_{23}$ in the mobile phase. The elution time of both proteins was increased at increasing micelle concentration. For BSA, the larger protein, this effect was larger than for Myo. This indicates that the selectivity can indeed be changed in-situ by changing the micelle concentration. This distribution behavior of the proteins is described by a model based on the excluded volume interactions between the proteins and the gel fibers, the proteins

and the micelles and the micelles and the gel fibers. This model adequately predicts the distribution behavior of both proteins in SASEC.

The ability to change the selectivity in-situ makes SASEC also suitable for gradient Simulated Moving Bed (SMB) chromatography. High affinity in the top sections and low affinity in the bottom sections can be established by using a high concentration of micelles in the top sections and a low concentration in the bottom sections. Also the distribution behavior of the micelles depends on the micelle concentration and is therefore implemented in the flow selection procedure for positioning the micelle gradient in the SMB. This procedure is described in chapter 3 and verified with several gradient-positioning experiments.

In chapter 4 viral clearance using SASEC is studied by the separation of the bacteriophage ϕ29 and bovine serum albumin (BSA). Although this bacteriophage can be seen as a model for a relative small virus (r=20 nm) it was too large to enter the pores of the gel matrix and adding micelles had no influence on the elution time of ϕ29. The added micelles only caused an increase the elution time of BSA. As a result, the resolution of the separation was increased at increasing surfactant concentrations. Experiments further show that SASEC results in higher productivity and lower solvent consumptions than compared with conventional SEC. This is not only shown in fixed bed chromatography but also in micellar gradient SMB. Gradient SASEC-SMB also shows an extra advantage of a non-diluted product. Appendix A contains a patent that was filed on part of this work.

In chapter 5 the separation of BSA and IgG was studied. Two resins have been tested (Sephacryl[TM] S200 and Sephacryl[TM] S300) as well as two different surfactants ($C_{12}E_{23}$ and Tween 20). Pulse experiments using SASEC showed that both BSA and IgG are more distributed towards the solid phase than compared to using SEC. This effect is larger on IgG, the largest component, than on BSA. As a consequence the mixture forms an azeotrope at a specific micelle concentration. Above this concentration the selectivity is reversed. Experiments show that at 7.5% (w/w) $C_{12}E_{23}$, BSA elutes before IgG. When the concentration is further increased the selectivity increases to values higher than obtained with conventional SEC. The productivity at 10% (w/w) $C_{12}E_{23}$ is increased with a factor 3 while the eluent consumption is decreased with a factor 1.2. Mathemetical simulations of the separation of BSA and IgG show a large increase in productivity (factor 40) and a decrease in eluent consumption (factor 15) when SASEC-SMB is applied compared to conventional SEC-SMB. The obtained product IgG is also concentrated by a factor 2 with SASEC-SMB.

Size-exclusion effects do not only appear between micelles and proteins or proteins and gel fibers but also between proteins and proteins. This leads to non-linear distribution behavior of these proteins. This is studied in chapter 6 by break-through experiments with highly concentrated BSA. The results show an increase in elution time with increasing concentration of BSA. This effect is however less then predicted by only excluded volume-effects. Apparently other interactions also play a role. Nevertheless, these concentration effects are still large enough to play an important in the design of separation processes using SEC in fixed bed or SMB chromatography systems.

The final chapter discusses the choice of micelle-gel systems to be used in SASEC. The selectivity is depending on two radius ratios; the radius ratio of the solute versus the gel fiber and the radius ratio of the micelle versus the gel fiber. The effect of these ratios is first evaluated on a theoretical base. This evaluation shows that the ratio of the solute versus the gel fiber should be as large as possible while the ratio of the micelle versus the gel fiber should be as small as possible. The second part of this chapter discusses the characteristics of some of the available micelles and gel materials to see the real limits of these ratios. The ratios needed to improve the selectivity are well inside the limits of the real available ratios. It is therefore possible to find a micelle-gel system for a specific separation. Chapter 7 finishes with some remarks concerning viscosity, acceptance of micelles in bioprocesses, and possible removal of the surfactants afterwards.

Danielle Horneman

Samenvatting

Bioscheidingen met behulp van Surfactant-Aided Size-Exclusion Chromatography

In de meeste bioprocessen worden een of meerder chromatografiestappen gebruikt voor het zuiveren van het eindproduct. Gelfiltratie behoort vaak tot een van deze stappen. Het scheidingsmechanisme van gelfiltratie is gebaseerd op het verschil in grootte en vorm van de te scheiden componenten. Het wordt veelal gebruikt voor de scheiding van componenten die chemisch gezien nagenoeg gelijk zijn aan elkaar. Een voorbeeld hiervan is de scheiding van dimeren en monomeren. De selectiviteit van gelfiltratie is afhankelijk van de geleigenschappen: het volume van de gelfibers en de diameterverhouding van de gelfibers in de gel en de te scheiden componenten. Deze eigenschappen liggen vast waardoor elke specifieke scheiding een specifieke gel nodig heeft. Naast deze lage flexibiliteit wordt gelfiltratie ook gekarakteriseerd door een lage efficiency die weer veroorzaakt wordt door de beperkte selectiviteit van het gelmateriaal. Hoge resolutie is weliswaar mogelijk maar heeft wel als gevolg dat het eluensverbruik en het verbruik van gelmateriaal relatief hoog ligt en dat bovendien de procestijden omhoog gaan terwijl de productconcentratie daalt. Dit alles heeft een negatieve invloed op de productiekosten. Er is dus duidelijk een behoefte aan verbeteringen of alternatieven voor deze chromatografiestap. Dit proefschrift beschrijft een nieuwe methode die gebaseerd is op een combinatie van gelfiltratie met een selectieve mobiele fase met niet-ionische micellen.

In hoofdstuk 2 wordt een gedetailleerde beschrijving gegeven van deze nieuwe methode die surfactant-aided size-exclusion chromatography (SASEC) genoemd wordt. De verdeling van biomoleculen ten opzichte van een mobiele fase met "inerte" micellen van niet-ionische surfactanten is afhankelijk van dezelfde soort parameters als in gelfiltratie: het volume van de micellen en de diameterverhouding van de micellen en de te scheiden componenten. Hoe groter de component hoe meer deze zal worden uitgesloten van de micelrijke mobiele fase. In theorie zou de gelfase niet selectief moeten zijn voor de te scheiden componenten maar wel selectief de micellen moeten buitensluiten. In dat geval zullen de kleinere componenten eerder elueren en is de selectiviteit dus omgekeerd ten opzichte van conventionele gelfiltratie. In hoofdstuk 2 is ook het bewijs gegeven van dit principe. Pulsexperimenten zijn uitgevoerd met de modeleiwitten Bovine Serum Albumin (BSA) en Myoglobine (Myo). Aan de mobiele fase is $C_{12}E_{23}$ of $C_{16}E_{20}$ als niet-ionische surfactant toegevoegd. De elutietijden van beide eiwitten gingen omhoog na verhoging van de micel concentratie. Dit effect was het groter voor BSA, het grootste eiwit, dan voor

Myo. Dit duidt erop dat de selectiviteit inderdaad in-situ kan worden veranderd door het veranderen van de micelconcentratie. Deze verdeling van de eiwitten over de twee fases is beschreven door een model dat is gebaseerd op de sterische interacties tussen de eiwitten en de gelfibers, de eiwitten en de micellen en tussen de micellen en de gelfibers. Het model geeft een nauwkeurige voorspelling van deze verdeling.

De mogelijkheid om de selectiviteit in-situ te veranderen maakt SASEC ook geschikt voor gradiënt Simulated Moving Bed (SMB) chromatografie. Door een hoge micelconcentratie in de top secties en een lage micelconcentratie in de onderste secties aan te brengen kan een hoge affiniteit in de top secties en een lage affiniteit in de onderste secties worden bereikt. De micellen die gebruikt zijn in deze studie worden echter niet selectief van de vaste fase uitgesloten. De verdeling van deze micellen over de beide fasen is afhankelijk van de micelconcentratie en is geïmplementeerd in de ontwerpprocedure voor het positioneren van de micelgradiënt in de SMB. Deze procedure is beschreven in hoofdstuk 3 en is experimenteel geverifieerd.

In hoofdstuk 4 is met de scheiding van de bacteriofaag $\phi29$ en BSA een virusverwijderingsstap bestudeerd. De bacteriofaag kan gezien worden als een model voor een relatief klein virus van ongeveer 40 nm. Het is echter te groot om in de poriën van het gelmateriaal te kunnen binnengaan. Het toevoegen van micellen heeft dan ook geen invloed op de elutietijd van $\phi29$. De toegevoegde micellen hebben dus alleen effect op de elutietijden van BSA met als gevolg dat de resolutie van de scheiding toeneemt naar mate de micelconcentratie wordt verhoogd. De experimenten laten verder zien dat met SASEC een hogere productiviteit en een lager eluensverbruik verkregen kan worden dan met conventionele gelfiltratie. Dit is niet alleen gebleken bij de fixed-bed experimenten maar ook bij de SASEC-SMB experimenten. Gradiënt SASEC-SMB heeft bovendien ook nog het voordeel dat het verkregen product niet verdund is. In appendix A is ook een patent te vinden dat gebaseerd is op een deel van dit werk.

In hoofdstuk 5 is de scheiding van BSA en IgG bestudeerd. Hierbij zijn 2 gelmaterialen (Sephacryl^{TM} S200 en Sephacryl^{TM} S300) en 2 surfactanten ($C_{12}E_{23}$ en Tween 20) getest. Uit de pulsexperimenten blijkt dat BSA en IgG in SASEC zich meer verdelen naar de vaste fase dan in gelfiltratie. Dit effect is groter voor IgG, het grootste eiwit, dan voor BSA. Bij een bepaalde surfactant concentratie zal hierdoor een azeotroop ontstaan en boven deze concentratie is de selectiviteit omgekeerd. Bij een concentratie van 7.5% (w/w) elueert BSA al voor IgG. Wanneer de concentratie nog verder verhoogd wordt gaat ook de selectiviteit omhoog. De te bereiken selectiviteiten zijn hoger dan dat met conventionele gelfiltratie mogelijk zouden zijn. Bij een concentratie van 10% (w/w) van $C_{12}E_{23}$ is de productiviteit gestegen met een factor 3 ten opzichte van gelfiltratie. Het

eluensverbruik is dan tegelijkertijd afgenomen met een factor 1.2. Simulaties van dezelfde scheiding met SASEC-SMB voorspellen een grote toename in de productiviteit (factor 40) in vergelijking met gelfiltratie SMB. Het product dat verkregen wordt met SASEC-SMB is bovendien zelfs tweemaal geconcentreerd.

Sterische effecten zijn er niet alleen tussen micellen en eiwitten of tussen eiwitten en de gelfibers maar ook tussen de eiwitten onderling. Dit leidt tot niet-lineaire isothermen van deze eiwitten. Dit is bestudeerd in hoofdstuk 6 voor BSA. Bij een verhoging van de eiwitconcentratie neemt ook de elutietijd van dit eiwit toe. Dit effect is echter minder groot dan voorspeld wordt door alleen de sterische interacties. Blijkbaar spelen ook andere interacties een rol. De effecten zijn echter groot genoeg om van invloed te kunnen zijn in het ontwerp van een scheidingsproces met gelfiltratie of gelfiltratie SMB.

In SASEC is de selectiviteit afhankelijk van een aantal ratio's: de diameterratio van de componenten en de gelfiber en de diameterratio van de micellen en de gelfiber. Het effect van beide ratio's is bestudeerd in hoofdstuk 7. Maximale selectiviteit wordt bereikt door een zo groot mogelijke diameterratio tussen de component en de gel fiber en een zo laag mogelijke diameterratio tussen de micel en de gelfiber. Verder zijn de eigenschappen van bestaande micellen en gelmaterialen besproken. Hieruit blijkt dat binnen deze bestaande groep van micellen en gelmaterialen een ruime keuze lijkt te zijn voor vele specifieke scheidingen. Het hoofdstuk eindigt met een aantal opmerkingen wat betreft de viscositeit, de acceptatie van micellen in bioprocessen en de mogelijke verwijdering van de micellen na deze scheidingsstap.

Danielle Horneman

Curriculum Vitae

Danielle Horneman is op 5 november 1975 geboren te Leiden. In 1996 behaalde zij haar VWO diploma aan het Oranje Nassau College te Zoetermeer. Vervolgens ging zij Scheikundige Technologie & Bioprocestechnologie studeren aan de Technische Universiteit Delft. Tijdens deze studie heeft zij o.a stage gelopen bij Novo Nordisk te Kopenhagen in Denemarken waar ze heeft gekeken naar het menggedrag in verschillende bioreactoren. Tijdens haar afstudeeropdracht bij Delft Gelatin heeft zij de demineralisatie van dierlijke beenderen bestudeerd en de demineralisatiestap in het gelatineproductieproces geoptimaliseerd.

In 2000 begon zij met haar promotieonderzoek bij de afdeling Bioseparation Technology van de faculteit Technische Natuurwetenschappen te Delft. Sinds februari 2006 is zij werkzaam als bioprocess scientist bij Xendo te Leiden.

Publications

Horneman DA, Ottens M, Keurentjes JTF, van der Wielen LAM. 2006. "Concentration effects in size-exclusion chromatography" *submitted for publication in J. Chromatogr.*

Horneman DA, Ottens M, Keurentjes JTF, van der Wielen LAM. 2006. "Surfactant-aided size-exclusion chromatography for the purification of IgG" *submitted for publication in Biotechnol Bioeng*

Horneman DA, Ottens M, Keurentjes JTF, van der Wielen LAM. 2006. "Viral clearance using surfactant-aided size-exclusion chromatography" *accepted for publication in AICHE journal*

Horneman DA, Ottens M, Keurentjes JTF, van der Wielen LAM. 2006. "Micellar gradients in size-exclusion simulated moving bed chromatography" J.Chrom A. 1113: 130-139

Horneman DA, Ottens M, Hoorneman M, van der Wielen LAM, Tesson M. 2004. "Reaction and diffusion during demineralization of animal bone" Aiche journal 50: 2682-2690.

Horneman DA, Wolbers M, Zomerdijk M, Ottens M, Keurentjes JTF, van der Wielen LAM. 2004. "Surfactant-aided size-exclusion chromatography". J. of chromatogr. B 807: 39-45.

Horneman DA, Ottens M. 2004. "Viral clearance and virus handling - 4th Biosafe symposium" Bionieuws 10: 14-14.

Houwing J, Horneman DA, Ottens M. van der Wielen LAM. 2004. "Separation of proteins using Simulated Moving Bed chromatography" NPT procestechnologie 4: 14-15.

Horneman DA, Ottens M, van den Broeke LJP, van Roosmalen D, Keurentjes, JTF, van der Wielen LAM. 2004. "Separation method for bioparticles" Patent EP1491246.

Horneman DA, Ottens M, Tesson M. van der Wielen LAM. 2002. "Improving gelatin plant production by modelling the demineralisation process of animal bones". In: Grievink & van Schijndel (ed.), Computer Aided Chemical Engineering, 10: 691-696

Horneman DA, Zomerdijk M, Ottens M, Keurentjes JTF, van der Wielen, LAM. 2001. "Protein separation using surfactant-aided gel filtration equipment". In: Bryan A., Serbezov (ed.) *Aiche Separation Technology topical conference; 2001 AICHE Annual Meeting, Reno, Nevada*, 1248-1251

Dankwoord

Eindelijk is het proefschrift dan af en alhoewel vaak wordt beweerd dat een promovendus een eenzaam bestaan heeft, heb ik daar niet veel van gemerkt. Ik kan niet anders zeggen dat dit proefschrift niet mogelijk was geweest zonder de hulp en aanwezigheid van vele andere personen.

In de eerste plaats wil ik graag mijn promotor Luuk van der Wielen bedanken voor al zijn wetenschappelijke ideeën, het zichtbaar maken van de grote lijnen en het vertrouwen in de goede afloop. Marcel Ottens wil ik bedanken voor alle begeleiding, input en vertrouwen en het vele malen doorlezen van mijn teksten. Dit project is gedaan in samenwerking met Jos Keurentjes, mijn copromotor, Dick van Roosmalen en Peter van den Broeke van de Technische Universiteit Eindhoven. Jullie wil ik ook allemaal bedanken voor de fijne samenwerking en de discussies die we gevoerd hebben. De leden van de gebruikersgroepcommissie wil ik graag bedanken voor al hun input tijdens de halfjaarlijkse voortgangsbesprekingen. Met name wil ik hierbij Marc Bisschops en Michel Eppink noemen die ook buiten deze besprekingen vaak de tijd hebben genomen om over delen van het project mee te denken en hun input hierbij te geven.

Ik heb ook veel hulp gehad met een groot deel van het experimentele werk beschreven in dit proefschrift. Maroesja, Max, Noortje, Niels en Stef hebben voor kortere of langere tijd een bijdrage geleverd aan het eindresultaat. Behalve experimentele resultaten leverde jullie aanwezigheid op het lab ook altijd veel gezelligheid op. Bedankt hiervoor! Ik wil ook graag Noortje, Sander en Koenraad bedanken, jullie hebben ieder als student zeker een bijdrage kunnen leveren aan de inhoud van dit proefschrift.

Verder zijn er een aantal mensen in het Kluyverlaboratorium bij wil je altijd terechtkunt, bij Carla voor alle administratieve zaken, afspraken met Luuk en nog veel meer, Marcel en Hans voor alle computerproblemen en bij Sjaak voor bijna alles. Jullie hebben heel veel zorgen weggenomen, bedankt hiervoor.

Ontspanning heb je ook nodig en dat kon ik vaak vinden aan de koffietafel waar ik heel wat collega's in de afgelopen jaren heb gezien en gesproken. Sommige bijna dagelijks andere wat minder regelmatig, maar altijd was het gezellig (met of zonder taart). Daarom bedankt aan iedereen die ik daar ben tegengekomen. Aan dezelfde koffietafel heb ik ook met veel plezier gezeten met de biotourcommissie, deze wil ik samen met alle deelnemers van de biotour bedanken voor de fantastische weken in Canada.

Ik ben ook bijzonder dankbaar voor alle mensen die tijdens moeilijkere tijden langs kwamen en tijd namen voor een praatje of een luisterend oor hebben aangeboden. Dat heeft mij heel veel goed gedaan. Bedankt!

Met Marco heb ik vele momenten mogen delen die bij een promotietraject horen. De blijdschap wanneer iets eindelijk lukt, maar ook de momenten waarop ik het niet meer zag zitten. Bedankt voor al je geduld en steun in de afgelopen jaren.

Danielle